OXIDATIVE STRESS IN PLANTS AND THE MALARIAL PARASITE *PLASMODIUM FALCIPARUM*

By

Suong Thi Thu Cu

Bachelor of Biotechnology (Hons.)

A thesis submitted in partial fulfillment of the requirements for the
Degree of Doctor of Philosophy in the
School of Biological Sciences,
Faculty of Science and Engineering
Flinders University

Adelaide
April, 2009

Table of contents

Summary

This thesis is divided into three main parts. Part A of the project aimed to investigate the effects of the mixed-culture of wheat (*Triticum aestivum* L.) with white lupin (*Lupinus albus* L.) on the availability of soil-P to the wheat and to study the mechanisms by which white lupin mobilises P from unavailable soil-P pools making it more available to the wheat crop partner. P limitation is a major problem for many agricultural systems, particularly in the tropics and subtropics. White lupin is well-known for its ability to mobilise P from a P pool that is normally unavailable to plants. In this study, white lupin was grown in a mixed culture with wheat and the effects of the mixed culture on the availability of P to the wheat was investigated using a novel leaching system. The results show that while lupin was capable of mobilising the P that was locked up in the soil, as the level of the immobile P pool was significantly lower in the presence of white lupin compared to the wheat monoculture. This ability of white lupin to mobilise the unavailable P was demonstrated to have beneficial effects on the growth and P uptake of the wheat when they were grown in a mixed-culture.

Part B and C of this study focuses on the 2-Cys peroxiredoxin proteins of malarial parasite *Plasmodium falciparum*; *Pf*Prx-1 and *Pf*Prx-2 respectively. Malaria parasites are highly exposed to oxidative burden due to a large amount of reactive oxygen and nitrogen species produced by haemoglobin degradation in the food vacuole of the parasite and the immune effects of the host in response to parasite infection. Therefore, inside erythrocytes, the ability of the parasite to defend itself against

oxidative damage is of vital importance for parasite survival. Such defences are thus expected to be potential targets for malaria control strategies. This study focuses on the 2-Cys peroxiredoxin (Prx) system of *P. falciparum*; these enzymes are mainly responsible for the detoxification of hydrogen peroxide and other organic peroxides in the parasite, thereby protecting the parasite against oxidative stress.

Part B of the project aimed to study the factors influencing the oligomeric states of the *P. falciparum Pf*Prx-1 protein recombinantly expressed in *E. coli* and to investigate its three dimensional structure using X-ray crystallography. Firstly, the *Pf*Prx-1 gene was successfully expressed in *E.coli* for protein production. Following high-level expression, the *Pf*Prx-1 protein was purified to homogeneity. The purified *Pf*Prx-1 protein was studied for its Prx activity and its oligomeric structure. The *Pf*Prx-1 protein exists in both decameric and dimeric forms. High pH (8.5) and high concentrations of urea (2.8 M) seem to favour the formation of dimers. Attempts at crystallization of the protein yielded crystals, of which one diffracted to around 6-7 Å. Eventhough these data were not enough to sovle the structure of the protein, they could serve as a ground for further studies in order to obtain the full details of *Pf*Prx-1 3-D structure enabling inhibitor studies for structure-based drug design.

Part C of this study aimed to develop a *Pichia pastoris* expression system for the *P. falciparum Pf*Prx-2 protein and to investigate the oligomeric states and the subcellular localization of the recombinant *Pf*Prx-2 protein. The *P. pastoris* expression system was demonstrated to be able to translate this *P. falciparum* A+T rich sequence and recognise the mitochondrial targeting sequence of the protein.

This production system could be up-scaled to obtain sufficient quantities of recombinant *Pf*Prx-2 protein to enable structural and functional studies for structure-based drug design. Evidence for the production by *P. pastoris* of the *Pf*Prx-2 protein as an oligomer (decamer and larger) was obtained by gel filtration chromatography, SDS-PAGE and Western blotting. It was found that purification of the functionally active *Pf*Prx-2, by Ni-affinity chromatography, resulted in the protein being "locked" in the dimeric state and it could not be converted to the monomer by a variety of reducing agents as indicated by SDS-PAGE.

Declaration

"I certify that this thesis does not incorporate without acknowledgement any material previously submitted for a degree or diploma in any University; and that to the best of my knowledge and belief it does not contain any material previously published or written by another person except where due reference is made in the text".

Suong T. T. Cu

Acknowledgements

The completion of this thesis would have not been possible without the involvement of many exceptional individuals. First I would like to express my greatest appreciation to my principal supervisor, Dr. Kathy Schuller, for giving me the opportunity to work on this project and for her limitless guidance and support. I would also like to acknowledge my co-supervisors, Dr. Ian Menz, for his support with the works involved molecular biology and protein crystallography and Dr. John Hutson for his guidance with the works involved soil chemistry. I would like to thank many academic staffs at the School of Biological Sciences at the Flinders University; A. Prof. Kathleen Soole, Dr. Cathy Abbott, Dr. Peter Anderson for their generosity in providing essential chemicals plus many useful advices. I would also like to thank many post-doctorates and postgraduate students; Dr. Simon Schmidt for his help with the use of HPLC system and Dr. Tong Chen for her help with the use of confocal microcopy. I am grateful for having great support from all the technical staffs; Lidia, Geoff, Dough, Dick, Bob, Bruce, Tim and Andrew.

My special thanks go to Dr. Jenny Martin and Karl Byriel at the University of Queensland for their generous help with analysing my protein crystals and to Prof. Shin-ichiro Kawazu at the International Medical Research Centre of Japan for providing me the *Pf*Prx-2 antibody.

My PhD has been a long journey and I am very grateful to my PhD fellows for making the journey fun and enjoyable; in particular I would like to thank Janene

Publications

Part of the work in this thesis has been published or is in preparation for submission for publication. The publications are listed below:

Cu STT, Hutson J, Schuller KA (2005) Mixed culture of wheat (*Triticum aestivum* L.) with white lupin (*Lupinus albus* L.) improves the growth and phosphorus nutrition of the wheat. **Plant and Soil**, 272(1-2): 143-151

Suong T.T. Cu, R. Ian Menz and Kathryn A. Schuller (in preparation) Expression, purification, crystallization and preliminary X-ray analysis of *Pf*Prx-1, a cytosolic 2-Cys peroxiredoxin from *Plasmodium falciparum. Journal of Biochemistry.*

Suong T.T. Cu, R. Ian Menz and Kathryn A. Schuller (in preparation) Expression, purification and characterisation of a recombinant *Plasmodium falciparum* mitochondrial 2-Cys peroxiredoxin in *Pichia pastoris. Protein Expression and Purification.*

Cu, S TT and Schuller, KA (2005) Intercropping lupin and wheat for better phosphorus acquisition. Oral presentation at the XV International Plant Nutrition Colloquium, Beijing, China, September 14-20.

List of symbols and abbreviations

Å   angstrom (10^{-10} m)

Amp   ampicillin

AOP   antioxidant protein

AOX   alcohol oxidase

A_x absorbance at x nm

ATP   adenosine triphosphate

βME   β-mercapto ethanol

BMGY   buffered minimal glycerol

BMMY   buffered minimal methanol

bp   base pair

BPB   bromophenol blue

BSA   bovine serum albumin

BT   Bis-Tris, bis (2-hydroxyethyl)imino-tris(hydroxymethyl)methane

cDNA   complementary DNA

CHAPS   3-(3-Cholamidopropyl)dimethylamino-1-propanesulphonate

Ch   chloramphenicol

Cys   cysteine

Da   dalton

dH_2O milliQ water

DMSO   dimethylsulphoxide

DNA   deoxyribonucleic acid

DNase   deoxyribonuclease

dNTP   deoxynucleotides triphosphate

dsDNA   double-stranded DNA

DTT   dithiothreitol

EDTA   ethylendiaminetetraacetate

eg   for example

EGTA   ethylene glycol-bis(2-aminoethylether)-N,N,N,N-tetra acetic acid

ESI-MS   electrospray ionisation mass spectrometry

Fig.   figure

FPLC   fast performance liquid chromatography

g   gram

g   acceleration of gravity

GF   gel filtration chromatography

GPx   glutathione peroxidase

GSH   glutathione

GSR   glutathione reductase

GST   glutathione S-transferase

h   hour

H_2O_2 hydrogen peroxide

HEPES   N-2-hydroxyethyl-piperazine-N-2-ethanesulfonic acid

HPLC	high performance liquid chromatography
His$_6$-tag	(polyhistidine)$_6$ tag
IPTG	isopropyl β-D-1-thiogalactopyranoside
Kan	kanamycin
kb	kilobase
kDa	kilodalton
lacI	gene encoding the lac repressor
l	litre
LB	Luria-Bertani
m	milli (10^{-3})
μ	micro (10^{-6})
M	molar
MALDI	matrix assisted laser desorption ionization
MCS	multiple cloning site
MES	2-(N-morpholino)ethane sulphonic acid
min	minute
mRNA	messenger RNA
MS	mass spectrometry
MW	molecular mass
NADH	nicotinamide adenine dinucleotide (reduced form)
NADPH	nicotinamide adenine dinucleotide phosphate

NMR	nuclear magnetic resonance spectroscopy
NKEF	natural killer enhancing factor
n	nano (10^{-9})
$O_2^{\bullet-}$	superoxide
$ONOO^-$	peroxynitrite
OD_x	optical density at x nm
ORF	open reading frame
PAGE	polyacrylamide gel electrophoresis
PBS	phosphate buffer saline
PCR	polymerase chain reaction
PDB	protein data bank
PEG	polyethyleneglycol
pI	isoelectric point
Prx	peroxiredoxin(s)
PVDF	polyvinylidene fluoride
RBC	red blood cell
RNA	ribonucleic acid
RNase	ribonuclease
rmp	revolutions per minute
ROS	reactive oxygen species
s	second

SAP	shimp alkaline phosphatase
SDS	sodium dodecyl sulphate
SDS-PAGE	sodium dodecyl sulphate polyacrylamide gel electrophoresis
SOD	superoxide dismutase
ssDNA	single-stranded DNA
Taq	*Thermus aquaticus*
TAE	Tris-acetate-EDTA buffer
TB	Tris buffer
TBE	Tris-borate- EDTA buffer
TCA	Trichloroacetic acid
TE	Tris-EDTA buffer
TEMED	N,N,N,N-tetramethylendiamine
TPx	thioredoxin peroxidase
Tris	Tris(hydroxymethyl)aminomethane
tRNA	transfer RNA
Trx	thioredoxin
TrxR	thioredoxin reductase
TSA	thiol-specific antioxidant
UV	ultraviolet
V	volt
vol	volume

v/v	volume per volume
w/v	weight per volume
w/w	weight per weight
wt	wild-type
YEP	yeast extract peptone
YNB	yeast extract nitrogen base

List of figures

List of tables

Chapter 1   Introduction

1.1 Generation of reactive oxygen species and other oxidants

1.1.1   Reactive oxygen species

Reactive oxygen species (ROS) is a term that describes the chemical species that are formed upon incomplete reduction of oxygen to water. They include the superoxide anion (O_2^{-}), hydrogen peroxide (H_2O_2) and the hydroxyl radical (OH^{-}) (D'Autréaux and Toledano, 2007). Molecular oxygen is relatively non-reactive. In its ground state, triplet oxygen $^3O_2$ is unlikely to react with organic molecules unless it is activated (Briviba et al., 1997). Activation of oxygen can occur by various mechanisms (summarised in Fig. 1.1). The mechanisms are as follows:

(i)   absorption of sufficient energy to reverse the spin on one of the unpaired electrons, or monovalent reduction. If triplet oxygen absorbs sufficient energy, excitation of this molecule will occur leading to a change in electron distribution in the molecule forming molecular species with all electrons paired (singlet oxygen, Fig. 1.1) (Afanas'ev, 1991)

(ii)   stepwise monovalent reduction of oxygen. In living organisms, the utilisation of oxygen for aerobic respiration involves a four-electron reduction (cytochrome oxidase adds four electrons to an oxygen molecule which leads to the formation of water). However, one- and two- electron reductions also occur leading to the formation of ROS (Elstner and Osswald, 1993).

(iii)   Transition metals and organic electron donors reduce $^3O_2$ and produce

superoxide ($O_2^{\cdot-}$) and metal-oxygen complexes such as perferryl and related

species (Dalton et al., 1999),

(iv)   abstraction of one electron (or hydrogen) from an organic compound. In this

case, carbon radicals resulting from hydrogen abstraction by hydroxyl

radicals react with $^3O_2$ and produce peroxyl radicals (Dalton et al., 1999)

(v)   enzymatic activation of oxygen. The production of nitric oxide via nitric

oxide synthase is one example of this case (Dalton et al., 1999).

Superoxide is the primary product of NADPH oxidase activity and the initial oxidant

that escapes the mitochondrial electron transport chain (Winterbourn and Hampton,

2008). Superoxide has extremely limited permeability through lipid membranes and

is largely restricted to the compartment where it is generated (Takahashi and Asada,

1983). Superoxide can act as either an oxidant or a reductant; it can oxidise sulphur,

ascorbic acid and NADPH; it can reduce cytochrome c and metal ions. In its

protonated form (pKa = 4.8) superoxide forms the perhydroxyl radical (Fig. 1.1)

which is a powerful oxidant but its biological relevance is probably minor because

of its low concentration at physiological pH (Gebicki and Bielski, 1981)
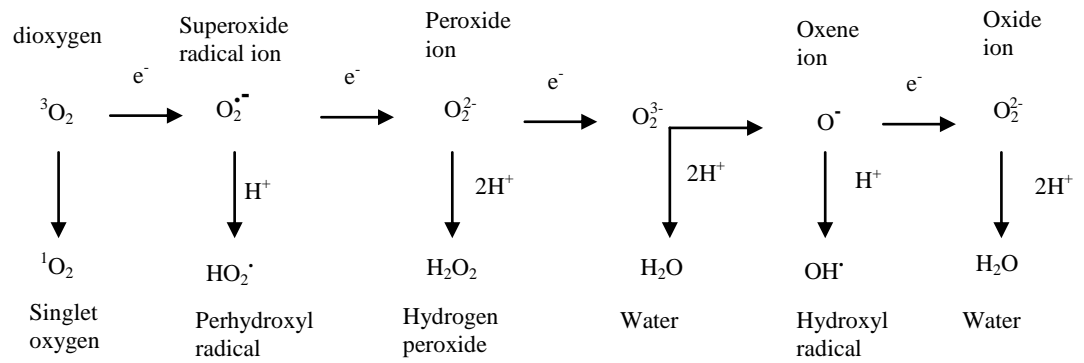
Figure 1.1: Generation of various ROS by energy transfer or sequential
univalent reduction of ground state triplet oxygen (adapted from Apel and Hirt,
2004)

Hydrogen peroxide is generated both directly (for example, as a secondary product of the superoxide generated by NADPH oxidases) and as a by-product of mitochondrial respiration and other metabolic processes (Winterbourn and Hampton, 2008). Superoxide dismutation occurs spontaneously but can be accelerated through catalysis by intracellular or extracellular superoxide dismutases. Hydrogen peroxide is uncharged and it can readily diffuse through membranes. Therefore it is not compartmentalised in the cell (Apel and Hirt, 2004). Hydrogen peroxide has a high reduction potential and is therefore a strong oxidizing agent. However, most of its reactions have high activation energies and are, therefore, slow (Winterbourn and Hampton, 2008). Numerous enzymes (peroxidases) use hydrogen peroxide as a substrate in oxidation reactions involving the synthesis of complex organic molecules.

In the presence of a metal reductant such as iron, hydrogen peroxide can be oxidised to form the highly reactive **_hydroxyl radical_** which is the strongest oxidising agent known; the reaction was named the "Fenton" reaction

$$Fe^{2+} + H_2O_2 \rightarrow Fe^{3+} + {}^{\cdot}OH + OH^{-}$$

Metals other than iron may also participate in these electron transfer reactions by cycling between oxidised and reduced states. The hydroxyl radical is very harmful because it reacts with organic molecules at extremely high rates (Afanas'ev, 1991).

ROS are formed by the action of various physical and chemical factors on living organisms and also as unavoidable by-products of aerobic metabolism (Table 1.1). The most significant metabolic source of superoxide ($O_2^{\cdot-}$) in animal cells is the

respiratory chain of mitochondria where 1-2% of oxygen is subject to one-electron reduction (Boveris, 1984). ROS may also come from the reduction of oxygen by NADPH-dependent oxidase systems (e.g. those present in phagocytes, B lymphocytes and some plasma membranes) as a result of a variety of pathological conditions (Apel and Hirt, 2004, Babior, 1999)

In plant cells, apart from mitochondria, another important site of $O_2^{-\cdot}$ production is chloroplasts where the O_2 concentration is very high (up to 300 mol m^{-3}) (Navari-Izzo et al., 1996). The major sites of $O_2^{-\cdot}$ production in chloroplasts are the thylakoid membrane-bound primary electron acceptor of photosystem I and ferredoxin (Furbank and Badger, 1983). Other sources of $O_2^{-\cdot}$ production are the electron transport chains of the endoplasmic reticulum and the NADH- or NADPH-utilising electron transport chain of the nuclear envelope (Gille and Sigler, 1995). Plant peroxisomes and cell walls also produce $O_2^{-\cdot}$ and H_2O_2 (Del Rio and Donaldson, 1995).

Table 1.1. Sources of oxidative stress (adopted from Winterbourn and Hampton, 2008)

Condition	Proposed source	Likely reactive oxygen species produced
Hyperoxia Hypoxia	Mitochondria, NADPH oxidases; Xanthine oxidase, nitric oxide synthases	Superoxide Hydrogen peroxide Nitric oxide, Peroxynitrite
Inflammation	Phagocyte NADPH oxidase Myeloperoxidase, nitric oxide synthase	Oxyradicals, nitrogen dioxide, carbonate radical Nitric oxide, peroxynitrite
Activation of receptors to agonists	NADPH oxidases, mitochondria Nitric oxide synthases	Superoxide Hydrogen peroxide Nitric oxide
Xenobiotic metabolism	Peroxidases, flavoprotein reductases, autoxidation	Oxyradicals Superoxide Hydrogen peroxide

This table lists significant sources of reactive oxygen species but is not intended to be all-inclusive.

1.1.2   Oxidative stress damage

In every aerobic cell there is a dynamic equilibrium between reactions generating oxidants and those generating antioxidants. A change in this equilibrium favouring the production of oxidants leads to cellular damage referred to as oxidative stress (Sies, 1991).

Damage caused by the rapid and non-specific reactions of ROS under oxidative stress conditions affects all classes of biomolecules. Damaging effects of ROS include lipid peroxidation, inactivation of enzymes and other functional proteins and base modifications and strand breaks in DNA (Breen and Murphy, 1995, Fridovich, 1978, Stadtman, 1992). For example, one of the targets of ROS in both plant and animal cells is the Ca^{2+}-ATPase. Inhibition of this enzyme contributes to increased cytoplasmic Ca^{2+}, a common symptom of cellular damage by ROS (Price et al., 1994). In plants, ROS can also target the thiol-containing enzymes participating in the CO_2-fixation cycle such as fructose-1,6-bisphosphatase, glyceraldehyde-3-phosphate dehydrogenase and ribulose-5-phosphate kinase (Asada, 1992). Though ROS are well known for their toxicity, they also participate in key signaling events (Rhee et al., 2005). Thus, cells require at least two different mechanisms to regulate their intracellular ROS − one that enables fine modulation of low levels of ROS for signaling purposes, and one that enables the detoxification of excess ROS, especially during oxidative stress (Mittler, 2002).

1.1.3   Oxidative stress and nutrient deficiency especially phosphorus (P) deficiency in plants

In plant cells, the level of ROS is kept under tight control by antioxidant systems (details described in section 1.2) under normal conditions. However, severe stress conditions can disturb the balance between ROS generation and its scavenging machinery, which initiates signaling responses, enzyme activation, gene expression, programmed cell death and cellular damage (Niell et al., 2002, Mahalingam and Fedoroff , 2003, Tewari et al., 2004). Deficiency of major structural constituents like nitrogen (N) or phosphorus (P) is expected to reduce the frequency of electron carriers of electron transport systems (Grossman and Takahashi 2001). Potassium (K) deficiency retards CO_2 uptake due to stomatal closure leading to an accumulation of reducing power (NADPH), over-reduction of electron transport carriers (Grossman and Takahashi 2001) and generation of the superoxide radical (O_2^-) and other ROS (Grossman and Takahashi 2001). The increase in activities of antioxidant enzymes was reported in spinach and maize deficient in macronutrients (Logan et al., 1999, Tewari et al., 2004)

P starvation is a stress condition that can increase ROS formation and cause oxidative stress in plant tissues. Previous studies have shown that that prolonged phosphate deficiency causes a decline in inorganic phosphate (Pi) concentration in bean root tissues accompanied by a lower respiration rate via the cytochrome pathway and increased alternative respiration using alternative oxidase (Gniazdowska et al., 1998, Mikulska et al., 1998). Under these conditions, electron

flow through the cytochrome pathway in the mitochondria was restricted, resulting in increased ROS production by the electron transport chain (Juszczuk et al., 2001b). Malusà et al., (2002) reported that P-deficient bean roots had a significant increase in ROS production (specifically hydrogen peroxide and 5,5-dimethyl-L-pyrroline-N-oxide). The ROS production increased as the duration of the phosphate deficiency increased. Apart from the increase in ROS formation, other reported effects of oxidative stress caused by P deficiency were an increase in membrane lipid peroxidation and a change in membrane phospholipid composition (Gniazdowska et al., 1999, Juszczuk et al., 2001a).

Although P deficiency is known to cause symptoms of oxidative stress in plant cells, studies on the antioxidant protection mechanisms in plant cells suffering from P-deficiency are quite limited. Malusà and Rychter (1997) reported changes in peroxidase, catalase and superoxide dismutase enzyme activities in bean roots under P deficiency and identified peroxidase enzymes as the most active. Juszczuk et al., (2001a) reported that there was an increase in catalase and total peroxidase activity in the roots of P-deficient bean plants while the activities of superoxide dismutase and ascorbate peroxidase were not affected by P stress. The peroxidase activity reported by these researchers could be catalyzed by a number of different enzymes (see above). Unfortunately, the researchers did not investigate which peroxidase enzymes were involved. Further studies in this area would improve our understanding of antioxidant-mediated protection against oxidative stress under P deficiency in plants.

With regards to the link between improved P nutrition and oxidative stress, Gunes *et al.* (2009) studied the effects of arsenic and P supply on chickpea plants and showed that increasing the availability of P in the form of phosphate protected chickpea plants against arsenic-induced oxidative stress as indicated by decreased lipid peroxidation (Gunes et al., 2009). Since intercropping systems are supposed to improve P-uptake in P-inefficent plants, it is expected that this system would affect the P-deficiency induced oxidative stress in plants and their antioxidant mechanisms. This is of interest to investigate this hypothesis.

1.2 Antioxidant systems

1.2.1   General

As aerobic organisms produce toxic oxygen derivatives, they also possess elaborate defense mechanisms for ROS detoxification in order to maintain ROS at a "safe" level (Miller et al., 2002). The defense mechanisms can be grouped into two types: enzymatic and non-enzymatic (Fig. 1.2).
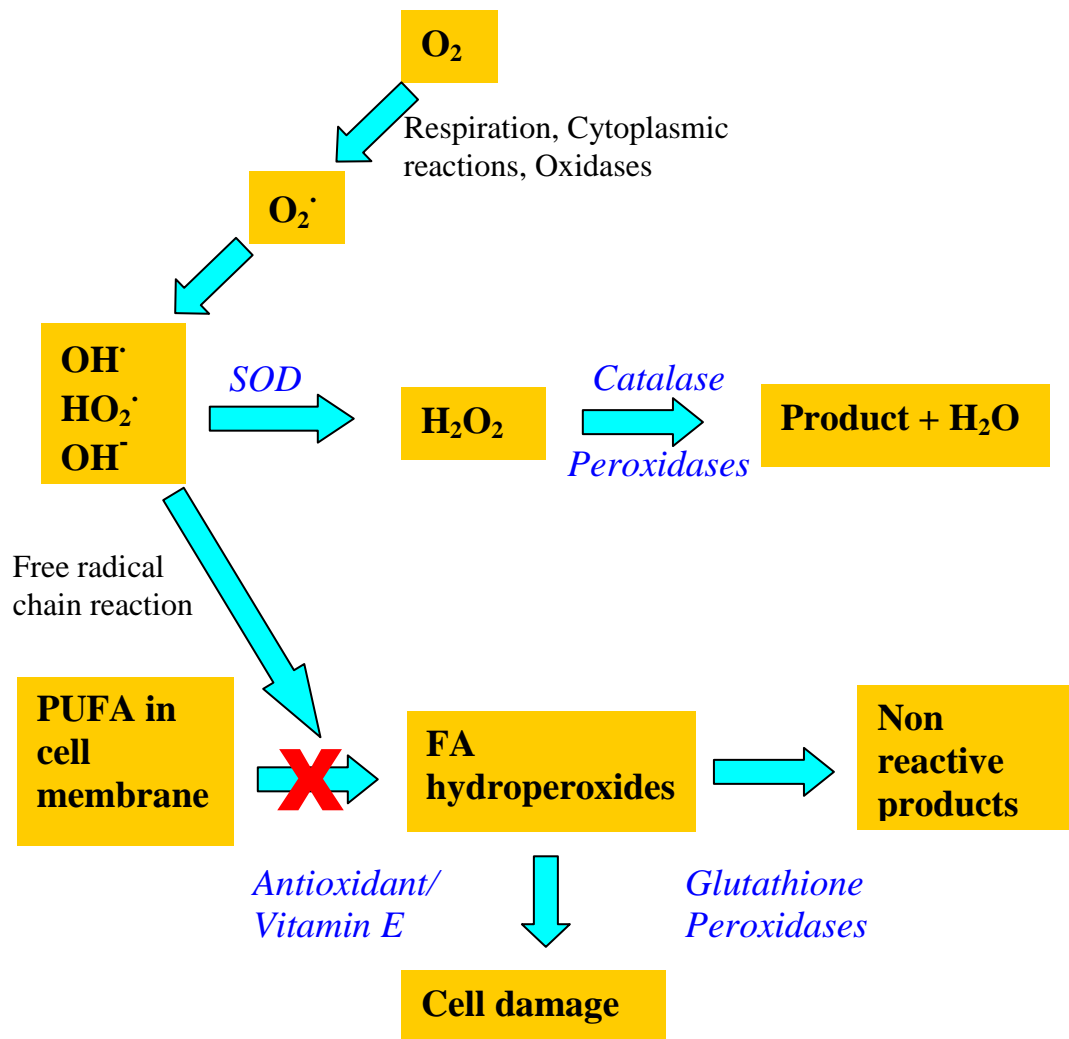
Figure 1.2. **Non-enzymatic and enzymatic mechanisms of ROS detoxification** (adapted from Cowey et al., 1985). Cellular reactions produce oxygen radicals which need to be removed otherwise they may cause damage to cells such as reaction with polyunsaturated fatty acids (PUFA) causing lipid peroxidation, particularly in cellular membranes. These oxygen radicals can be removed by the actions of antioxidant enzymes e.g. superoxide dismutase (SOD), catalase and various peroxidases. Non-enzymatic antioxidants such as vitamin E also function as ROS scavengers.

Non-enzymatic protection is provided by organic antioxidants such as ascorbic acid, glutathione and vitamin E (Mittler et al., 2004). These compounds scavenge ROS, thus preventing oxidative damage. Vitamin E (α-tocopherol) is a lipid-soluble antioxidant compound that plays an important role in preventing membrane damage (Mittler et al., 2004). Glutathione and ascorbic acid (vitamin C) are both essential in cellular antioxidant protection (Mittler et al., 2004).

Major ROS-scavenging enzymes in plants include superoxide dismutases (SODs), ascorbate peroxidases (APxs), catalases (CATs), glutathione peroxidases (GPxs) and peroxiredoxins (Prxs) (Mittler et al., 2004). In general, SODs convert oxygen radicals to H_2O_2 which is then detoxified by CATs, GPxs, APxs or Prxs.

1.2.2   Superoxide dismutases

SODs are the first line of defense against ROS. They catalyse the dismutation of superoxide anions to form hydrogen peroxide.

$$O_2^{\cdot -} + O_2^{\cdot -} + 2\ H^+ \rightarrow H_2O_2 + O_2$$

This catalyzed reaction occurs approximately 10,000-fold faster than spontaneous superoxide dismutation (Bowler et al., 1992).

SOD isozymes are present in all aerobic organisms and in all subcellular compartments susceptible to oxidative stress (Blokhina et al., 2003). There are three major types of SODs each defined by their metal cofactor(s), i.e., manganese

12

(MnSOD), iron (FeSOD) and copper and zinc (Cu/ZnSOD). Animals have SODs

containing active-site manganese (MnSOD) in the mitochondrial matrix, plus SODs

with copper and zinc (Cu/ZnSOD) in the mitochondrial intermembrane space and in

the rest of the cell (Fridovich, 1995). In addition to the two above forms, some

plants also have iron-containing SODs (FeSOD) in the chloroplast (Alscher et al.,

2002). Bacteria often have CuZnSOD plus MnSOD and/or FeSOD; a few even have

nickel-containing SOD (Halliwell and Gutteridge, 2006). All forms of SODs

catalyze the above reaction (Fridovich, 1995; Halliwell and Gutteridge, 2006).

1.2.3   Catalases

CATs are heme containing enzymes with the potential to directly dismutate

hydrogen peroxide into water and oxygen

$$H_2O_2 \rightarrow 2\,H_2O + O_2$$
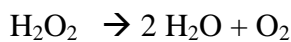
CAT has one of the highest turnover rates for all enzymes: one molecule of CAT

can convert approximately 6 million molecules of H_2O_2 to H_2O and O_2 per minute

(Willekens et al., 1995; Halliwell, 2006), therefore the enzyme plays an important

role in in defense against ROS (Feierabend, 2005, Willekens et al., 1997).

The CAT family is highly diverse with CATs from different organisms have a broad

range of subunit sizes, a variety of quaternary structures, at least two different

prosthetic groups, and even substantially different amino acid sequences (Halliwell,

2006). Generally, the most common type of CAT, the monofunctional, are active as

homotetramers, but dimers, hexamers, and even an unusual heterotrimer structure (from *Pseudomonas aeruginosa*) are found (Halliwell, 2006).

Most CATs in plants and animals are in peroxisomes, and they are indispensable for the removal of H_2O_2 generated in peroxisomes by oxidases involved in β-oxidation of fatty acids, photorespiration and purine catabolism (Schrader and Fahimi, 2004). In most bacteria, CATs are not essential for growth and survival of microbial cells under common laboratory conditions, but these enzymes play important roles in a number of environmental situations (Halliwell, 2006).

1.2.4   Ascorbate peroxidases

APx is believed to play the most essential role in scavenging ROS and protecting cells in higher plants, algae, euglena and other organisms (Baier et al., 2000). This enzyme catalyses the reduction of H_2O_2 to H_2O using ascorbate as the electron donor. Reduced ascorbate is regenerated by the action of MDA reductase or dehydroascorbate (DHA) reductase using NADPH as the electron donor (Fig. 1.3). APx enzymes are activated in the presence of ascorbate and they are inhibited by cyanide and azide which ligate to the haem group. They are also inhibited by thiol reagents which is different from other peroxidases (Shigeoka et al., 2002).

The APx family consists of at least five different isoforms including thylakoid (tAPx) and glyoxysome membrane forms (gmAPx), as well as chloroplast stromal soluble forms (sAPx), cytosolic forms (cAPx) (Yoshimura et al., 2000).

APx has a higher affinity for H_2O_2 (mM range) than CAT and it may have a more crucial role in the management of ROS during stress. Enhanced expression of APx in plants has been demonstrated during different environmental stress conditions such as ozone exposure, low temperature, high light intensity, salinity and drought (Mittler and Zilinskas, 1994, Schöner and Heinrich Krause, 1990, Tanaka et al., 1985, Wang et al., 1999, Willekens et al., 1994)
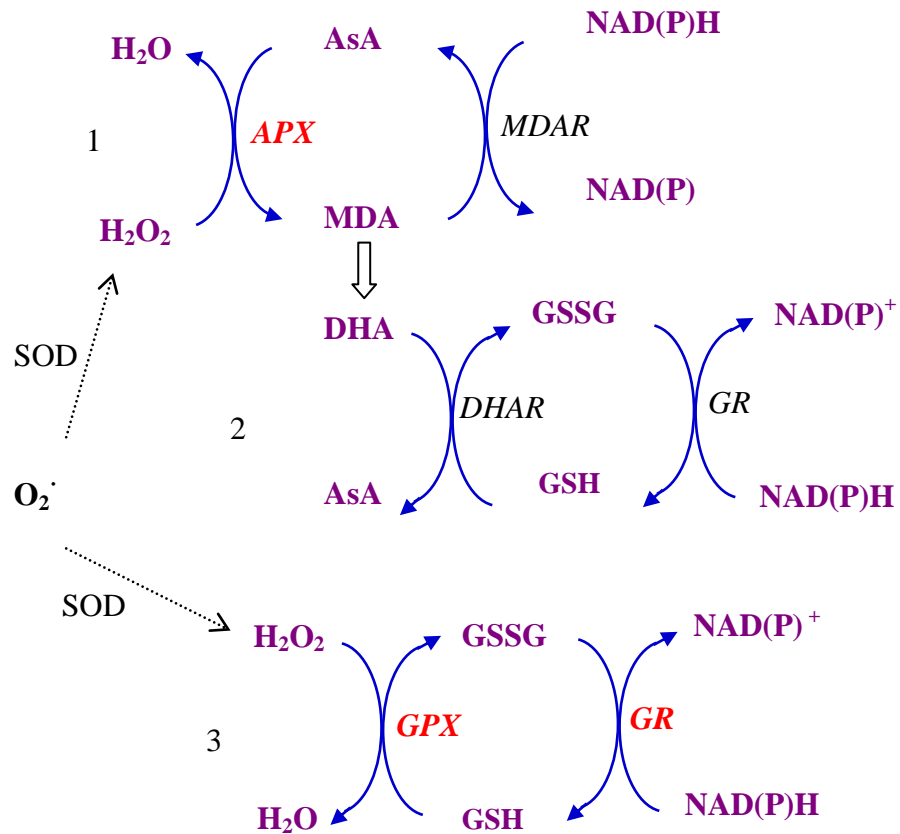
Figure 1.3. Catalytic mechanism of H_2O_2 removal by two key enzymes APX and GPX. APX reduces H_2O_2 to water at the expense of AsA oxidation (1). The oxidized AsA is then re-reduced by the action of either MDAR (1) or DHAR (2) using NAD(P)H or GSH respectively as the electron donor. The reduction of H_2O_2 to water by GPX (3) is coupled with the oxidation of the electron donor GSH. The oxidized GSH produced by either DHAR or GPX is regenerated by the action of the enzyme GR using NAD(P)H (Dalton et al., 1986)

1.2.5   Glutathione peroxidase and phospholipid hydroperoxide glutathione peroxidase (PHGPx)

GPxs comprise another family of enzymes using GSH to reduce H_2O_2, lipid hydroperoxides, and other hydroperoxides (Eshdat, 1997; Halliwell, 2006).

$H_2O_2 + 2GSH \rightarrow GSSG + 2H_2O$
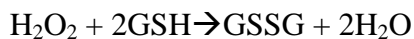
The product, oxidized glutathione (GSSG), consists of two GSH molecules linked by a disulphide bridge, and can be converted back to GSH by glutathione reductase enzymes (Fig. 1.3).

In mammals, the GPx family consists of 5 subclasses: cytosolic GPx (GPx1), gastro-intestinal GPx (GPx2), plasma GPx (GPx3), phospholipid hydroperoxide GPx (GPx4 or PHGPx) and selenium-independent epididymal GPx (GPx5) (Chu, 1994, Drevet, 2000). All mammalian GPx enzymes, with the exception of the epididymal GPx, contain the rare amino acid selenocysteine (Sec) encoded by TGA which is normally a stop codon. This amino acid is the catalytic residue of the enzyme. GPx enzymes contain selenium in place of sulphur in the Cys residue at the active site and this selenium contributes to the greater nucleophilic power of selenocysteine-containing enzymes compared with those that contain cysteine (Eshdat et al., 1997). In terms of protein structure, PHGPx is a monomer in its native conformation whereas the other GPx isoforms are homotetramers. This monomeric structure is likely to explain the difference in substrate specificity between PHGPx isozymes and the other GPx isozymes. PHGPxs can use complex lipid hydroperoxides as substrates and they prefer these over H_2O_2 (Eshdat el al., 1997).

In contrast to the large amount of published research on mammalian GPx genes and enzymes, the amount of published research on plant GPx genes and enzymes is rather limited (Herbette et al., 2002). In plants, cDNAs encoding proteins similar to animal GPxs have been identified (Depege et al., 1998, Holland et al., 1993). Plant GPx-like proteins showed highest sequence similarity to mammalian PHGPx rather than to any of the other members of the GPx family (Blokhina et al., 2003). They contained a catalytic cysteine residue instead of a selenocysteine suggesting that the plant GPx enzymes should be less active than the animal enzymes. Plant GPxs are found mainly in the cytosol, chloroplasts, mitochondria, and endoplasmic reticulum (Churin et al., 1999, Rodriguez Milla et al., 2003). They are believed to be involved in the protection of plant cells against oxidative damage, particularly via the removal of lipid hydroperoxides thus protecting cellular membranes of those organelles under environmental stresses (Blokhina et al., 2003).

1.2.6   Peroxiredoxins (Prxs)

The peroxiredoxins (Prxs) are a relatively newly-discovered family of peroxidases. The first Prx proteins were identified in yeast (Kim et al., 1988) and mammals (Kim et al., 1989). They were shown to be able to protect glutamine synthetase and DNA from oxidative damage in a thiol/Fe^{3+}/O_2 mixed function pro-oxidant system. Prxs are found in all kingdoms of life and they detoxify cytotoxic peroxides by reducing them to non-toxic products (Baier and Dietz, 1996, Chae et al., 1994a, Chae et al., 1994b, Lim et al., 1998, Storz et al., 1989).The substrate specificity of Prx enzymes

is rather broad including H_2O_2, organic hydroperoxides and peroxynitrite (Lim et al., 1993).

Different from many other enzymes, Prx proteins do not contain redox cofactors, such as heme, flavin, or metal ions, thus their reactions are robust and independent of sensitive cofactors (Dietz, 2003). The redox reactions are dependent on Cys at the active sites. The Prx family was originally divided into two categories, the 1-Cys and 2-Cys Prxs, based on the number of cysteinyl residues directly involved in catalysis. The 2-Cys Prxs was further divided into two classes called the 'typical' and 'atypical' 2-Cys Prxs (Wood et al., 2003). Details of the plant and animal Prx subclasses are summarized in Tables 1.2 and 1.3

All Prx classes contain a conserved cysteine residue at the N-terminus that is oxidized to sulfenic acid (Cys-SOH) during the catalytic reaction. This Cys is referred to as the peroxidatic Cys (Cys_P-SH) and serves as the site of oxidation by H_2O_2. Typical 2-Cys Prx form a homodimer during the catalytic reaction; oxidation of Cys_P-SH to Cys_P-SOH is followed by formation of an intermolecular disulfide bond between Cys_P and the second conserved Cys at the C-terminus of the other subunit, which is referred to as the resolving Cys (Cys_R-SH). Finally, the 2-Cys disulfide is reduced by another biothiol, such as thioredoxin (Trx), and the dimer dissociates into two regenerated monomers (Chae et al., 1999, Wood et al., 2003). Atypical 2-Cys Prxs contain one conserved Cys_P and another non-conserved Cys residue for the catalytic reaction. An intramolecular disulfide bond (between the two Cys residues of the same unit) is formed that is also reduced by Trx (Wood et al.,

2002). In 1-Cys Prxs, Cysp-SOH is reduced directly by a redox partner such as glutathione or dithiothreitol (DTT) (Wood et al., 2003). Apart from thioredoxin, the atypical 2-Cys Prxs can be reduced by glutaredoxin as well (Finkemeier et al., 2005, Rouhier et al., 2001). Fig. 1.4 summarises the catalytic cycle of 2-Cys Prx proteins.

It has recently been realized that Prxs may be the most important H_2O_2-removal enzymes in animals, bacteria, and possibly plants (Rhee et al., 2005). This is due to their low K_m for H_2O_2 (<20 μM), the large amounts of Prxs present (up to 0.8% of total soluble protein in some animal cells) and their locations in all subcellular organelles as well as in the cytosol.

Table 1.2: Prx subclasses from plants

Prx Type	Sub-group	No. of conserved Cys residues	Cell location	Reference
2-Cys Prx (typical 2-Cys)	2-Cys Prx	2	Plastid	Horling et al. (2003)
Prx Q (atypical 2-Cys)	PrxQ	2	Plastid	Lamkemeyer et al. (2006)
Type-II Prx (atypical 2-Cys)	PrxII B & C	2	Cytosol	Horling et al. (2002)
	PrxII E	2	Plastid	Horling et al. (2003)
	PrxII F	2	Mitochondria	Finkemeier et al. (2005)
	PrxII D	2	Unidentified	Dietz et al. (2006)
1-Cys Prx	1-Cys Prx	1	Nucleus Cytosol	Stacy et al. (1999)

Table 1.3. Prx subclasses from mammals (adopted from Wood et al. 2003)

Prx type	No. of conserved Cys residues	Subcellular location	No. aa	Other nomenclature
PrxI	2	Cytosol, Nucleus	199	TPx-A, NKEF A, MSP23, HBP23
PrxII	2	Cytosol,	198	TPx-B, NKEF B, Calpromotin, Torin, TSA
PrxIII	2	Mitochondrion	256	AOP 1, MER5, SP22
PrxIV	2	Cytosol, Golgi, secreted	271	AOE372, TRANK
PrxV (atypical)	2	Mitochondria, peroxisome, cytosol	214	AOEB166, PMP20, AOPP
PrxVI	1	Cytosol	224	ORF06, LTW4, AOP2

PrxSH

Catalytic
cycle

Inactivation-
Reactivation
cycle

H_2O_2
ROOH

Thioredoxin
Glutaredoxin
Glutathione

Sulfiredoxin
(ATP)

Prx-SOH

Prx-SH

H_2O_2

Prx-S-S-Prx

Prx-SO$_2$H
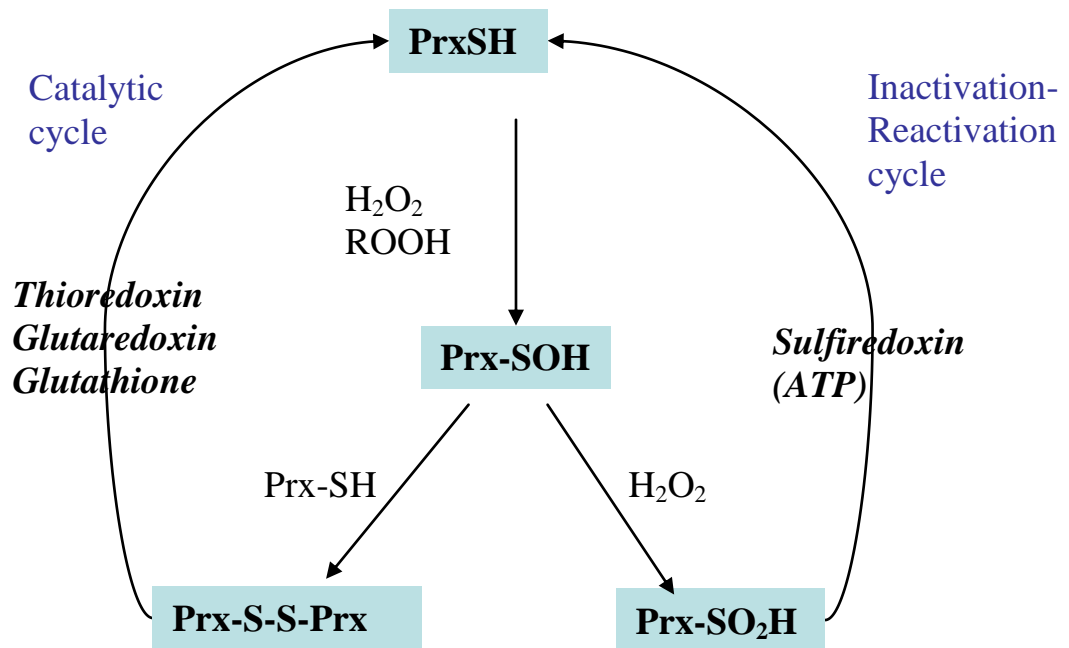
Figure 1.4. Reaction cycle of peroxiredoxins. The catalytic Cys is oxidized to
sulphenic acid (SOH). A disulphide bridge (S-S) is formed involving a
conformational switch of the protein. The disulphide-oxidized Prx is regenerated by
electron donors such as Trx, Grx, and glutathione. Over-oxidation of the catalytic
Cys to the sulphinic acid form (SO$_2$H) withdraws Prx from the cycle. This is thought
to be involved in regulatory and potentially signalling mechanisms (adapted from
Rhee et al., 2005 and Dietz et al., 2006).

1.3   Antioxidant system in the malaria parasite *Plasmodium falciparum*

1.3.1   Malaria, the disease

Malaria is caused by parasites belonging to the genus *Plasmodium*. The most important in terms of mortality and morbidity in humans is *P. falciparum*. Despite huge efforts to eliminate malaria, it remains one of the world's most serious infectious diseases (Sachs and Malaney, 2002*).*The World Health Organisation (WHO) estimates that more than 3 billion people are at risk of malaria and that between 300 and 500 million are infected causing the deaths of one to three million people annually and these numbers are increasing. Infection results in severe complications during pregnancy and most fatal cases happen in children under five (WHO, *World Malaria Report 2008*, http://www.who.int/malaria/wmr2008/, viewed 12, December, 2008).

There are a number of factors contributing to increasing mortality and morbidity from malaria. Firstly, increasing numbers of populations of *P. falciparum* are becoming resistant to traditional anti-malarial treatments. Secondly, the female *Anopheles* mosquitoes responsible for the transmission of the disease are developing resistance to the commonly-used insecticides. Thirdly, displacement of people living in areas of high transmission by natural or man-made changes in the environment is creating new breeding grounds for mosquitoes (Kumar, 2004). Of these, the most important is the development by the malaria parasite of resistance to cheap and

effective drugs such as chloroquine and sulphadoxine/pyrimethamine (Greenwood and Mutabingwa, 2002). The absence of any effective vaccine against the malaria parasite and the rapid emergence of resistance to the currently administered drugs are making the situation progressively worse. Thus, there is an urgent need to develop new strategies to combat the disease.

1.3.2   The malaria parasite

Malaria is caused by members of the genus *Plasmodium*. *Plasmodium* species belong to the phylum Apicomplexa, a group of highly derived protists. There are more than 120 different *Plasmodium* species that infect vertebrates including reptiles, birds and mammals (Sherman, 1998). Of these, only four infect humans, i.e. *P. falciparum, P. vivax*, *P. ovale* and *P. malariae*. Among these, *P. vivax* is responsible for most of the malaria cases. However, *P. falciparum* is the culprit causing the most severe form of the disease and is responsible for the most malaria related deaths (Sherman, 1998).

Unlike many other major infectious diseases such as AIDS and tuberculosis where the pathogens are transmitted directly from human to human, malaria is transmitted via an insect vector, the female *Anopheles* mosquito. *Plasmodium* parasites undergo various stages of sexual and asexual development during their complex life cycle as summarized in Fig. 1.5 (Sherman, 1998).
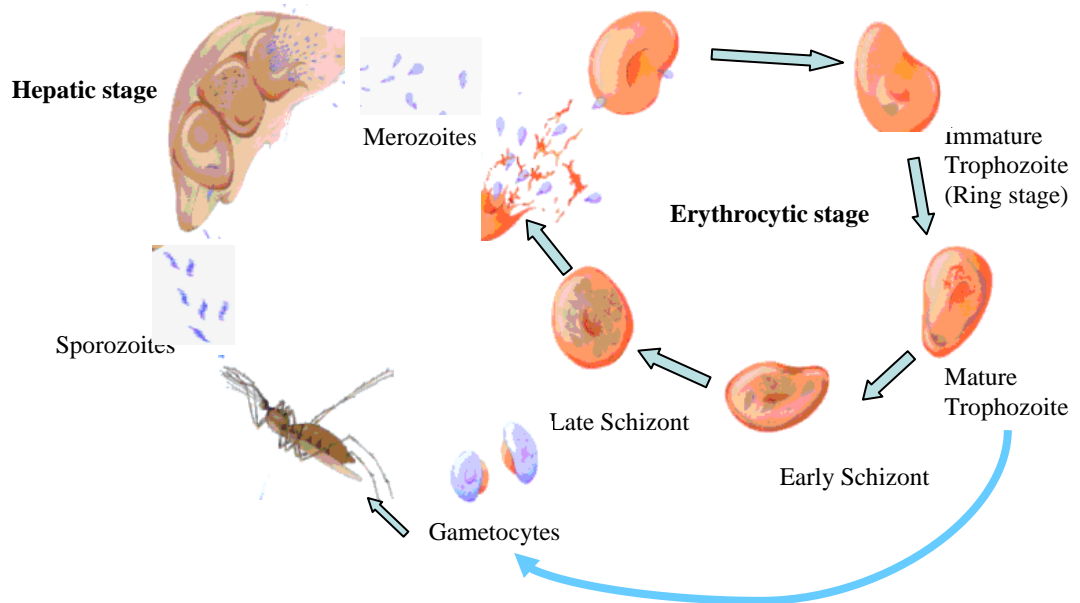
Figure 1.5. The life cycle of the parasite *Plasmodium falciparum* (adapted from Sherman, 1998). When a parasite-infected mosquito feeds on a human, it injects the parasites in their sporozoite form. These travel to the liver, where they develop through several stages, finally producing merozoites which invade and multiply (ring stage) via the trophozoite stage, in red blood cells (RBCs). The ring stage trophozoites mature into schizonts, which rupture the RBCs releasing merozoites. Some parasites differentiate into sexual erythrocytic stages (gametocytes). Clinical features of malaria, including fever and chills, anaemia and cerebral malaria are all associated with infected red blood cells, and most current drugs target this stage of the life cycle. When another mosquito bites the infected human, it takes up blood containing gametocytes, which develop into male and female reproductive cells (gametes). These fuse in the insect's gut to form a zygote. The zygote in turn develops into the ookinete, which crosses the wall of the gut and forms a sporozoite-filled oocyst. When the oocyst bursts, the sporozoites move to the mosquito's salivary glands, and the process begins again.

The entire genome sequence of *P. falciparum* (strain 3D7) was completed in 2002 (Gardner et al., 2002). The genome of *P. falciparum* is composed of 22.8 Mb of nuclear DNA distributed amongst 14 linear chromosomes and two extra-chromosomal genomes – a linear 6 kb mitochondrial genome (Vaidya et al., 1989) and a circular 35 kb apicoplast genome (Wilson et al., 1996). The entire genome contains ca. 5,300 predicted open reading frames (ORFs) with more than 60% showing no homology to any known protein (Gardner et al., 2002).

1.3.3   The malaria parasite and oxidative stress

The malaria parasite is exposed to oxidative stress at various stages of its life cycle (Atamna and Ginsburg, 1993). A major contributor to this stress is the host's immune response (Schirmer et al., 1987). Another is the oxygen-rich environment of the host's red blood cells (RBCs) in which the parasite resides during various life-cycle stages (Fig. 1.5) and the release of iron as the highly-metabolically active parasite degrades the host's haemoglobin (Schirmer et al., 1987). Degradation of the haemoglobin in the host's RBCs is central to the oxidative stress suffered by the parasite (Loria et al., 1999). Following entry into the host's RBCs, the malaria parasite uses the host's hemoglobin as a source of amino acids for its own replication. This degradation of haemoglobin in an acidic food vacuole results in the production of toxic free haem (ferri/ferroprotoporphyrin IX; FP) and ROS. Most of the haem forms an inert pigmented polymer inside the vacuole (Loria et al., 1999, Zhang et al., 1992). However, a small amount escapes the neutralization process and becomes a major iron-based catalyst for the formation of oxidants such as

superoxide and hydrogen peroxide (Guerra et al., 2005). These highly reactive

oxidants form covalent bonds with proteins, nucleic acids and lipids, thus impairing

their function.

1.3.4 The antioxidant defense system of P. falciparum

P. falciparum defends itself against oxidative stress with enzymes that convert ROS

to less reactive molecules and with enzymes that repair damaged cellular molecules

(Becker et al., 2005). Without these enzymes, the genome and the lipid membranes

of *P. falciparum* would be vulnerable to oxidative damage. Many of these key

enzymes have been identified.

1.3.4.1 Superoxide dismustase and catalase

P. falciparum has two distinct SOD genes, one encoding a cytosolic FeSOD (SOD-

1) (Gratepanche et al., 2002) and the other encoding a mitochondrial MnSOD (SOD-

2) (Sienkiewicz et al., 2004). Thus the *P. falciparum* SOD family is different from

that of more highly derived eukaryotes that possess cytosolic Cu/ZnSODs and

mitochondrial MnSOD, (Müller, 2004). The *SOD-1* gene was expressed during the

erythrocytic stage of the life cycle of *P. falciparum*. A related gene has been found

in *P.ovale, P.malariae* and *P.vivax* as well as in other apicomplexan (*Toxoplasma*

gondii) and trypanosomatid (*Leishmania* and *Trypanosoma*) parasites (Bécuwe et

al., 1996, Dive et al., 2003, Meshnick et al., 1983). There is evidence that *P.*

falciparum can take up large amounts of Cu/Zn-SOD from the erythrocytes of its

host and that host erythrocyte SOD activity decreases upon infection with the

parasite (Fairfield et al., 1988, 1983, Stocker et al., 1985)

No gene coding for catalase has so far been identified in the *P. falciparum* genome

and it is doubtful that it exists (Clarebout et al., 1998). The absence of this enzyme

has also been reported in trypanosomatids (Boveris et al., 1980).

1.3.4.2   The glutathione system

Glutathione (GSH)

GSH is found in all types of cells (Sies, 1986). It plays a vital role in the antioxidant

defense systems of cells through the maintenance of the redox status of protein

sulphydryl groups and the reduction of H_2O_2 and lipid hydroperoxides (Nickel et al.,

2006). It is also a substrate for antioxidant enzymes such as glutathione-S-

transferases (GSTs) and GPxs. Oxidized glutathione (GSSG) is reduced to GSH by

the enzyme glutathione reductase (GR) using NADPH as the electron donor (Becker

et al., 2003b).

Glutathione reductase (GR)

GR is the enzyme responsible for recycling oxidized glutathione. GR is a member of

a group of enzymes known as flavo-disulphide oxidoreductases which also contains

thioredoxin reductases (Williams, 1992). *P. falciparum* GR (*Pf*GR) has been

functionally characterised in both its native form (isolated from malaria parasites)

and its recombinant form (Bohme et al., 2000, Farber et al., 1998, 1996, Gilberger et

al., 2000, Krauth-Siegel et al., 1996). The three-dimensional structure of *Pf*GR has

been solved (Sarma et al., 2003) and *Pf*GR inhibitors are under study for the

development of new anti-malarial drugs (Table 1.4) (Biot et al., 2003, Buchholz et

al., 2007).

Glutathione S-transferase (GST)

GST serves in the intracellular detoxification of toxic chemicals which can

contribute to drug clearance in parasites (Bruns et al., 1999). *P. falciparum* has only

one *Pf*GST isoenzyme and this protein has low sequence similarity to any GST from

other organisms (less than 37%) (Becker et al., 2004). The enzyme represents 1–

10% of the parasite's cellular protein and it exhibits peroxidase activity with H_2O_2,

cumene hydroperoxide and *tert*-butyl hydroperoxide using glutathione as its

reducing partner (Harwaldt et al., 2002, Liebau et al., 2002). In solution, *Pf*GST is a

homotetramer which dissociates into dimers in the presence of glutathione. A *Pf*GST

crystal structure (solved at 1.9 Å) shows that this enzyme does not belong to any

known GST class, thus representing a novel GST isoform (Fritz-Wolf et al., 2003).

This distinct structure makes *Pf*GST an interesting target for developing antimalarial

drugs and a number of *Pf*GST inhibitors are under study for drug development

(Table 1.4) (Hiller et al., 2006).

Table 1.4: Summary of the antioxidant enzymes in *P. falciparum* (adopted from Rahlfs and Becker, 2006)

Name	Abbreviation used in this study	Other nomenclature	Subcellular location	Biochemical function	Three-dimensional structural data and identified inhibitors
2-Cys peroxiredoxin 1	*Pf*Prx-1	*Pf* Tpx1 *Pf* Px-1 *Pf* Trx-Px1	Cytosol	Detoxify peroxides and peroxynitrite with *Pf*Trx1, *Pf*Grx-1, *Pf*Plrx1 as reductants	Not available
2-Cys peroxiredoxin 2	*Pf*Prx-2	*Pf* Tpx2 *Pf* Px-2 *Pf* Trx-Px2	Mitochondrion	Detoxify ROS and with *Pf*Trx2 and to a lesser extent *Pf*Trx1 as reductants	A truncated version of *Pf*Prx-2 has its structure solved at 1.8 Å resolution (Boucher et al., 2006)
1-Cys peroxiredoxin	*Pf* 1-Cys Prx	*Pf*-1-Cys Tpx *Pf* 1-Cys Px *Pf* 1-Cys Trx Px *Pf* Px-1	Cytosol	Detoxify peroxides with glutathione, dithiothreitol and to a lesser extent *Pf*Trx1 as reductants	Not available
Antioxidant protein	*Pf*AOP		Apicoplast (predicted)	Detoxify peroxides with *Pf*Trx1, *Pf*Grx-1, *Pf*Plrx1 as reductants	Structure solved at 1.8 Å resolution (Sarma et al. 2005)
GPx-like peroxiredoxin	*Pf* GPx-like Prx	*Pf*GPx *Pf*TPx$_{GL}$	Apicoplast (predicted)	Detoxify peroxides using *Pf*Trx1 as reductant	Not available

Table 1.4   continued

Name	Abbreviation used in this study	Other nomenclature	Subcellular location	Biochemical function	Three-dimensional structural data and identified inhibitors
Thioredoxin reductase	*Pf*TrxR		Cytosol	Reduce oxidized Trx Shown to be a validated drug target by gene knock out (Komaki-Yasuda et al., 2003)	Structural data is not available but inhibitors have been tested for drug development (Andricopulo et al., 2006) Inhibitors: Mannich bases, various inhibitors
Glutathione reductase	*Pf*GR			Reduce oxidized glutathione	Structure solved at 2.6 Å resolution (Sarma et al. 2003) Inhibitors: methylene blue, isoalloxanzine derivatives, dimerization inhibitors
Glutathione-S transferase	*Pf*GST		Cytosol	Peroxidase activity	Structure solved at 1.9 Å (Fritz-Wolf et al., 2003) Inhibitors: S-hexylglutathione; various inhibitors
Superoxide dismutase 1	*Pf*Fe-SOD	*Pf*SOD1	Cytosol	Carry out the dismutation of superoxide ions	Not available
Superoxide dismutase 2	*Pf*Mn-SOD	*Pf*SOD2	Mitochondrion	Carry out the dismutation of superoxide ions	Not available

Abbreviations: *Pf: Plasmodium falciparum*, Trx1: cytosolic thioreodoxin, Trx2: mitochondrial thioredoxin, Grx: glutaredoxin; Plrx1: cytosolic plasmoredoxin;

Glutathione peroxidase (GPx)

A genuine GPx has not been found in *P. falciparum* (Kawazu et al., 2008). A *P. falciparum* enzyme that was described as GPx (Gamain et al., 1996) was subsequently re-classified as a thioredoxin peroxidase or peroxiredoxin because it preferred thioredoxin (Trx) over glutathione as its reducing partner (Sztajer et al., 2001). As a GPx homologue it had the characteristic selenocysteine replaced by a cysteine making its reactions with hydroperoxides and GSH three orders of magnitude slower than the typical seleno-GPx enzymes found in mammals (Sztajer et al., 2001).

1.3.4.3   The thioredoxin system

The thioredoxin superfamily

P. falciparum possesses a number of proteins belonging to the thioredoxin superfamily. These are characterized by a specific active site CXXC motif with a typical thioredoxin fold in their structure (Rahlfs et al., 2003). Members of this family include thioredoxin (Trx), glutaredoxin and other thioredoxin-like proteins (Müller, 2004). These proteins interact with a variety of redox active proteins such as peroxidases and low-molecular weight thiols (Fernandes and Holmgren, 2004). They are reduced by thioredoxin reductases (TrxR) and are involved in antioxidant defense, ribonucleotide reduction and reduction of peroxidases and transcription factors (Rahlfs et al., 2002).

Genes encoding five Trx and Trx-like proteins have been identified in the *P.*

falciparum genome, and the proteins act as redox-active molecules donating

electrons through the Trx system to peroxidases (Kanzok et al., 2000, Nickel et al.,

2006). In addition to Trx proteins, *P. falciparum* possesses a typical glutaredoxin

(Grx) as well as Grx-like proteins (Deponte et al., 2005, Rahlfs et al., 2001).

Furthermore, there is a redox active protein with homology to Trx proteins, named

plasmoredoxin (Plrx). This protein is only found in malaria parasites (Becker et al.,

2003a, Nickel et al., 2006).

Thioredoxin reductase (TrxR)

The *P. falciparum* TrxR (*Pf*TrxR) is homodimeric with a subunit molecular mass of

55 kDa (Becker et al., 1996, Müller et al., 1995). *Pf*TrxR is a flavin-dependent TrxR

that reduces Trx via a Cys-Cys pair located near the C-terminal end of the enzyme

(Gilberger et al., 1998, 1997). In this respect, *Pf*TrxR differs significantly from its

human counterpart which bears a Cys-Sec redox pair at the same position (Arscott et

al., 1997, Williams et al., 2000). *Pf*TrxR has been shown to be involved in

antioxidant defense and redox regulation in the parasite (Becker et al., 2000) and

gene knock-out studies have shown that it is essential for the survival of the parasite

during the erythrocytic stage (Krnajski et al., 2002). No crystal structure for *Pf*TrxR

has yet been solved, however, known inhibitors are currently being studied for the

purpose of developing new anti-malarial drug therapies (Table 1.4) (Andricopulo et

al., 2006, Becker et al., 2004).

Peroxiredoxins

CAT and GPx proteins seem to be absent from *P. falciparum.*Therefore, Prx proteins appear to be the main antioxidant enzymes responsible for peroxide-detoxification (Hofmann et al., 2002, McGonigle et al., 1998, Schröder and Ponting, 1998). Apart from the GPx-like Prx mentioned above, four other Prx proteins that act in different subcellular compartments have been described in *P. falciparum*. The four proteins are *Pf*Prx-1 and *Pf*Prx-2 which are both typical 2-Cys peroxiredoxins, a 1-Cys Prx and an antioxidant protein (AOP) (Nickel et al., 2006). AOP is a 1-Cys Prx.

***Pf*Prx-1** is the best studied Prx from *P. falciparum*. This enzyme has been localized to the cytosol and it is constitutively expressed throughout the erythrocytic stage of the life cycle of the parasite suggesting that it plays a housekeeping role including defense against oxidative stress (Kawazu et al., 2003, Yano et al., 2005). The characteristics of *Pf*Prx-1 are described in detail in Chapter 3.

***Pf*Prx-2** has a calculated molecular mass of 25.8 kDa for it monomer, slightly larger than *Pf*Prx-1, and the two proteins share 51.8% sequence identity (Rahlfs and Becker, 2001). The *Pf*Prx-2 protein is located in the parasite's mitochondria and it is expressed in both the trophozoite and schizont stages (Yano *et al.* 2005). Full details of *Pf*Prx-2 characteristics are in Chapter 4.

The **Pf 1-Cys Prx** gene was first isolated and expressed in *E. coli* by Kawazu *et al.* (2000). The deduced *Pf* 1-Cys Prx amino acid sequence contained the conserved Cys47 and showed greatest similarity to its homologue in *Onchocerca volvulus* (50.5% identity) and rice (41.7% identity). The *Pf* 1-Cys Prx protein obtained from expression in *E. coli* appeared as a 25 kDa band in a Western blot using mouse anti-*Pf* 1-Cys Prx antiserum (Kawazu et al., 2001, Krnajski et al., 2001).The protein demonstrated *in vitro* thiol peroxidase activity to remove H_2O_2 and protect DNA against oxidative damage by ROS in the presence of either DTT or glutathione (Kawazu et al., 2001, Krnajski et al., 2001, Rahlfs et al., 2002). *Pf* 1-Cys Prx showed increased expression during the trophozoite and early schizont stages in the parasite cytoplasm (Yano et al., 2005) and was suggested to bind to ferriprotoporphyrin (FP), slowing the rate of GSH-mediated FP degradation and consequent iron generation, protecting proteins against iron-derived ROS (Kawazu et al., 2005).

PfAOP is a *P. falciparum* antioxidant protein (*Pf*AOP) with a high level of sequence similarity to human Prx V (Table 1.3) (Nickel et al., 2005). *Pf*AOP gene transcription is high throughout the erythrocytic stage of the life cycle of *P. falciparum* and the protein is predicted to be targeted to the apicoplast by signal peptide prediction programs (Nickel et al., 2005). *Pf*AOP was the first glutaredoxin-dependent peroxidase reported in *P. falciparum* and it could also use thioredoxin and to a lesser extent plasmoredoxin as electron donors (Nickel et al., 2006). It preferred *tert*-butylhydroperoxide and phosphatidylcholine hydroperoxide as substrates compared to H_2O_2 and cumene hydroperoxide (Nickel et al., 2006). The crystal structure of *Pf*AOP has been solved and the enzyme has been shown to act

on the basis of a 1-Cys Prx mechanism (Sarma et al., 2005). Without the putative

targeting sequence, recombinant *Pf*AOP formed non-covalently bound dimers

(Sarma et al., 2005).

1.3.5   Existing anti-malarial drugs and the need for new drug development

To control malaria, there are three major strategies: (i) vaccination, (ii) mosquito

control and (iii) anti-malaria drugs (Tilley et al., 2006). The use of antimalarial

drugs is currently the main line of defence (Buchholz et al., 2007). The traditional

drugs used for the treatment of malaria are quinolines such as chloroquine, quinine,

mefloquine and primaquine and antifolates such as Fansidar (sulfadoxine

pyrimethamine) (Meshnick et al., 1996, Tilley et al., 2006). However, there is a

rising problem with the resistance of malaria parasites to existing drugs. For

example, most of the *P. falciparum* strains have now become resistant to

chloroquine and some have developed resistance to mefloquine, antifolates and

halofantrine (Macreadie et al., 2000, Wernsdorfer, 1994). The development of new

drugs is therefore urgently needed.

1.3.6   The parasite antioxidant system, a potential target for antimalarial drug design

As stated in section 1.3.3, *P. falciparum* is subjected to oxidative stress throughout

its life cycle. Thus, to survive, the parasite needs an efficient antioxidant system.

This system could be a good target for antimalarial drug design.

The thioredoxin-dependent peroxiredoxin-linked antioxidant system has been proven to play a crucial function in defence against oxidative stress in *P. falciparum* as the disruption of the gene encoding thioredoxin reductase, is fatal for the parasites (Krnajski *et al.*, 2002). Given that the parasites lack catalase and glutathione peroxidase, it has been suggested that peroxiredoxins are key antioxidants that guarantee parasite survival under enhanced oxidative stress (Müller, 2004). However, *Pf*Prx-1 was shown to be important but not essential to the survival of the parasites under oxidative and nitrosative stresses (Komaki-Yasuda *et al.*, 2003). Similar approaches using reverse genetics to knock-out one or more genes of the Prx family should be done in future studies in order to elucidate the precise roles of the Prx system thus helping to gain a better understanding of the mechanisms that the parasites have employed to protect themselves against fatal oxidative damage. The results from such studies will elucidate the potential of *Pf*Prxs as drug targets.

There are many current anti-malarial drugs working on the susceptibility of the malaria parasite to oxidative stress such as endoperoxides of which the most effective are artemisinin and its derivatives (Borstnik et al., 2002). These drugs are widely used in China and South East Asia where resistance to the common antimalarial drugs is significant (Hien and White, 1993). These endoperoxides are believed to kill malarial parasites via burdening the parasites with substantial oxidative stress while having no significant effect on the human host. For example, artemisinin having an endoperoxide bridge (C-O-O-C) can produce oxygen free radicals and/or even turn itself into a free radical by a reaction with hemoproteins and alkylate the malaria proteins in infected erythrocytes. However with regards to the mechanism of artemisinin, there is also an alternative hypothesis proposing that

artemisinins inhibit *Pf*SERCA, the *P. falciparum* Sarco(endo)plasmic reticulum Ca^{2+}ATPase, and thus possibly act by perturbing calcium homeostasis of the intracellular parasite (Eckstein-Ludwig et al., 2003).No reaction between artemisinin and any protein of the intact erythrocytes was detected (Meshnick et al., 1996). The disadvantage of endoperoxides is their short half-life. Thus, effective levels are retained for relatively short periods (Meshnick et al., 1996).

Differences between the antioxidant system of the malaria parasite and its human host with respect to substrate specificity, mechanism of action and efficacy are the subject of many current studies with the aim of developing drugs that overstrain the malaria antioxidant system but are safe for the human host. Three members of the antioxidant enzyme family of *P. falciparum*; i.e *Pf*TrxR, *Pf*GR and *Pf*GST have been identified as potential targets for antimalarial drug development and their inhibitors are under study (Table 1.4). However, the Prxs, one of the most important antioxidant enzyme families, have not been investigated sufficiently with regards to their kinetic properties, physiological functions and crystal structures (Deponte et al., 2007). To date it is unknown whether *Plasmodium* Prxs are involved in signal transduction (Hofmann *et al*., 2002, Wood *et al*., 2003a), or whether they possess a kind of chaperone activity (Jang *et al*., 2004) as demonstrated for Prx from other organisms. Apart from functional studies, three out of five Prx proteins have their crystal structures unsolved (i.e *Pf*Prx-1, 1-Cys Prx and GPx-like Prx). Further studies of these aspects would improve our understanding of the role of this enzyme family and help demonstrate whether the Prx proteins of *P. falciparum* are suitable candidates for antimalarial drug development.

1.4 Aims and significance of the project

This project was comprised of three main parts:

Part A: Mixed culture of wheat (*Triticum aestivum* L.) with white lupin (*Lupinus albus* L.) improves the growth and phosphorus nutrition of the wheat

This part of the project aimed to study the effect of the mixed-culture of wheat with white lupin on the availability of soil-P to the wheat and to investigate the mechanisms by which white lupin mobilises P from unavailable soil-P pools making it more available to the wheat crop partner. The outcome of this part improved our understanding in the areas of P mobilisation from the soil by crop plants and may lead to the development of mixed culture or intercropping systems that are more efficient in mobilising and using P from soil, thus reducing the need for P fertiliser application. Reduction in phosphate fertiliser use would cut down farmer costs and lessen the risk of pollution and eutrophication of water resources.

The work in this part has been published as:

Cu STT, Hutson J, Schuller KA (2005) Mixed culture of wheat (*Triticum aestivum* L.) with white lupin (*Lupinus albus* L.) improves the growth and phosphorus nutrition of the wheat. *Plant and Soil*, 272(1-2): 143-151

Part B: Cloning, expression, purification, crystallization and preliminary X-ray analysis of *Pf*Prx-1, a cytosolic 2-Cys peroxiredoxin from *Plasmodium falciparum*

This part of the project aimed to investigate the factors influencing the oligomeric states of the *P. falciparum Pf*Prx-1 protein recombinantly expressed in *E. coli* and to investigate its three dimensional structure using X-ray crystallography. The outcomes of this part provided a better understanding in the areas of transitioning of the oligomeric states of *Pf*Prx-1 in particular and of the typical 2-Cys peroxidoxin family in general. The structural data obtained from the X-ray crystallography study provides a background for further studies in order to obtain the full details of *Pf*Prx-1 3D structure which will facilitate the development of the *Pf*Prx-1 protein as a novel antimalarial drug target.

Part C: Expression, purification and characterisation of a recombinant *Plasmodium falciparum* mitochondrial 2-Cys peroxiredoxin in *Pichia pastoris*.

This part of the project aimed to develop a *Pichia pastoris* expression system for the *P. falciparum Pf*Prx-2 protein and to investigate the oligomeric states and the sub-cellular localization of the recombinant *Pf*Prx-2 protein. In particular, the aim was to determine whether *P. pastoris* could translate this *P. falciparum* A+T rich sequence and recognise the mitochondrial targeting sequence of the protein. The outcomes of this part firstly provided a better understanding of the transitions between the oligomeric states of the *Pf*Prx-2 protein. Secondly, the success in developing an

expression and purification system for *Pf*Prx-2 in *P. pastoris* should open the way

for further investigations of this enzyme both *in vivo* and *in vitro*. This will facilitate

the development of the *Pf*Prx-2 protein as a novel antimalarial drug target.

References

Afanas'ev, I. B. (1991) Generation of active oxygen species by superoxide ion: the formation of HO, HO$_2$, HO$^-$, and H$_2$O$_2$. *Superoxide Ion: Chemistry and Biological Implications.* Boca Raton, FL, CRC Press.

Alscher R.G., Erturk N., Heath L.S. (2002) Role of superoxide dismutases (SODs) in controlling oxidative stress in plants, *Journal of Experimental Botany*, 53, 1331–1341

Andricopulo, A. D., Akoachere, M. B., Krogh, R., Nickel, C., McLeish, M. J., Kenyon, G. L., Arscott, L. D., Williams, C. H., Davioud-Charvet, J., E. & Becker, a. K. (2006) Specific inhibitors of *Plasmodium falciparum* thioredoxin reductase as potential antimalarial agents. *Bioorganic and Medicinal Chemistry Letters,* 16**,** 2283-2292.

Apel, K. & Hirt, H. (2004) Reactive oxygen species: metabolism, oxidative stress, and signal transduction. *Annual Review of Plant Biology,* 55**,** 373-399.

Arscott, L. D., Gromer, S., Schirmer, R. H., Becker, K. & Williams, C. H. (1997) The mechanism of thioredoxin reductase from human placenta is similar to the mechanisms of lipoamide dehydrogenase and glutathione reductase and is distinct from the mechanism of thioredoxin reductase from *Escherichia coli*. *Proceedings of the National Academy of Science of USA,* 94**,** 3621-3626.

Asada, K. (1992) Ascorbate peroxidase-a hydrogen peroxide-scavenging enzyme in plants. *Physiologia Plantarum,* 85**,** 235-241.

Atamna, H. & Ginsburg, H. (1993) Origin of reactive oxygen species in erythrocytes infected with *Plasmodium falciparum. Molecular and Biochemical Parasitology,* 61, 231-241.

Babior, B. M. (1999) NADPH oxidase: an update. *Blood,* 93, 1464-1476.

Baier, M. & Dietz, K. J. (1996) Primary structure and expression of plant homologues of animal and fungal thioredoxin-dependent peroxide reductases and bacterial alkyl hydroperoxide reductases. *Plant Molecular Biology,* 31, 553-564.

Baier, M., Noctor, G., Foyer, C. H. & Dietz, K. J. (2000) Antisense suppression of 2-cysteine peroxiredoxin in Arabidopsis specifically enhances the activities and expression of enzymes associated with ascorbate metabolism but not glutathione metabolism. *Plant Physiology,* 124, 823-832.

Becker, K., Gromer, S., Schirmer, R. H. & Muller, S. (2000) Thioredoxin reductase as a pathophysiological factor and drug target. *European Journal of Biochemistry,* 267, 6118-6125.

Becker, K., Kanzok, S. M., Iozef, R., Fischer, M., Schirmer, R. H. & Rahlfs, S. (2003a) Plasmoredoxin, a novel redox-activie protein unique for malarial parasites. *European Journal of Biochemistry,* 270, 1057-1064.

Becker, K., Koncarevic, S. & Hunt, H. H. (2005) Oxidative stress and antioxidant defense in malarial parasites. In Sherman, I. W. (Ed.) *Molecular Approaches to Malaria.* Washington, D.C., ASM Press.

Becker, K., Muller, S., Keese, M. A., Walter, R. D. & Schirmer, R. H. (1996) A

glutathione reductase-like flavoenzyme of the malaria parasite *Plasmodium*

falciparum: structural considerations based on the DNA sequence. *Biochemical*

Society Transactions, 24**,** 67-72.

Becker, K., Rahlfs, S., Nickel, C. & Schirmer, R. H. (2003b) Glutathione-function

and metabolism in the malarial parasite *Plasmodium falciparum. Journal of*

Biological Chemistry, 348**,** 551-566.

Becker, K., Tilley, L., Vennerstrom, J. L., Roberts, D., Rogerson, F. & Ginsburg, H.

(2004) Oxidative stress in malaria parasite-infected erythrocytes: host-parasite

interactions. *International Journal for Parasitology,* 34**,** 163-189.

Biot, C., Dessolin, J., Grellier, P. & Davioud-Charvet, E. (2003) Double-drug

development against antioxidant enzymes from *Plasmodium falciparum. Redox*

Report, 8**,** 280-283.

Blokhina, O., Virolainen, E. & Fagerstedt, K. V. (2003) Antioxidants, Oxidative

Damage and Oxygen Deprivation Stress: a Review *Annals of Botany,* 91**,** 179-

194.

Bohme, C. C., Arscott, L. D., Becker, K., Schirmer, R. H. & Williams, C. H. (2000)

Kinetic characterization of glutathione reductase from the malarial parasite

Plasmodium falciparum comparison with the human enzyme. *Journal of*

Biological Chemistry, 275**,** 37317-37323.

Borstnik, K., Paik, I., Shapiro, T. A. & Posner, G. H. (2002) Antimalarial

chemotherapeutic peroxides: artemisinin, yingzhaosu A and related compounds.

International Journal for Parasitology, 32**,** 1661-1667.

Boucher, I.W., McMillan, P.J., Gabrielsen,M., Akerman, S.E., Brannigan, J.A., *et al.* (2006) Structural and biochemical characterization of a mitochondrial peroxiredoxin from *Plasmodium falciparum*, *Molecular Microbiology*, 61, 948–959

Boveris, A. (1984) Determination of the production of superoxide radicals and hydrogen peroxide in mitochondria. *Methods in Enzymology,* 105**,** 429-435

Boveris, A., Sies, H., Martino, E. E., Docampo, R., Turrens, J. F. & Stoppani, A. O. (1980) Deficient metabolic utilization of hydrogen peroxide in *Trypanosoma cruzi*. *Biochemical Journal,* 188**,** 643-648.

Bowler, C., Montagu, M. V. & Inze, D. (1992) Superoxide dismutase and stress tolerance. *Annual Review of Plant Biology,* 43**,** 83-116.

Breen, A. P. & Murphy, J. A. (1995) Reactions of oxyl radicals with DNA. *Free Radical Biology and Medicine,* 18**,** 1033-1077.

Briviba, K., Klotz, L. O. & Sies, H. (1997) Toxic and signaling effects of photochemically or chemically generated singlet oxygen in biological systems. *Biological chemistry Hoppe-Seyler,* 378**,** 1259-1265.

Bruns, C. M., Hubatsch, I., Ridderström, M., Mannervik, B. & Tainer, J. A. (1999) Human glutathione transferase A4-4 crystal structures and mutagenesis reveal the basis of high catalytic efficiency with toxic lipid peroxidation products. *Journal of Molecular Biology,* 288**,** 427-439.

Buchholz, K., Mailu, M., Schirmer, H. & Becker, K. (2007) Structure-Based Drug Development Against Malaria. *Frontiers in Drug Design & Discovery: Structure-Based Drug Design in the 21st Century,,* 3**,** 225-255.

Chae, H. Z., Chung, S. J. & Rhee, S. G. (1994a) Thioredoxin-dependent peroxide

reductase from yeast. *Journal of Biological Chemistry,* 269**,** 27670-27678.

Chae, H. Z., Kang, S. W. & Rhee, S. G. (1999) Isoforms of mammalian

peroxiredoxin that reduce peroxides in presence of thioredoxin. *Methods in*

Enzymology, 300**,** 219-226.

Chae, H. Z., Robison, K., Poole, L. B., Church, G., Storz, G. & Rhee, S. G. (1994b)

Cloning and sequencing of thiol-specific antioxidant from mammalian brain:

alkyl hydroperoxide reductase and thiol-specific antioxidant define a large

family of antioxidant enzymes. *Proceedings of the National Academy of*

Sciences of USA, 91.

Chu, F. F. (1994) The human glutathione peroxidase genes GPX2, GPX3, and

GPX4 map to chromosomes 14, 5, and 19, respectively. *Cytogenetics and Cell*

Genetics, 66**,** 96-98.

Churin, Y., Schilling, S. & Börner, T. (1999) A gene family encoding glutathione

peroxidase homologues in Hordeum vulgare (barley). *FEBS Letters,* 459**,** 33-38.

Clarebout, G., Slomianny, C., Delcourt, P., Leu, B., Masset, A., Camus, D. & Dive,

D. (1998) Status of Plasmodium falciparum towards catalase *British Journal of*

Haematology, 103**,** 52-59.

Cowey, C. B., Bell, J. G., Knox, D., Fraser, a. and Youngson, A. 1985, Lipids and

lipid antioxidant systems in developing eggs of salmon (*Salmo salar*), *Lipids*,

20, 567-572

D'Autréaux, B. & Toledano, M. B. (2007) ROS as signalling molecules:

mechanisms that generate specificity in ROS homeostasis. *Nature Reviews*

Molecular Cell Biology, 8**,** 813-824.

Dalton, T. P., Shertzer, H. G. & Puga, A. (1999) Regulation of gene expression by reactive oxygen. *Annual Review of Pharmacology and Toxicology,* 39**,** 67-101.

Dalton, D.A., Russell, S.A., Hanus, F.J., Pascoe, G.A., Evans, H.J. (1986) Enzymatic reactions of ascorbate and glutathione that prevent peroxide damage in soybean root nodules. *Proceedings of the National Academy of Sciences USA*, 83, 3811-3815

Del Rio, L. A. & Donaldson, R. P. (1995) Production of superoxide radicals in glyoxysomal membranes from castor bean endosperm. *Plant Physiology,* 146**,** 283-287.

Depege, N., Drevet, J. & Boyer, N. (1998) Molecular cloning and characterization of tomato cDNAs encoding glutathione peroxidase-like proteins. *European Journal of Biochemistry,* 253**,** 445-451.

Deponte, M., Becker, K. & Rahlfs, S. (2005) *Plasmodium falciparum* glutaredoxin-like proteins. *Biological Chemistry,* 386**,** 33-40.

Deponte, M., Rahlfs, S. & Becker, K. (2007) Peroxiredoxin systems of protozoal parasites. IN Flohé, L. & Harris, J. R. (Eds.) *Peroxiredoxin Systems: Structure and Functions.* Springer Netherlands.

Dietz, K. J., Jacob, S., Oelze, M. L., Laxa, M., Tognetti, V., de Miranda, S. M. N., Baier, M. & Finkemeier, I. (2006) The function of peroxiredoxins in plant organelle redox metabolism. *Journal of Experimental Botany,* 57**,** 1697-1709.

Dive, D., Gratepanche, S., Yera, H., Becuwe, P., Daher, W., Delplace, P., Odberg-Ferragut, C., Capron, M. & Khalife, J. (2003) Superoxide dismutase in *Plasmodium*: a current survey. *Redox Report,* 8**,** 265-267.

Drevet, J. R. (2000) *Glutathione peroxidases expression in the mammalian epididymis and vas deferens,* Andrology, Litografia Brandolini, Chieti, Italy.

Elstner, E. F. & Osswald, W. (1993) Mechanisms of oxygen activation during plant stress. *Proceedings of the Royal Society of Edinburgh-B-Biological Sciences,* 102**,** 131-154.

Eshdat, Y., Holland, D., Faltin, Z. & Ben-Hayyim, G. (1997) Plant glutathione peroxidases. *Physiologia Plantarum,* 100**,** 234-240.

Eckstein-Ludwig, U., Webb, R.J., van Goethem ,I.D., East, J.M., Lee, A.G., *et al.* (2003) Artemisinins target the SERCA of *Plasmodium falciparum*, *Nature*, 424, 957–961.

Fairfield, A. S., Abosch, A., Ranz, A., Eaton, J. W. & Meshnick, S. R. (1988) Oxidant defense enzymes of *Plasmodium falciparum. Molecular and Biochemical Parasitology,* 30**,** 77-82.

Fairfield, A. S., Meshnick, S. R. & Eaton, J. W. (1983) Malaria parasites adopt host cell superoxide dismutase. *Science,* 221**,** 764-766.

Farber, P. M., Arscott, L. D., Williams, C. H., Becker, K. & Schirmer, R. H. (1998) Recombinant *Plasmodium falciparum* glutathione reductase is inhibited by the antimalarial dye methylene blue. *FEBS Letters,* 422**,** 311-314.

Farber, P. M., Becker, K., Muller, S., Schirmer, R. H. & Franklin, R. M. (1996) Molecular Cloning and Characterization of a Putative Glutathione Reductase Gene, the *Pf*GR2 Gene, from *Plasmodium falciparum. European Journal of Biochemistry,* 239**,** 655-661.

Feierabend, J. (2005) Catalases in plants: molecular and functional properties and role in stress defence. IN Smirnoff, N. (Ed.) *Antioxidants and Reactive Oxygen Species in Plants.* Oxford, Blackwell Publishing.

Fernandes, A. P. & Holmgren, A. (2004) Glutaredoxins: glutathione-dependent redox enzymes with functions far beyond a simple thioredoxin backup system. *Antioxidants and Redox Signaling,* 6**,** 63-74.

Finkemeier, I., Goodman, M., Lamkemeyer, P., Kandlbinder, A., Sweetlove, L. J. & Dietz, K.-J. (2005) The mitochondrial type II peroxiredoxin F is essential for redox homeostasis and root growth of *Arabidopsis thaliana* under stress. *Journal of Biological Chemistry,* 280**,** 12168-12180.

Fridovich, I. (1978) The biology of oxygen radicals. *Science,* 201**,** 875-880.

Fridovich, I. (1995) Superoxide radical and SODs. Annu al Reviews of *Biochemistry*, 64,97–112

Fritz-Wolf, K., Becker, A., Rahlfs, S., Harwaldt, P., Schirmer, R. H., Kabsch, W. & Becker, K. (2003) X-ray structure of glutathione S-transferase from the malarial parasite *Plasmodium falciparum. Proceedings of the National Academy of Sciences,* 100**,** 13821-13826.

Furbank, R. T. & Badger, M. R. (1983) Oxygen exchange associated with electron transport and photophosphorylation in spinach thylakoids. *Biochimica et Biophysica Acta,* 723**,** 400-409.

Gamain, B., Langsley, G., Fourmaux, M. N., Touzel, J. P., Camus, D., Dive, D. & Slomianny, C. (1996) Molecular characterization of the glutathione peroxidase gene of the human malaria parasite *Plasmodium falciparum. Molecular and Biochemical Parasitology,* 78**,** 237-248.

Gardner, M. J., Hall, N., Fung, E., White, O., Beriman, M., Hyman, R. W., Carlton, J. M., Pain, A., Nelson, K. E. & al., e. (2002) The genome sequence of the human malaria parasite *Plasmodium falciparum*. *Nature,* 419**,** 498-511.

Gebicki, J. M. & Bielski, B. H. J. (1981) Comparison of the capacities of the perhydroxyl and the superoxide radicals to initiate chain oxidation of linoleic acid. *Journal of American Chemistry Society,* 103**,** 7020-7022.

Gilberger, T. W., Bergmann, B., Walter, R. D. & Müller, S. (1998) The role of the C-terminus for catalysis of the large thioredoxin reductase from *Plasmodium falciparum. FEBS Letters,* 425**,** 407-410.

Gilberger, T. W., Schirmer, R. H., Walter, R. D. & Müller, S. (2000) Deletion of the parasite-specific insertions and mutation of the catalytic triad in glutathione reductase from chloroquine-sensitive *Plasmodium falciparum* 3D7. *Molecular & Biochemical Parasitology,* 107**,** 169-179.

Gilberger, T. W., Walter, R. D. & Muller, S. (1997) Identification and characterization of the functional amino acids at the active site of the large thioredoxin reductase from *Plasmodium falciparum. Journal of Biological Chemistry,* 272**,** 29584-29589.

Gille, G. & Sigler, K. (1995) Oxidative stress and living cells. *Folia Microbiologica,* 40**,** 131-152.

Gniazdowska, A., Mikulska, M. & Rychter, A. M. (1998) Growth, nitrate uptake and respiration rate in bean roots under phosphate deficiency. *Biologia Plantarum,* 41**,** 217-226.

Gniazdowska, A., Szal, B. & Rychter, A. M. (1999) The effect of phosphate

deficiency on membrane phospholipid composition of bean (*Phaseolus vulgaris*

L.) roots. *Acta Physiologiae Plantarum,* 21**,** 263-270.

Gratepanche, S., Ménage, S., Touati, D., Wintjens, R., Delplace, P., Fontecave, M.,

Masset, A., Camus, D. & Dive, D. (2002) Biochemical and electron

paramagnetic resonance study of the iron superoxide dismutase from

Plasmodium falciparum. Molecular & Biochemical Parasitology, 120**,** 237-246.

Greenwood, B. & Mutabingwa, T. (2002) Malaria in 2002. *Nature,* 415**,** 670-672.

Grossman, A., Takahashi, H. (2001). Macronutrient utilisation by photosynthetic

eukaryotes and the fabric of interactions. *Annual Reviews of Plant Physiology*

and Plant Molecular Biology, 52, 163–210.

Guerra, R., Shaw, C., Christian, B., Fox, G., Noyola-Martinez, J., Stevens, M., Garg,

N. & Gustin, M. (2005) Oxidative stress genes in *Plasmodium falciparum* as

indicated by temporal gene expression. *Critical Assessment of Microarray Data*

Analysis Conference.

Gunes, A., Pilbeam, D. J. & Inal, A. (2009) Effect of arsenic–phosphorus interaction

on arsenic-induced oxidative stress in chickpea plants. *Plant and Soil,* 314**,** 211-

220.

Halliwell, B. (2006), Reactive species and antioxidants. Redox biology is a

fundamental theme of aerobic life, *Plant Physiology*, 141, 312-322.

Halliwell, B. and Gutteridge J.M.C. (2006) Free Radicals in Biology and Medicine,

Ed 4. Clarendon Press, Oxford

Harwaldt, P., Rahlfs, S. & Becker, K. (2002) Glutathione S-transferase of the

malarial parasite *Plasmodium falciparum*: characterization of a potential drug

target. *Biological Chemistry,* 383**,** 821-830.

Herbette, S., Lenne, C., Leblanc, N., Julien, J. L., Drevet, J. R. & Roeckel-Drevet, P.

(2002) Two GPx-like proteins from *Lycopersicon esculentum* and *Helianthus*

annuus are antioxidant enzymes with phospholipid hydroperoxide glutathione

peroxidase and thioredoxin peroxidase activities. *European Journal of*

Biochemistry, 269**,** 2414-2420.

Hien, T. T. & White, N. J. (1993) Qinghaosu. *Lancet,* 341**,** 603-608.

Hiller, N., Fritz-Wolf, K., Deponte, M., Wende, W., Zimmermann, H. & Becker, K.

(2006) *Plasmodium falciparum* glutathione S-transferase—Structural and

mechanistic studies on ligand binding and enzyme inhibition. *Protein Science,*

15**,** 281-289.

Hofmann, B., Hecht, H.-J. & Flohé, L. (2002) Peroxiredoxins. *Biological Chemistry,*

383**,** 347-364.

Holland, D., Ben-Hayyim, G., Faltin, Z., Camoin, L., Strosberg, A. D. & Eshdat, Y.

(1993) Molecular characterization of salt-stress-associated protein in citrus:

protein and cDNA sequence homology to mammalian glutathione peroxidases.

Plant Molecular Biology, 21**,** 923-927.

Horling, F., König, J. & Dietz, K.-J. (2002) Type II peroxiredoxin C, a member of

the peroxiredoxin family of *Arabidopsis thaliana*: its expression and activity in

comparison with other peroxiredoxins. *Plant Physiology and Biochemistry,* 40**,**

491-499.

Horling, F., Lamkemeyer, P., König, J., Finkemeier, I. & al., e. (2003) Divergent

light-, ascorbate- and oxidative stress-depedent regulation of expression of the

peroxiredoxin gene family in *Arabidopsis*. *Plant Physiology,* 131**,** 317-325.

Jang, H. H., Lee, K. O., Chi, Y. H., Jung, B. G., Park, S. K., Park, J. H. Lee, J. R.,

Lee, S. S., Moon, J. C et al. (2004), Two enzymes in one: Two yeast

peroxiredoxins display oxidative stress-dependent switching from a peroxidase

to a molecular chaperone function, *Cell*, 117, 625-635

Juszczuk, I., Malusà, E. & Rychter, A. M. (2001a) Oxidative stress during phosphate

deficiency in roots of bean plants (Phaseolus vulgaris L.). Journal of plant

physiology, 158, 1299-1305.

Juszczuk, I. M., Wagner, A. M. & Rychter, A. M. (2001b) Regulation of alternative

oxidase activity during phosphate deficiency in bean roots (*Phaseolus vulgaris*).

Physiologia Plantarum, 113**,** 185-192.

Kanzok, S. M., Schirmer, R. H., Turbachova, I., Iozef, R. & Becker, K. (2000) The

thioredoxin system of the malaria parasite *Plasmodium falciparum:* Glutathione

reduction revisited. *Journal of Biological Chemistry,* 275**,** 40180-40186.

Kawazu, S., Ikenoue, N., Takemae, H., Komaki-Yasuda, K. & Kano, S. (2005)

Roles of 1-Cys peroxiredoxin in haem detoxification in the human malaria

parasite *Plasmodium falciparum. FEBS Journal,* 272**,** 1784-1791.

Kawazu, S., Komaki-Yasuda, K., Oku, H. & Kano, S. (2008) Peroxiredoxins in

malaria parasites: Parasitologic aspects. *Parasitology International,* 57**,** 1-7.

Kawazu, S., Komaki, K., Tsuji, N., Kawai, S., Ikenoue, N., Hatabu, T., Ishikawa, H., Matsumoto, Y., Himeno , K. & Kano, S. (2001) Molecular characterization of a 2-Cys peroxiredoxin from the human malaria parasite *Plasmodium falciparum*. *Molecular and Biochemical Parasitology,* 116**,** 73-79.

Kawazu, S., Nozaki, T., Tsuboi, T., Nakano, Y., Komaki-Yasuda, K., Ikenoue, N., Torii, M. & Kano, S. (2003) Expression profiles of peroxiredoxin proteins of the rodent malaria parasite *Plasmodium yoelii*. *International Journal for Parasitology,* 33**,** 1455-1461.

Kawazu, S., Tsuji, N., Hatabu, Kawai, S., Matsumoto, Y. & Kano, S. (2000) Molecular cloning and characterization of a peroxiredoxin from the human malaria parasite *Plasmodium falciparum*. *Molecular and Biochemical Parasitology,* 109**,** 165-169.

Kim, I. H., Kim, K. & Rhee, S. G. (1989) Induction of an antioxidant protein of *Saccharomyces cerevisiae* by O_2, Fe_3^+, or β-mercaptoethanol. *Proceedings of the National Academy of Sciences,* 86**,** 6018-6022.

Kim, K., Kim, I. H., Lee, K. Y., Rhee, S. G. & Stadtman, E. R. (1988) The isolation and purification of a specific protector Q protein which inhibits enzyme inactivation by a thiol/Fe(III)/O2 mixed-function oxidation system. *Journal of Biological Chemistry,* 263**,** 4704– 4711.

Krauth-Siegel, R. L., Muller, J. G., Lottspeich, F. & Schirmer, R. H. (1996) Glutathione reductase and glutamate dehydrogenase of *Plasmodium falciparum*, the causative agent of tropical malaria. *European Journal of Biochemistry,* 235**,** 345-350.

Krnajski, Z., Gilbeger, T. W., Walter, R. D., Cowman, R. F. & Müller, S. (2002) Thioredoxin reductase is essential for the survival of *Plasmodium falciparum* erythrocytic stage. *Journal of Biological Chemistry,* 277**,** 25970-25975.

Krnajski, Z., Gilberger, T. W., Walter, R. D. & Müller, S. (2001) The malaria parasite *Plasmodium falciparum* possesses a functional thioredoxin system. *Molecular and Biochemical Parasitology,* 112**,** 219-228.

Kumar, N. (2004) Malaria: a grand challenge. *International Journal for Parasitology,* 34**,** 3-4.

Lamkemeyer, P., Laxa, M., Collin, V., Li, W., Finkemeier, I., Schottler, M. A., Holtkamp, V., Tognetti, V. B., Issakidis-Bourguet, E. & Kandlbinder, A. (2006) Peroxiredoxin Q of Arabidopsis thaliana is attached to the thylakoids and functions in context of photosynthesis. *The Plant Journal,* 45**,** 968-981.

Liebau, E., Bergmann, B., Campbell, A. M., Teesdale-Spittle, P., Brophy, P. M., Lüersen, K. & Walter, R. D. (2002) The glutathione S-transferase from *Plasmodium falciparum. Molecular & Biochemical Parasitology,* 124**,** 85-90.

Lim, M. J., Chae, H. Z., Rhee, S. G., Yu, D.-Y., Lee, K.-K. & Yeom, Y. I. (1998) The type II peroxiredoxin gene family of the mouse: molecular structure, experssion and evolution. *Gene,* 216**,** 197-205.

Lim, Y. S., Cha, M. K., Kim, H. K., Uhm, T. B., Park, J. W., Kim, K. & Kim, I. H. (1993) Removals of hydrogen peroxide and hydroxyl radical by thiol-specific antioxidant protein as a possible role in vivo. *Biochemical and Biophysical Research Communications,* 192**,** 273-280.

Logan, B.N., Demmig-Adams B., Rosenstiel T.N., Adams, W.W. (1999). Effect of nitrogen limitation on foliar antioxidants in relationship to other metabolic characteristics. *Planta* 209, 213–220.

Loria, P., Miller, S., Folley, M. & Tilley, L. (1999) Inhibition of the peroxidative degradation of haem as the basis of action of chloroquine and other quinoline antimalarials. *Biochemical Journal,* 339**,** 363-370.

Macreadie, I., Ginsburg, H., Sirawaraporn, W. & Tilley, L. (2000) Antimalarial drug development and new targets. *Parasitology Today,* 16**,** 438-443.

Mahalingam, R. & Fedoroff, N. (2003), Stress response, cell death andsignalling: The many faces of reactive oxygen species. *Physiologia Plantarum*, 119, 56–68

Maiorino, M., Aumann, K. D., Brigelius-Flohé, R., Doria, D., van Den Heuvel, J., McCarthy, J., Roveri, A., Ursini, F. & Flohé, L. (1995) Probing the presumed catalytic triad of selenium-containing peroxidases by mutational analysis of phospholipid hydroperoxide glutathione peroxidase (PHGPx). *Biological chemistry Hoppe-Seyler,* 376**,** 651-660.

Malusà, E., Laurenti, E., Juszczuk, I., Ferrari, R. P. & Rychter, A. M. (2002) Free radical production in roots of *Phaseolus vulgaris* subjected to phosphate deficiency stress. *Plant Physiology et Biochemistry,* 40**,** 963-967.

Malusà, E. & Rychter, A. (1997) *Effect of phosphate deficiency on isoenzyme pattern of hydrogen peroxide scavenging enzymes in bean roots,* Bologna, Patron.

McGonigle, S., Dalton, J. P. & James, E. R. (1998) Peroxiredoxins: a new antioxidant family. *Parasitology Today,* 14**,** 139-145.

Meshnick, S. R., Taylor, T. E. & Kamchonwongpaisan, S. (1996) Artemisinin and the antimalarial endoperoxides: from herbal remedy to targeted chemotherapy. *Microbiological Reviews,* 60**,** 301-315.

Meshnick, S. R., Trang, N., Kitchener, K., Cerami, A. & Eaton, J. W. (1983) Iron-containing superoxide dismutases in trypanosomatids. IN Cohen, G. & Greenwald, R. (Eds.) *Oxy Radicals and their Scavenger Systems: Molecular Aspects.* New York, Elsevier.

Mikulska, M., Bomsel, J. L. & Rychter, A. M. (1998) The influence of phosphate deficiency on photosynthesis, respiration and adenine nucleotide pool in bean leaves. *Photosynthetica,* 35**,** 79-88.

Miller, L. H., Baruch, D. I., Marsh, K. & Doumbo, O. K. (2002) The pathogenic basis of malaria. *Nature,* 417**,** 673-679.

Mittler, R. (2002) Oxidative stress, antioxidants and stress tolerance. *Trends in Plant Science,* 7**,** 405-410.

Mittler, R., Vanderauwera, S., Gollery, M. & van Breusegem, F. (2004) Reactive oxygen gene network of plants. *Trends in Plant Science,* 9**,** 490-498.

Mittler, R. & Zilinskas, B. A. (1991) Purification and characterization of pea cytosolic ascorbate peroxidase 1. *Plant Physiology,* 97**,** 962-968.

Mittler, R. & Zilinskas, B. A. (1994) Regulation of pea cytosolic ascorbate peroxidase and other antioxidant enzymes during the progression of drought stress and following recovery from drought. *The Plant Journal,* 5**,** 397-405.

Müller, S. (2004) Redox and antioxidant systems of the malarial parasite *Plasmodium falciparum. Molecular Microbiology,* 53**,** 1291-1305.

Müller, S., Becker, K., Bergmann, B., Schirmer, R. H. & Walter, R. D. (1995)
Plasmodium falciparum glutathione reductase exhibits sequence similarities
with the human host enzyme in the core structure but differs at the ligand-
binding sites. *Molecular & Biochemical Parasitology,* 74**,** 11-18.

Navari-Izzo, F., Quartacci, M. F. & Sgherri, C. L. M. (1996) Superoxide production
in relation to dehydration and rehydration. *Biochemical Society Transactions,*
24**,** 447–450.

Neill, S., Desikan, R., Hancock, J. (2002), Hydrogen peroxide signaling. *Current
Opinion in Plant Biology*, 5, 388–395.

Nickel, C., Rahlfs, S., Deponte, M., Koncarevic, S. & Becker, K. (2006)
Thioredoxin networks in the malarial parasite *Plasmodium falciparum.*
Antioxidants and Redox Signaling, 8**,** 1227-1239.

Nickel, C., Trujillo, M., Rahlfs, S., Deponte, M., Radi, R. & Becker, K. (2005)
Plasmodium falciparum 2-Cys peroxiredoxin reacts with plasmoredoxin and
peroxynitrite. *Biological Chemistry,* 386**,** 1129-1136.

Ogawa, K., Kanematsu, S. & Asada, K. (1997) Generation of superoxide anion and
localization of Cu,Zn-superoxide dismutase in the vascular tissue of spinach
hypocotyls: their association with lignification. *Plant and Cell Physiology,* 38**,**
1118-1126.

Olliaro, P. L. & Goldberg, D. E. (1995) The *Plasmodium* digestive vacuole:
metabolic headquarters and choice drug target. *Parasitology Today,* 11**,** 294-
297.

Price, A. H., Taylor, A., Ripley, S. J., Griffiths, A., Trewavas, A. J. & Knight, M. R. (1994) Oxidative signals in tobacco increase cytosolic calcium. *Plant Cell,* 6**,** 1301-1310.

Rahlfs, S. & Becker, K. (2006) Interference with redox-active enzymes as a basis for the design of antimalarial drugs. *Mini Reviews of Medicinal Chemistry*, 6: 163–176.

Rahlfs, S. & Becker, K. (2001) Thioredoxin peroxidases of the malarial parasite *Plasmodium falciparum. European Journal of Biochemistry,* 268**,** 1404-1409.

Rahlfs, S., Fischer, M. & Becker, K. (2001) *Plasmodium falciparum* possesses a classical glutaredoxin and a second, glutaredoxin-like protein with a PICOT homology domain. *Journal of Biological Chemistry,* 276**,** 37133-37140.

Rahlfs, S., Nickel, C., Deponte, M., Schirmer, R. H. & Becker, K. (2003) *Plasmodium falciparum* thioredoxins and glutaredoxins as central players in redox metabolism. *Redox Report,* 8**,** 246-250.

Rahlfs, S., Schirmer, R. H. & Becker, K. (2002) The thioredoxin system of *Plasmodium falciparum* and other parasites. *Cellular and Molecular Life Sciences,* 59**,** 1024-1041.

Rhee, S. G., Kang, S. W., Jeong, W., Chang, T.-S., Yang, K.-S. & Woo, H. A. (2005) Intracellular messenger function of hydrogen peroxide and its regulation by peroxiredoxins. *Current Opinion in Cell Biology,* 17**,** 183-189.

Rodriguez Milla, M. A., Maurer, A., Rodriguez Huete, A. & Gustafson, J. P. (2003) Glutathione peroxidase genes in *Arabidopsis* are ubiquitous and regulated by abiotic stresses through diverse signalling pathways. *The Plant Journal,* 36**,** 602.

Rouhier, N., Gelhaye, E., Sautiere, P. E., Brun, A., Laurent, P., Tagu, D., Gerard, J., de Fay, E., Meyer, Y. & Jacquot, J. P. (2001) Isolation and characterization of a new peroxiredoxin from poplar sieve tubes that uses either glutaredoxin or thioredoxin as a proton donor. *Plant Physiology,* 127**,** 1299-1309.

Sachs, J. & Malaney, P. (2002) The economic and social burden of malaria. *Nature,* 415**,** 680-685.

Sarma, G. N., Nickel, C., Rahlfs, S., Fischer, M., Becker, K. & and Karplus, P. A. (2005) Crystal structure of a novel *Plasmodium falciparum* 1-Cys peroxiredoxin. *Journal of Molecular Biology,* 346**,** 1021-1034.

Sarma, G. N., Savvides, S. N., Becker, K., Schirmer, M., Schirmer, R. H. & Karplus, P. A. (2003) Glutathione reductase of the malarial parasite *Plasmodium falciparum*: Crystal structure and inhibitor development. *Journal of Molecular Biology,* 328**,** 893-907.

Schrader, M. and Fahimi, H.D. (2004) Mammalian peroxisomes and reactive oxygen species. *Histochem Cell Biol*, 122: 383–393

Schirmer, R. H., Schöllhammer, T., Eisenbrand, G. & Krauth-Siegel, R. L. (1987) Oxidative stress as a defense mechanism against parasitic infections. *Free Radical Research Communications,* 3**,** 3-12.

Schöner, S. & Heinrich Krause, G. (1990) Protective systems against active oxygen species in spinach: response to cold acclimation in excess light. *Planta,* 180**,** 383-389.

Schröder , E. & Ponting, C. P. (1998) Evidence that peroxiredoxins are novel members of the thioredoxin fold superfamily. *Protein Science,* 7**,** 2465 - 2468.

Sherman, I. W. (1998) *Malaria: Parasite Biology, Pathogenesis and Protection*, Blackwell Publishing.

Shigeoka, S., Ishikawa, T., Tamoi, M., Miyagawa, Y., Takeda, T., Yabuta, Y. & Yoshimura, K. (2002) Regulation and function of ascorbate peroxidase isoenzymes. *Journal of Experimental Botany,* 53**,** 1305-1319.

Sienkiewicz, N., Daher, W., Dive, D., Wrenger, C., Viscogliosi, E., Wintjens, R., Jouin, H., Capron, M., Müller, S. & Khalife, J. (2004) Identification of a mitochondrial superoxide dismutase with an unusual targeting sequence in *Plasmodium falciparum. Molecular and Biochemical Parasitology,* 137**,** 121-132.

Sies, H. (1986) Biochemistry of oxidative stress. *Angewandte Chemie International Edition in English,* 25.

Sies, H. (1991) Oxidative stress: from basic research to clinical application. *American Journal of Medicine,* 91**,** 31S-38S.

Stacy, R. A. P., Nordeng, T. W., Culianez-Macia, F. A. & Aalen, R. B. (1999) The dormancy-related peroxiredoxin anti-oxidant, PER1, is localized to the nucleus of barley embryo and aleurone cells. *Plant Journal,* 19**,** 1-8.

Stadtman, E. R. (1992) Protein oxidation and aging. *Science,* 257**,** 1220-1224.

Stocker, R., Hunt, N. H., Buffinton, G. D., Weidemann, M. J., Lewis-Hughes, P. H. & Clark, I. A. (1985) Oxidative stress and protective mechanisms in erythrocytes in relation to *Plasmodium vinckei* load. *Proceedings of the National Academy of Sciences,* 82**,** 548-551.

Storz, G., Jacobson, F. S., Tartaglia, L. A., Morgan, R. W., Silveira, L. A. & Ames, B. N. (1989) An alkyl hydroperoxide reductase induced by oxidative stress in *Salmonella typhimurium* and *Escherichia coli*: Genetic characterization and cloning of *ahp*. *Journal of Bacteriology,* 171**,** 2049-2055.

Sztajer, H., Gamain, B., Aumann, K.-D., Slomianny, C., Becker, K., Brigelius-Flohé, R. & Flohé, L. (2001) The putative glutathione peroxidase gene of *Plasmodim falciparum* codes for a thioredoxin peroxidase. *Journal of Biological Chemistry,* 276**,** 7397-7403.

Takahashi, M. A. & Asada, K. (1983) Superoxide anion permeability of phospholipid membranes and chloroplast thylakoids. *Archives of Biochemistry and Biophysics,* 226**,** 558.

Tanaka, K., Suda, Y., Kondo, N. & Sugahara, K. (1985) O_3 tolerance and the ascorbate-dependent H_2O_2 decomposing system in chloroplasts. *Plant and Cell Physiology,* 26**,** 1425-1431.

Tewari, R.K., Kumar, P., Tewari, N., Srivastava, S.& Sharma, P.N. (2004). Macronutrient deficiencies and differential antioxidant responsesinfluence on the activity and expression of superoxide dismutase in maize. *Plant Science*, 166, 687–694

Tilley, L., Davis, T. M. E. & Bray, P. G. (2006) Prospects for the treatment of drug-resistant malaria parasites. *Future Microbiology,* 1**,** 127-141.

Vaidya, A. B., Akella, R. & Suplick, K. (1989) Sequences similar to genes for two mitochondrial proteins and portions of ribosomal RNA in tandemly arrayed 6-kilobase-pair DNA of a malarial parasite. *Molecular and Biochemical Parasitology,* 35**,** 97-107.

Wang, J., Zhang, H. & Allen, R. D. (1999) Overexpression of an *Arabidopsis* peroxisomal ascorbate peroxidase gene in tobacco increases protection against oxidative stress. *Plant and Cell Physiology,* 40**,** 725-732.

Wernsdorfer, W. H. (1994) Epidemiology of drug resistance in malaria. *Acta Tropica,* 56**,** 143-156.

Willekens, H., Chamnongpol, S., Davey, M., Schraudner, M., Langebartels, C., van Montagu, M., Inzé, D. & van Camp, W. (1997) Catalase is a sink for H_2O_2 and is indispensable for stress defence in C_3 plants. *The EMBO Journal,* 16**,** 4806-4816.

Willekens, H., Inze´, D., van Montagu, M. a. & van Camp, W. (1995) Catalases in plants. *Molecular Breeding,* 1**,** 207–228.

Willekens, H., van Camp, W., van Montagu, M., Inze, D., Langebartels, C. & Sandermann Jr, H. (1994) Ozone, sulfur dioxide, and ultraviolet B have similar effects on mRNA accumulation of antioxidant genes in *Nicotiana plumbaginifolia* L. *Plant Physiology,* 106**,** 1007-1014.

Williams, C. H., Arscott, L. D., Muller, S., Lennon, B. W., Ludwig, M. L., Wang, P. F., Veine, D. M., Becker, K. & Schirmer, R. H. (2000) Thioredoxin reductase: two modes of catalysis have evolved. *European Journal of Biochemistry,* 267**,** 6110-6117.

Williams Jr, C. H. (1992) Lipoamide dehydrogenase, glutathione reductase, thioredoxin reductase, and mercuric ion reductase—a family of flavoenzyme transhydrogenases. IN Müller, F. (Ed.) *Chemistry and Biochemistry of Flavoenzymes.* Boca Raton, FL, CRC Press.

Wilson, R. J. M., Denny, P. W., Preiser, P. R., Rangachari, K., Roberts, K., Roy, A., Whyte, A., Strath, M., Moore, D. J., Moore, P. W. & Williamson, D. H. (1996) Complete gene map of the plastid-like DNA of the malaria parasite *Plasmodium falciparum*. *Journal of Molecular Biology,* 261**,** 155–172.

Winterbourn, C. C. & Hampton, M. B. (2008) Thiol chemistry and specificity in redox signaling. *Free Radical Biology and Medicine,* 45**,** 549-561.

Wood, Z. A., Poole, L. B., Hantgan, R. R. & Karplus, P. A. (2002) Dimers to doughnuts: redox-sensitive oligomerization of 2-cysteine peroxiredoxins. *Biochemistry,* 41**,** 5493– 5504.

Wood, Z. A., Schroder, E., Harris, J. R. & Poole, L. B. (2003) Structure, mechanism and regulation of peroxiredoxins. *Trends in Biochemical Sciences,* 28**,** 32-40.

Yano, K., Komaki-Yasuda, K., Kobayashi, T., Takemae, H., Kita, K., Kano, S. & and Kawazu, S. (2005) Expression of mRNAs and proteins for peroxiredoxins in *Plasmodium falciparum* erythrocytic stage. *Parasitology International,* 54**,** 35-41.

Yoshimura, K., Yabuta, Y., Ishikawa, T. & Shigeoka, S. (2000) Expression of spinach ascorbate peroxidase isoenzymes in response to oxidative stresses. *Plant Physiology,* 123**,** 223-234.

Zhang, F., Gosser, D. & Meshnick, S. R. (1992) Hemin-catalyzed decomposition of artemisinin (qinghaosu). *Biochemical Pharmacology,* 43**,** 1805-1809.

Chapter 2   Mixed culture of wheat (*Triticum aestivum L.*) with white lupin (*Lupinus albus* L.) improves the growth and phosphorus nutrition of the wheat

Note: The work described in this chapter has been published as: "Cu STT, Hutson J, Schuller KA (2005) Mixed culture of wheat (*Triticum aestivum* L.) with white lupin (*Lupinus albus* L.) improves the growth and phosphorus nutrition of the wheat. *Plant and Soil*, 272: 143-151". The other two authors (Dr. Kathy Schuller and Dr. John Hutson) are my principal and co-supervisors. They had supervisory roles as acknowledged in the acknowledgement section

Abstract

The aim of this study was to investigate how mixed culture of wheat (*Triticum aestivum* L.) with white lupin (*Lupinus albus* L.) improves the growth and phosphorus (P) nutrition of the wheat. Wheat and white lupin plants were grown either in mixed culture or in monoculture in soil columns containing an adequate supply of nitrogen but a limited supply of P. Mixed-culture of the wheat with the lupins increased shoot growth and shoot P uptake of the wheat by 33% and 45%, respectively, without significantly affecting the growth or P uptake of the lupins. After 6 weeks of plant growth, the soil columns were leached first with distilled water and then with 10 mM citric acid monohydrate (pH 4.0). In the initial fraction of the water leachate, the phosphate concentration for the lupin monocultures was as high as for the uncultivated soil and approximately 10-fold higher than for the wheat monocultures. In contrast, in the initial fraction of the citric acid leachate, the

phosphate concentration for the lupin monocultures was very low, approximately

only 10% of the concentration for the wheat monocultures. For the mixed cultures,

the phosphate concentrations for all fractions for both the water and the citric acid

leachates were consistently low. Thus, the lupin monocultures preferentially

depleted the citric acid-leachable soil P pool whereas the wheat monocultures

preferentially depleted the water-leachable soil P pool and the mixed cultures

depleted both pools. The lupin monocultures lowered the soil pH by 0.3 pH units

whereas the wheat monocultures raised it by 0.8 pH units and the mixed cultures

gave a soil pH intermediate between the two monocultures. Thus, the lupins in the

mixed cultures partially offset the alkalinisation of the soil caused by the wheat and

visa versa. This will be discussed in relation to the impact of soil pH on the plant

availability of soil P.

2.1 Introduction

In many agricultural systems, phosphorus (P) is the limiting nutrient for plant

growth. This is due not only to the low concentrations of P in many soils but also to

the poor plant availability of P in most soils (Hinsinger, 2001). Plants take up P as

the phosphate ions $H_2PO_4^-$ and HPO_4^{2-}. $H_2PO_4^-$ is the predominant form of P in soils

below pH 7.2 and it is also the preferred form of P taken up by the phosphate

transport proteins in plant roots (Raghothama, 1999). Phosphate becomes

unavailable to plants by reacting with soil cations to form either soluble complexes

or insoluble precipitates. In acid soils, the most important cations are Fe^{3+} and Al^{3+}

whereas in alkaline soils they are Ca^{2+} and Mg^{2+}. Phosphate can also become

unavailable to plants when it adsorbs to the surfaces of various positively charged

soil particles (Hinsinger, 2001).

Many plant species have evolved adaptations to extract P from low P soils and/or

soils where P is only sparingly available to most plants. One of the most striking

adaptations is the formation of proteoid roots first described in members of the

family Proteaceae (Purnell, 1960). The proteoid roots of the Proteaceae exude a

range of organic acid anions that make soil P more available to plants either by

chelating soil cations that interact with phosphate or by displacing phosphate from

adsorption sites on positively charged soil particles (Roelofs et al., 2001). Proteoid

roots are also found in agricultural species such as white lupin. As well as exuding

organic acid anions (predominantly the citrate anion), the proteoid roots of white

lupins also release protons (Dinkelaker et al., 1989, Gardner et al., 1983, Gardner

and Boundy, 1983, Gerke et al., 1994, Keerthisinghe et al., 1998, Neumann et al.,

2000). The protons acidify the rhizosphere which in alkaline soils high in calcium

increases the availability of P by dissolving calcium phosphate complexes. Thus,

two factors contribute to the ability of white lupins to extract soil P. One is the

chelation/displacement/desorption activity of the citrate anion and the other is the

acidification of the rhizosphere caused by proton release. The importance of soil

acidification depends on the soil type. In acid soils, the ability of citrate to displace

phosphate from complexes with Fe^{3+} and Al^{3+} is more important than rhizosphere

acidification caused by proton release.

Several studies have shown that mixed culture of wheat with white lupin improves the growth and P uptake of the wheat and from which it was concluded that this is due to the ability of the lupins to mobilize P from a citric acid soluble soil P pool not normally available to wheat (Gardner and Boundy, 1983, Horst and Waschkies, 1987, Kamh et al., 1999, Marschner et al., 1986). However, these studies did not provide any direct evidence of soil P mobilization. On the other hand, other studies have simulated the effects of citrate and/or proton exudation by plant roots by extracting soils with sodium citrate and citric acid. For example, Jones and Darrah (1994) found that both sodium citrate and citric acid were capable of mobilizing P from a soil high in calcium phosphate. This study used a novel system in which plants are grown in soil columns that can be leached at the end of the plant growth period to investigate changes in soil P pools. This system provided a direct demonstration that improved growth and P uptake by wheat in mixed culture with white lupin is due to the ability of the lupins to extract P from a citric acid soluble soil P pool not normally available to wheat.

2.2 Materials and methods

2.2.1 Plant growth

Seeds of white lupin (*Lupinus albus* L. cv. Merrit) and wheat (*Triticum aestivum* L. cv. Krichauft) were pre-germinated in a 1:1 (w/w) mixture of perlite and vermiculite for four days at 25ºC. After germination, the seedlings were transferred into soil

columns containing a low-P soil. The soil columns were designed so that the soil could be leached at the end of the plant growth period (as shown in Fig. 2.1A). Each soil column consisted of a piece of PVC piping (160 mm diameter x 165 mm high) fitted with a cap at the bottom. There was a small 10 mm diameter hole in the centre of the cap. The inside of the cap had a ridged surface and this was covered with a fine wire mesh and a finer cloth filter. This prevented the plant roots from blocking the outlet and facilitated the flow of the leaching solution through the column. Each column was filled with approximately 2 kg of a low P soil (4 parts washed sand, 1 part garden soil) amended with 100 mg of a fertiliser containing 23% nitrogen as urea, 20.8% potassium as K_2SO_4 and 8.5% sulphur as SO_4^{2-}. Prior to amendment, the results for the soil analysis were as follows: texture, 1.5; gravel, 5-10%; colour, light brown; nitrate nitrogen, 4 mg kg^{-1}; ammonium nitrogen, 1 mg kg^{-1}; phosphorus, 18 mg kg^{-1}; potassium, 72 mg kg^{-1}; sulphur, 88 mg kg^{-1} and pH in H_2O 7.7. Phosphorus was determined after extracting the soil with 0.5 M $NaHCO_3$ (pH 8.5) for 16 h at 25^oC with a soil:solution ratio of 1:100. Each soil column was sown with a lupin monoculture (10 lupin plants per column), a wheat monoculture (10 wheat plants per column) or a mixed culture of 5 lupin plants plus 5 wheat plants per column. The control columns were not sown to plants but in every other way were treated the same as the columns containing plants. There were 5 replicate columns per culture condition. All columns, including the control columns, were maintained at 80% of field capacity by daily watering. The plants were grown in a glasshouse with the temperature maintained at 25°C/18°C for a 16h/8h day/night cycle. The experiment was repeated twice with similar results. Only the results of the second experiment are shown here.

2.2.2   Leaching the soil

The plants were grown in the soil columns for 6 weeks. At the end of the plant growth period, each soil column was leached with 7 L of distilled water followed by 2 L of 10 mM citric acid monohydrate (pH 4.0) at a flow rate of approximately 1.8 L h^{-1}. To obtain even flow, the upper surface of each column was covered with the eluent (distilled water or citric acid) to a depth of 5 cm and this depth was maintained for the duration of the experiment (Fig. 2.1B). The leachate from each column was collected in a number of 1L fractions and a 50 mL sample of each fraction was saved at -20°C in the dark for later analysis. To remove any traces of P, all experimental glassware was pre-soaked in 10% (v/v) sulphuric acid overnight, rinsed extensively with distilled water and then left to air dry. All plasticware used was brand new.

2.2.3   Plant and soil leachate analyses

After the soil columns had been leached with water and citric acid, the plants were harvested and separated into shoots and roots. The roots were washed with water to remove any adhering soil and then both the shoots and the roots were dried in an oven at 80°C for 24 hours. The dried shoots and roots were weighed, ground to a fine powder and then analysed for P, Fe, Mn, B, Cu, Mo, Co, Ni, Zn, Ca, Mg, Na, K, S, Al, Cd using nitric acid digestion and inductively coupled plasma spectrometry (Zarcinas et al., 1987). Nitrogen was analysed using a total combustion gas chromatograph. The phosphate concentrations in the soil leachate fractions were

determined by the method of Murphy and Riley (1962). Prior to the phosphate analyses, the leachate fractions were filtered through a 0.45 µm nylon filter. The pH values of the filtered leachate fractions were measured using a pH meter.

2.2.4   Statistical analyses

The data were analysed by one-way ANOVA followed by a Tukey's post hoc test using SPSS 11.0 software.

A

B
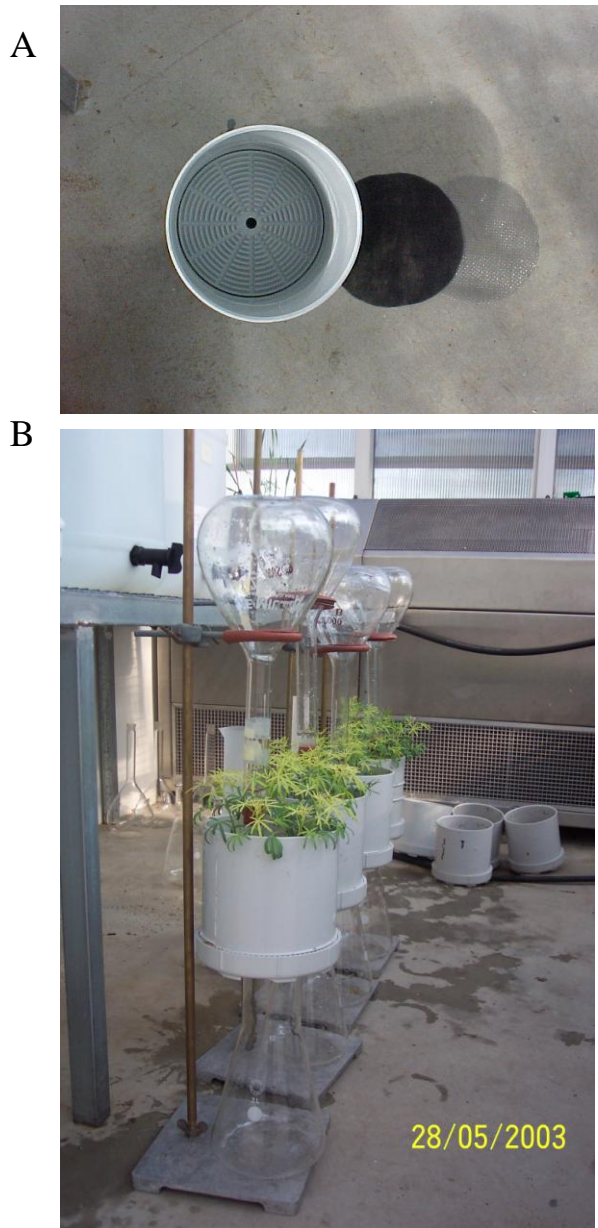
Figure 2.1. (A) Soil growth column and (B) Leaching experiment

2.3 Results

2.3.1   Plant growth and P uptake

Wheat and white lupin were grown either in mixed culture or in monoculture in soil columns filled with a low P soil. The reason for using the soil columns was so that they could be leached at the end of the plant growth period to determine the effects of plant growth on soil P pools and soil pH. The effects of mixed culture on plant growth and P uptake are shown in Table 2.1. Root dry mass, shoot P concentration (mg P kg^{-1} shoot dry mass), root P concentration (mg P kg^{-1} root dry mass) and root P content (mg P root^{-1}) were all significantly greater for the lupins than for the wheat regardless of the culture conditions. Mixed culture significantly increased the shoot growth and shoot P content (mg P shoot^{-1}) of the wheat but did not affect either of these parameters for the lupins. Thus, in the mixed cultures, as compared with the monocultures, the lupins continued to obtain an adequate supply of P but the supply of P to the wheat was enhanced. White lupins growing under low P conditions are known to exude large quantities of organic acid anions (mostly citrate) and protons from their roots and this has been shown to improve their P nutrition (Gardner et al., 1983; Dinkelaker et al., 1989; Gerke et al., 1994; Hocking et al., 1997; Keerthisinghe et al., 1998). Thus, the improved growth and P uptake of the wheat in the mixed cultures may be due to the lupins exuding citrate and protons from their roots, mobilizing P in excess of their own needs and then making the excess P available to their companion wheat plants. To investigate this further, the soil

columns the plants had been growing in were leached first with distilled water and then with 10 mM citric acid monohydrate (pH 4.0).

2.3.2   Effect of plant growth on the phosphate concentration in soil leachates

When the soil columns were leached with distilled water, the concentration of phosphate in the initial fractions for the lupin monocultures was very high whereas for the mixed cultures and the wheat monocultures it was very low (Fig. 2.2). In contrast, when the soils columns were leached with citric acid, the concentration of phosphate in the initial fractions for the lupin monocultures and the mixed cultures was very low whereas for the wheat monocultures it was very high (Fig. 2.3). These results suggest several conclusions. First, in the mixed cultures, both the water-leachable and the citric acid-leachable soil P pools became depleted presumably due to the cooperative action of the lupins and the wheat. Second, in the wheat monocultures, only the water-leachable soil P pool became depleted because of the inability of wheat to access the citric acid-leachable soil P pool. Third, the lupin monocultures appear to be accessing only the citric-acid soluble soil P pool and not the water soluble soil P pool. This third conclusion is counter-intuitive. The more likely conclusion is that when the soil columns containing the lupin monocultures were leached with water, there was already a considerable amount of citric acid in the soil due to the exudation of citric acid by the lupin roots. Thus, any phosphate in the soil was already 'mobile' (i.e. water-soluble). The observation that more phosphate in total (water-leachable + citric acid-leachable) was leached from the soil after the lupin monocultures than after the mixed cultures supports the conclusion

that white lupin is able to mobilise more P from the soil than it needs for growth thus making available P for wheat.

These results provide a clear demonstration that in the mixed cultures the lupins are making the citric acid-leachable soil P pool available to their companion wheat plants. This is most likely the explanation for the increased growth and P uptake of the wheat in the mixed cultures as compared with the wheat in the monocultures (Table 2.1). Interestingly, the concentration of phosphate in the citric acid leachates for the wheat monocultures was greater than for the uncultivated soil. In wheat monocultures, the soil pH was increase by 0.8 units. This increase in soil pH might have converted water-leachable to citric acid-leachable P leading to the high concentration of the latter. Another possibility could be mineralization of organic forms of P derived from the breakdown of dead plant material.

Table 2.1. **Effect of mixed culture on plant dry mass and P content**. Each value is the mean of 5 replicates. The means with the same letter in a row are not significantly different at $P \leq 0.05$ based on a Tukey's test.

Parameter	Wheat		Lupin	
	Mono-culture	Mixed culture	Mono-culture	Mixed culture
Shoot dry mass (mg shoot^{-1})	277a	368b	256a	236a
Root dry mass (mg root^{-1})	77a	88a	137b	127b
Shoot P concentration (mg P kg^{-1} dry mass)	1690a	1834a	2354b	2284b
Root P concentration (mg P kg^{-1} dry mass)	776a	640a	1106b	1100b
Shoot P content (mg P shoot^{-1})	0.47a	0.68b	0.60b	0.61b
Root P content (mg P root^{-1})	0.06a	0.05a	0.15b	0.14b
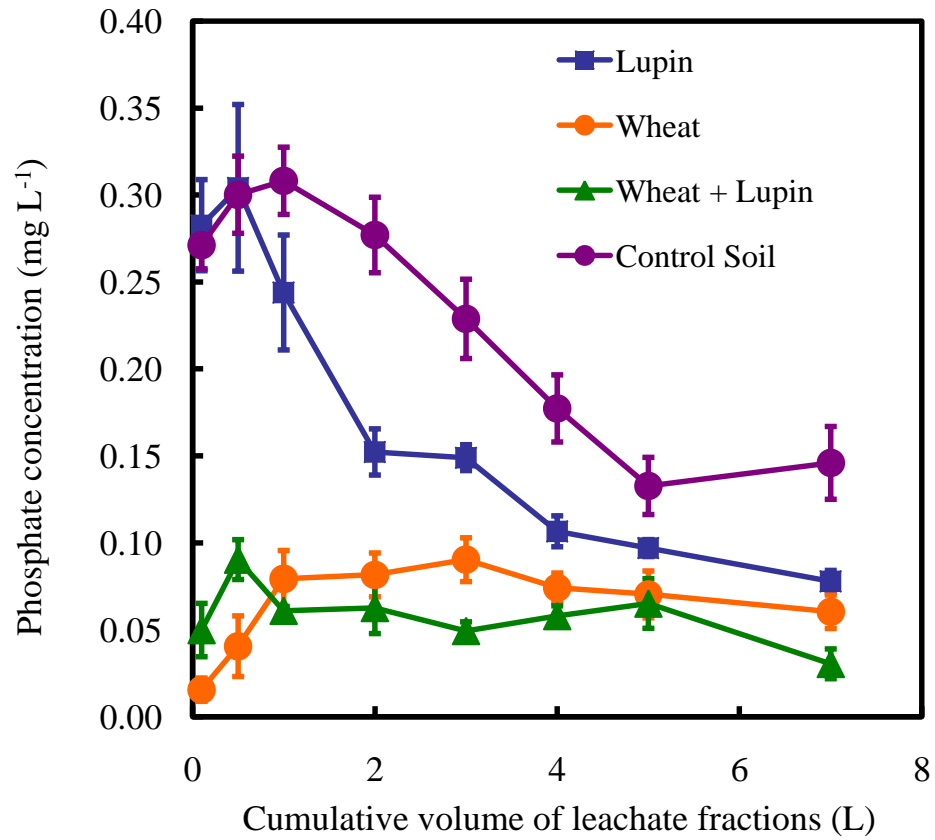
Figure 2.2. Effect of plant growth on the concentration of water-leachable phosphate in the soil. The plants were grown either in mixed culture or in monoculture for 6 weeks in soil columns containing a low P soil. At the end of the cultivation period, the soil columns were leached with 7 litres of distilled water followed by 2 litres of 10 mM citric acid monohydrate (pH 4.0). Each data point represents the mean of 5 replicate soil columns containing 10 plants each. The vertical bars represent the standard error of the mean (n=5).
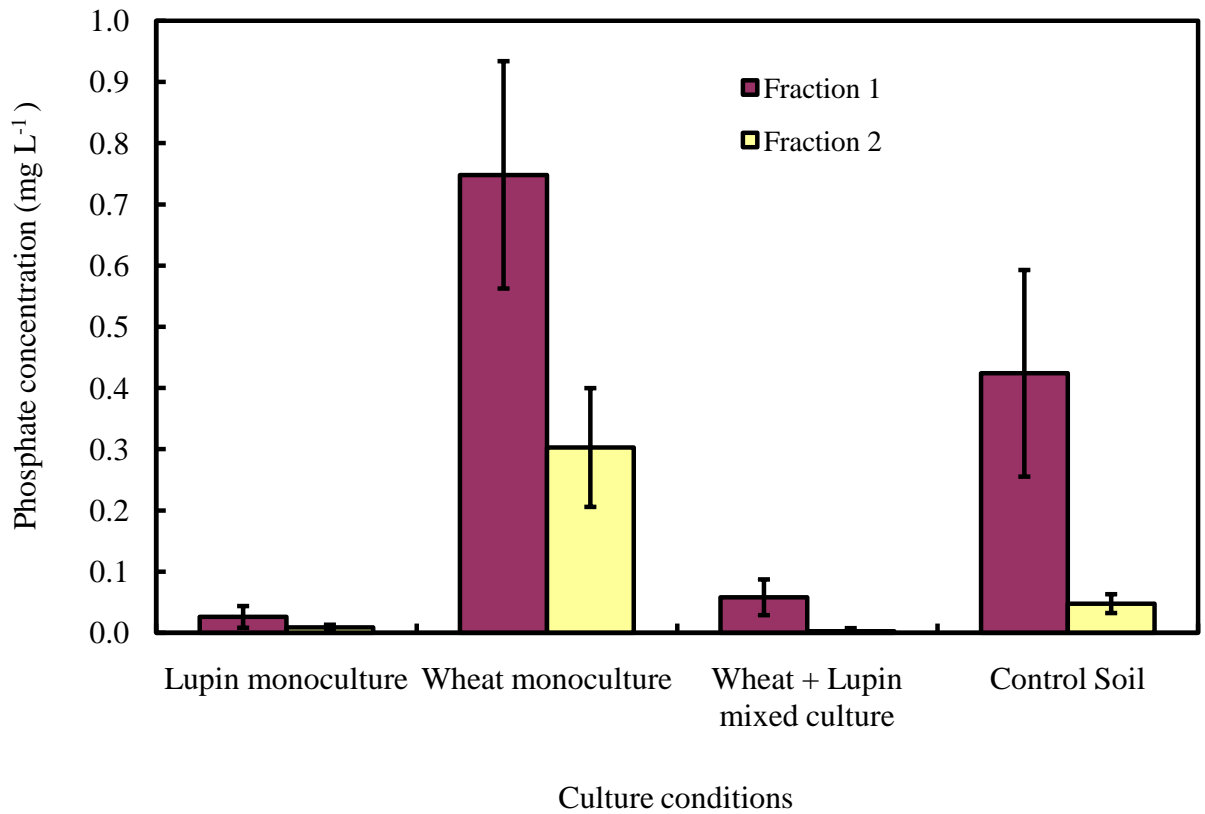
Figure 2.3. Effect of plant growth on the concentration of citric acid-leachable phosphate in the soil. The plants were grown and the soil columns were leached as described in the legend to Fig. 2.2. The data shown in this figure are for the citric acid leachate fractions obtained after the soil columns had already been leached with 7 litres of distilled water. Fraction 1 is the first and Fraction 2 is the second litre of the citric acid leachate. Each data point represents the mean of 5 replicate soil columns containing 10 plants each. The vertical bars represent the standard error of the mean (n=5).

2.3.3   Effect of plant growth on pH of soil leachate fractions

When the soil columns were leached with distilled water, the pH values for the initial fractions for the lupin monocultures were approximately 0.3 pH units below the pH values for the corresponding fractions for the uncultivated soil (Fig. 2.4). In contrast, the pH values for the initial fractions for the wheat monocultures were up to 0.8 pH units above the pH values for the corresponding fractions for the uncultivated soil control. Thus, the lupins were acidifying the soil whereas the wheat plants were causing soil alkalinisation. The leachate pH values for the mixed cultures were intermediate between the two monocultures. Thus, alkalinisation of the soil under the wheat was partially offset by acidification under the lupins and *vice versa*. As leaching proceeded, the pH values for the soils sown with plants converged towards the pH value for the uncultivated soil suggesting that the acidifying/alkalinising substances were being leached out.
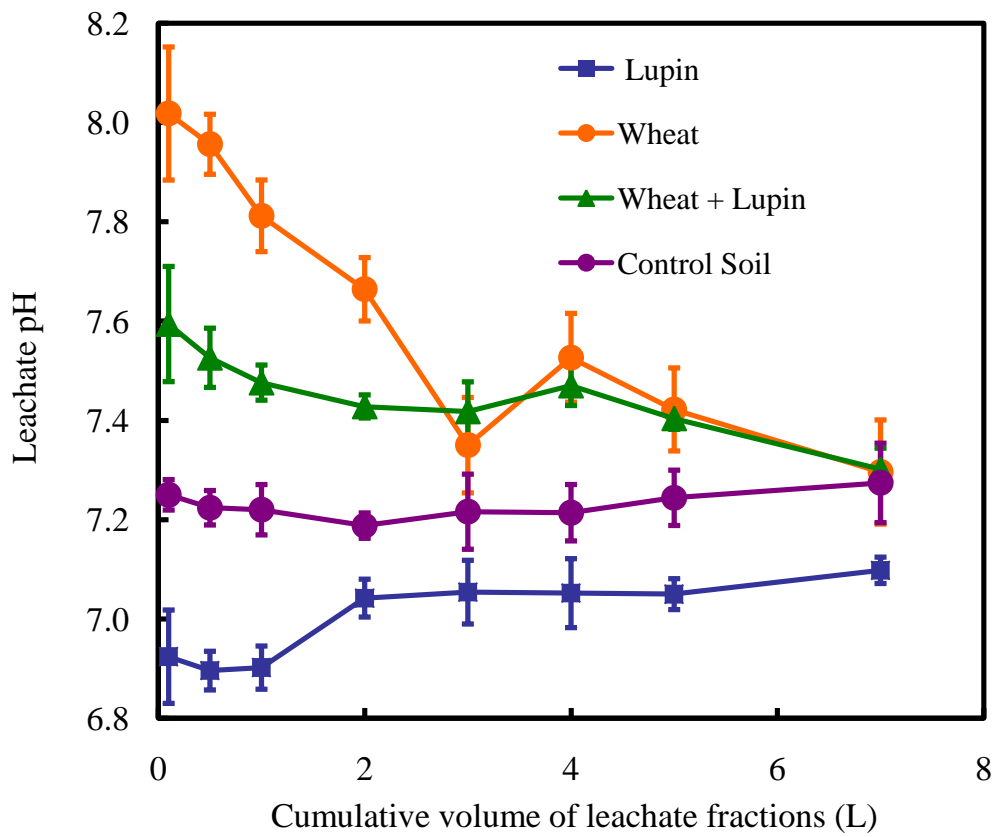
Figure 2.4. Effect of plant culture on soil leachate pH. The plants were grown and the soil columns were leached as described in the legend to Fig. 2.2. The data shown in this figure are for the water leachate fractions only. Each data point represents the mean of 5 replicate soil columns containing 10 plants each. The vertical bars represent the standard error of the mean (n=5).

2.3.4   Plant mineral element uptake

At the end of the plant growth period, the shoots and roots were analysed for a range of other mineral elements as well as P (Table 2.2). The nitrogen content of the shoots expressed per kg shoot dry mass was similar regardless of the species or the culture conditions. This indicates that the improved growth of the wheat in mixed culture with the lupins was not just simply due to improved nitrogen nutrition as might be expected when a cereal is grown together with a legume. Insufficient plant material was available for root nitrogen analyses but the results would be expected to be qualitatively similar to those obtained for the shoots.

There were some indications that Cu uptake differed between the mixed cultures and the monocultures but these results were not consistent between experiments (Table 2.2 and data not shown). The concentrations of the other mineral elements were not significantly affected by the culture conditions (i.e. mixed culture *vs.* monoculture) but there were large differences between the wheat and the lupins. For example, the lupin shoots accumulated approximately 10-fold more calcium, 5-fold more magnesium and 8-fold more sulphur than the wheat shoots.

Table 2.2. Mineral element composition of white lupin and wheat plants grown either in monoculture or in mixed culture. Each value is the mean of 5 replicates. Means in the same column with the same letter are not significantly different at $P \leq 0.05$ based on a Tukey's test. For the Tukey's test, shoots and roots were compared separately. So, for example, for Fe concentration in the shoots, the lupin monocultures were compared with the wheat monocultures, the lupins in the mixed cultures and the wheat in the mixed cultures.

		Mineral element concentration (mg kg^{-1} dry weight)															
		Fe	**Mn**	**B**	**Cu**	**Mo**	**Co**	**Ni**	**Zn**	**Ca**	**Mg**	**Na**	**K**	**N**	**S**	**Al**	**Cd**
Lupin shoot	Mono	368a	50.9a	39.5a	17.1b	1.2a	<0.8	1.4a	106a	22880a	5500a	828b	28000a	17000a	11640a	446a	<0.4
	Mixed	394a	59.2a	36.7a	9.0b	1.4a	<0.9	1.1a	117a	29000a	6700a	1074a	28200a	15000a	12780a	506a	<0.4
Wheat shoot	Mono	106b	18.4b	8.5b	9.3b	2.5b	<0.9	1.5a	55.6b	2116b	1298b	315c	26400a	17000a	1552b	89b	<0.4
	Mixed	114b	19.5b	9.7b	46.6a	3.0b	<0.8	1.5a	61.9b	1860b	1256b	189c	25000a	16000a	1412b	110b	<0.4
Lupin root	Mono	1626b'	22.7a'	19.9a'	12.4c'	<0.9	<0.9	4.3a'	136a'	12800a'	7080a'	15580a'	21360a'	-	19660a'	2476a'	<0.4
	Mixed	2046a'	24.1a'	20.0a'	14.9b'	<0.8	<0.8	1.9b'	130a'	12500a'	6620a'	12640b'	17460a'	-	16140b'	3400a'	<0.4
Wheat root	Mono	1624b'	16.4b'	28.9a'	19.6a'	<0.9	<0.9	1.2b'	96.0b'	2980b'	732b'	2782c'	8580b'	-	2128c'	3340a'	<0.4
	Mixed	1760b'	16.3b'	17.3a'	15.1b'	<0.9	<0.9	1.8b'	103b'	3110b'	920b'	2376c'	7300b'	-	2120c'	3500a'	<0.4

2.4 Discussion

We have demonstrated that mixed culture of wheat with white lupin increases the growth and P uptake of the wheat without detrimentally affecting the growth or P uptake of the lupins (Table 2.1). This confirms the results of Gardner and Boundy (1983), Marschner et al. (1986) and Kamh et al. (1989). In addition, we have used a novel system employing soil columns that can be leached at the end of the plant growth period to show that lupin monocultures preferentially depleted the citric acid-leachable soil P pool whereas wheat monocultures preferentially depleted the water-leachable soil P pool and mixed cultures depleted both pools (Figs. 2.2 and 2.3). These results provide direct evidence that the improved growth and P uptake of wheat in mixed culture with white lupin is due to the ability of the lupins to make soil P available to their companion wheat plants from a citric acid soluble soil P pool not normally available to wheat. It is well known that white lupins growing in low P soils exude large quantities of citrate and protons from their roots and that this improves their P nutrition (Dinkelaker et al., 1989, Gardner et al., 1983, Gerke et al., 1994, Hocking et al., 1997, Keerthisinghe et al., 1998) and it has also been shown several times that mixed culture of wheat with white lupin improves the growth and P uptake of the wheat (Gardner and Boundy, 1983; Marschner et al., 1986; Kamh et al., 1999). However, this work is the first to provide a direct demonstration of the link between these two phenomena.

The special ability of white lupin to access soil P pools only sparingly available to other plant species is due to a combination of factors: (a) chelation by the citrate

anion of Al, Fe, Ca and Mg cations that would otherwise form soluble and insoluble complexes with soil inorganic P; (b) displacement by the citrate anion of inorganic P in soluble complexes with soil cations ; (c) displacement by the citrate anion of inorganic P adsorbed to the surfaces of soil particles and (d) acidification of the rhizosphere leading to increased solubility of soil inorganic P in alkaline soils (Hinsinger et al., 2001). Here we have mimicked these effects by leaching the soils with citric acid and investigating the impact of plant growth on soil P pools at the end of the plant growth period. Besides showing that mixed culture of wheat with white lupin improves the growth and P uptake of the wheat, we have also shown that mixed culture of a 'P-mobilizing' species (e.g. white lupin) with a more competitive 'P-utilizing' species (e.g. wheat) leads to more effective utilization of soil P.

The results complement those of Braum and Helmke (1995) and Hocking et al. (1997) who used soils labelled with ^{32}P-orthophosphate to show that white lupin had access to a soil P pool only sparingly available to other plant species. Braum and Helmke (1995) used a soil with a low concentration of Bray-I extractable P and unknown total P status whereas Hocking et al. (1997) used a soil with a low concentration of Bray-I extractable P but a high total P status. Braum and Helmke (1995) compared white lupin with soybean whereas Hocking et al. (1997) tested a broad range of species. Both groups showed that, compared with the other plant species, white lupin exhibited a low value for specific ^{32}P activity and a high value for isotopically exchangeable P. This indicated that white lupin was accessing the unlabelled soil P pool to a greater extent than the other species. The ranking of the species obtained by Hocking et al. (1997) for specific ^{32}P activity in the plant shoots was white lupin < pigeon pea and narrow-leaf lupin, soybean and wheat < canola

and for isotopically exchangeable P, the ranking was white lupin >> pigeon pea > canola, sunflower and wheat > narrow-leaf lupin and soybean. These experiments demonstrate that white lupin has better access to soil P than the other species but it does not compete particularly effectively with the other species in terms of P utilization. The results confirm and extend this work using a simple system that does not require radioactive labelling of the soil or any sophisticated equipment to perform the analyses.

We have also shown that in the mixed cultures, acidification of the soil caused by the lupins partially offset alkalinisation caused by the wheat (Fig. 2.4). This may be part of the explanation for the improved availability of P to the wheat in the mixed cultures as compared with the wheat in the monocultures. Sas et al. (2001) have shown that as P supply to N_2-fixing white lupins is decreased there is an increase in H^+ release by the roots and at low levels of P supply, there is a strong positive correlation between H^+ release and citrate anion release. Thus, for white lupins growing under P deficiency, at least part of the reason for soil acidification is the release of protons to balance the charge on the citrate anion. Soil pH is a major determinant of P availability to plants (Hinsinger et al., 2001). In alkaline soils, such as the soil used here, P becomes unavailable when it forms insoluble complexes predominantly with Ca^{2+} and Mg^{2+}. Acidification of alkaline soils tends to increase the solubility of Ca^{2+}- and Mg^{2+}-phosphates thus increasing the plant availability of phosphate. Thus, the fact that the soil under the mixed cultures was more acid than the soil under the wheat monocultures may have contributed to the improved P nutrition of the wheat in the mixed cultures by making phosphate more available (soluble).

Soil acidification/alkalinisation as a result of plant cultivation occurs because plants need to maintain their internal pH and charge balance (Hinsinger et al., 2003). In other words, plants taking up an excess of cations over anions exude H^+ from their roots whereas plants taking up an excess of anions over cations exude OH^-. In this study we observed that the lupin shoots accumulated approximately 10-fold more calcium, 5-fold more magnesium and 8-fold more sulphur than the wheat shoots regardless of whether they were grown in monoculture or mixed culture (Table 2.2). Tang et al. (1998) calculated excess cations in the shoots of five pasture species using the following formula $[(K^+ + Ca_{0.5}^+ + Mg_{0.5}^+ + Na^+) - (H_2PO_4^- + SO_{4(0.5)}^- + Cl^-)]$ cmol/kg dry mass. Unfortunately we do not have data for Cl^- but we can still apply the formula of Tang et al. (1998) excluding Cl^- from the calculations. If we do this we obtain the following results for excess cations in cmol/kg dry mass: (a) wheat monoculture 75, (b) wheat in mixed culture 70, (c) lupin monoculture 154 and (d) lupin in mixed culture 190. Clearly, the lupins show a greater excess of cation over anion uptake than the wheat and this is regardless of the culture conditions. Thus, the lupins would be expected to have a greater soil acidification potential than the wheat which is consistent with the data for the water leachates from the soil columns (Fig. 2.4). In future studies, the analysis should include Cl^- in order to obtain a more accurate calculation of excess cations if required.

McLay et al. (1997) have compared the soil acidification potential of ten different grain legume species and found that white lupin ranked near the top when the plants were ranked according to H^+ production per plant however when they were ranked according to H^+ production per unit plant dry mass there was little difference between the different species. From this, they concluded that, in general, large-

seeded species produced more H^+ than small-seeded species because of the more rapid early growth of the large-seeded species. It would be interesting to know how these species compare in relation to organic acid anion exudation from their roots. It would also be interesting to determine whether or not they can improve the growth and P uptake of wheat in mixed culture. Clearly, for intercropping to be successful in a practical sense it is important to find a combination of plant species where the P mobilising species does not compete too strongly with the P beneficiary species in terms of P uptake and/or plant vigour.

In conclusion, we have demonstrated that mixed culture of wheat with white lupin in a low P soil improves the growth and P uptake of the wheat without detrimentally affecting either the growth or the P uptake of the white lupin. The beneficial effect of mixed culture on the wheat appears to be due to the ability of white lupin to mobilise P from a citric acid soluble P pool in the soil, a pool not normally available to wheat. Apparently the lupins in the mixed-cultures mobilized P in excess of their own needs and made it available to their companion wheat plants without suffering any signs of P deficiency themselves. The next step will be up-scaling this experiment to field trials in order to assess the benefit of mixed culture or intercropping on the yield and mineral nutrition of wheat and lupin.

References

Braum, S. M. & Helmke, P. A. (1995) White lupin utilizes soil phosphorus that is unavailable to soybean. *Plant and Soil,* 176**,** 95-100.

Dinkelaker, B., Romheld, V. & Marschner, H. (1989) Citric acid excretion and precipitation of calcium citrate in the rhizosphere of white lupin (*Lupinus albus* L.). *Plant, Cell and Environment,* 12**,** 285-292.

Gardner, W. K., Barber, D. A. & Parbery, D. G. (1983) The acquisition of phosphorus by *Lupinus albus* L. *Plant and Soil,* 70**,** 107-124.

Gardner, W. K. & Boundy, K. A. (1983) The acquisition of phosphorus by *Lupinus albus* L. The effect of interplanting wheat and white lupin on the growth and mineral composition of the two species. *Plant and Soil,* 70**,** 391-402.

Gerke, J., Romer, W. & Jungk, A. (1994) The excretion of citric and malic acid by proteoid roots of *Lupinus albus* L.: Effects on soil solution concentrations of phosphate, iron, and aluminum in the proteoid rhizosphere in samples of an oxisol and a luvisol. *Zeitschrift fur Pflanzenernahrung und Bodenkunde,* 157**,** 289-294.

Hinsinger, P. (2001) Bioavailability of soil inorganic P in the rhizosphere as affected by root-induced chemical changes: A review. *Plant and Soil,* 237**,** 173-195.

Hinsinger, P., Plassard, C., Tang, C. & Jaillard, B. (2003) Origins of root-mediated pH changes in the rhizosphere and their responses to environmental constraints: A review. *Plant and Soil,* 248**,** 43-59.

Hocking, P. J., Keerthisinghe, G., Smith, F. W. & Randall, P. J. (1997) Comparison of the ability of different crop species to access poorly-available soil phosphorus. In Ando, T., Fujita, K., Mae, T., Matsumoto, H., Mori, S. & Sekiya, J. (Eds.) *Plant nutrition for sustainable food production and environment.* Dordrecht, Kluwer Academic Publishers.

Horst, W. J. & Waschkies, C. (1987) Phosphorus nutrition of spring wheat (*Triticum aestivum* L.) in mixed culture with white lupin (*Lupinus albus* L.). *Z Pflanzenernähr Bodenkd,* 150**,** 1–8.

Jones, D. L. & Darrah, P. R. (1994) Role of root derived organic acids in the mobilization of nutrients from the rhizosphere. *Plant and Soil,* 166**,** 247-257.

Kamh, M., Horst, W. J., Amer, F., Mostafa, H. & Maier, P. (1999) Mobilization of soil and fertilizer phosphate by cover crops. *Plant and Soil,* 211**,** 19-27.

Keerthisinghe, G., Hocking, P. J., Ryan, P. R. & Delhaize, E. (1998) Effect of phosphorus supply on the formation and fuction of proteiod roots of white lupin (*Lupinus albus* L.). *Plant, Cell and Environment,* 21**,** 467-478.

Marschner, H., Romheld, V., Horst, W. J. & Martin, P. (1986) Root-induced changes in the rhizosphere: Importance for the mineral nutrition of plants. *Zeitschrift fur Pflanzenernahrung und Bodenkunde,* 149**,** 441-456.

McLay, C. D. A., Barton, L. & Tang, C. (1997) Acidification potential of ten grain legume species grown in nutrient solution. *Australian Journal of Agricultural Research,* 48**,** 1025-1032.

Murphy, J. & Riley, J. P. (1962) A modified single solution method for the determination of phosphate in natural waters. *Analytica Chimica Acta,* 27**,** l-36.

Neumann, G., Massonneau, A., Langlade, N., Dinkelaker, B., Hengeler, C., Romheld, V. & Martinoia, E. (2000) Physiological aspects of cluster root function and development in phosphorus-deficient white lupin (*Lupinus albus* L.). *Annals of Botany,* 85**,** 909-919.

Purnell, H. M. (1960) Studies of the family Proteaceae. I. Anatomy and morphology of the roots of some Victorian species. *Australian Journal of Botany,* 8**,** 38-50.

Raghothama, K. G. (1999) Phosphate acquisition. *Annual Review of Plant Physiology and Plant Molecular Biology,* 50**,** 665-693.

Roelofs, R. F. R., Rengel, Z., Cawthray, G. R., Dixon, K. W. & Lambers, H. (2001) Exudation of carboxylates in Australian Proteaceae: Chemical composition. *Plant, Cell and Environment,* 24**,** 891-904.

Sas, L., Rengel, Z. & Tang, C. (2001) Excess cation uptake, and extrusion of protons and organic acid anions by *Lupinus albu*s under phosphorus deficiency. *Plant Science-Kidlington,* 160**,** 1191-1198.

Tang, C., Barton, L. & Raphael, C. (1998) Pasture legume species differ in their capacity to acidify soil. *Australian Journal of Agricultural Research,* 49**,** 53-58.

Zarcinas, B. A., Cartwright, B. & Spouncer, L. R. (1987) Nitric acid digestion and multi-element analysis of plant material by inductively coupled plasma spectrometry. *Communications in Soil Science and Plant Analysis,* 18**,** 131-146.

Chapter 3   Cloning, expression, purification, crystallization and preliminary X-ray analysis of *Pf*Prx-1, a cytosolic 2-Cys peroxiredoxin from *Plasmodium falciparum*

Abstract

The causative agent of malaria, *Plasmodium falciparum*, possesses a cytosolic 2-Cys peroxiredoxin (*Pf*Prx-1) which represents a potential drug target for treatment of the disease. *Pf*Prx-1 is an antioxidant enzyme responsible for removing reactive oxygen/nitrogen species, thereby protecting the parasite against oxidative stress. In order to enable the design of *Pf*Prx-1 inhibitors we set out to study its properties and to determine its 3D structure. Firstly, the *Pf*Prx-1 gene was successfully expressed in *E.coli* for protein production. Following high-level expression, the *Pf*Prx-1 protein was purified to homogeneity. The purified *Pf*Prx-1 protein was studied for its Prx activity and its oligomeric structure. The *Pf*Prx-1 protein exists in both decameric and dimeric forms. High pH (8.5) and high concentrations of urea (2.8 M) seem to favour the formation of dimers. Attempts at crystallization of the protein yielded crystals, of which one diffracted to around 6-7 Å. Although a complete native data set was collected to 6 Å resolution, it was impossible to integrate and merge all the data. However, indexing of selected images revealed that the crystal belongs to space group P2, with unit-cell parameters a= 117.37; b= 67.11; c= 118.36; α=90.00°; β= 119.53°; γ= 90.00°.

3.1 Introduction

*Pf*Prx-1 is a 2-Cys peroxiredoxin (2-Cys Prx) located in the cytosol of the malaria parasite, *P. falciparum*. *Pf*Prx-1 is expressed constitutively throughout the erythrocytic stage of the parasite's lifecycle and it is one of the most abundantly expressed proteins in the parasite cytosol accounting for approximately 0.25% of the total parasite cellular protein during the trophozoite stage (Kawazu *et al*., 2001).

The cloning and characterization of the *PfPrx-1* gene was published almost simultaneously by three independent research groups (Kawazu *et al*., 2001, Krnajski *et al*., 2001a, Rahlfs and Becker, 2001). The 588 bp *Pf*Prx-1 coding region is located on chromosome 14 and encodes a predicted protein of 194 amino acids (approx. 21.8 kDa). The deduced amino acid sequence of *Pf*Prx-1 contains two conserved cysteine residues Cys49 and Cys168 equivalent to Cys47 and Cys170 in yeast Prx, respectively (Kawazu *et al*., 2001, Krnajski *et al*., 2001a, Rahlfs and Becker, 2001). Cys47 serves as the primary catalytic site of oxidation by peroxide substrates with the Cys_P-SH being oxidised to sulfenic acid (Cys_P-OH) while Cys170 functions in the recycling of the sulfenic acid back to the reduced state. All three research groups showed that *Pf*Prx-1 expressed in *E. coli* catalyses the reduction of H_2O_2, cumene hydroperoxide and *tert*-butylhydroperoxide using reducing equivalents from the NADPH/thioredoxin/thioredoxin reductase system thus demonstrating that it is a member of the 2-Cys Prx family. The catalytic mechanism involving the two conserved Cys residues (Cys^{49} and Cys^{168}, the peroxidatic and resolving Cys residues, respectively) has been predicted based on site-directed mutagenesis and

molecular modeling (Nickel *et al*., 2005) but no crystal structure is available (Kawazu, 2008). A crystal structure is needed to more precisely determine the fine details of the reaction mechanism.

From BLAST analyses, the genome of *P. falciparum* is more similar overall to those of the plants (*Arabidopsis* and *Oryza*) than to any of the non-apicomplexan organisms whose sequences are currently available in Genbank (Kawazu *et al*. 2001, Krnaijski *et al*. 2001). This may be a consequence of genetic transfer from an algal endosymbiont to the parasite nucleus during evolution (Kawazu *et al*. 2001)**.** Among the currently known six subfamilies of mammalian Prx genes, *Pf*Prx-1 showed the highest identity at the amino acid level (46.6%) to the PrxII subfamily (also known as human natural killer-enhancing factor B or calpromotin, refer to Table 1.4) (Kawazu *et al*. 2001)**.**

Investigations into the characteristics of the *Pf*Prx-1 enzyme have suggested that it plays an important role in the detoxification of reactive oxygen species (ROS) and reactive nitrogen species (RNS) (Nickel *et al*. 2005). For example, *Pf*Prx-1 reacts very efficiently with H_2O_2 with a low K_m (~0.25 µM) and a high k_{cat}/k_m (catalytic efficiency ~ 6.7×10^6 $M^{-1}s^{-1}$ at 30°C) (Akerman and Müller, 2003). It is also able to carry out the reduction of peroxynitrite using either thioredoxin or plasmoredoxin as reducing substrates (Nickel *et al*., 2005). *Pf*Prx-1 reduces H_2O_2 via a thioredoxin (Trx) dependent catalytic cycle (Kanzok *et al*., 2002).

With regards to expression profiles of gene products of the Trx system in *P. falciparum*, whereas several processes of the transcription of the many participating genes were coordinated, there were some outstanding deviations reported (Bozdech and Ginsburg, 2004; Yano *et al*., 2005). Bozdech and Ginsburg (2004) showed that the transcript of the Trx-coding sequence is high immediately following invasion and remains highly expressed throughout the ring stage. The transcript of the plasmoredoxin-coding gene (plasmoredoxin is a 22-kDa protein occurring only in *Plasmodium*) peaks at 20 hours post-invasion (HPI) while TrxR peaks considerably later, at 30 HPI. The transcription of all Prx coding sequences was temporally similar with that of TrxR. The fact that the Trx or plasmoredoxin genes were transcribed before TrxR genes (TrxR is necessary for the control of the reduction state of these substrates) suggests that there might be another novel, non-classical pathways that necessitates further investigations (Bozdech and Ginsburg, 2004).

Similar to 2-Cys Prx proteins in other organisms, the *Pf*Prx-1 protein forms homodecamers with a doughnut-like shape consisting of five homodimers (Akerman and Müller, 2003). The formation of *Pf*Prx-1 decamers is favoured under reducing conditions (1 mM DTT). This finding agrees with the earlier findings of Wood *et al*., (2003b) who also stated that the decameric forms of 2-Cys Prx proteins in a number of organisms had higher enzyme activity than their dimeric forms.

Homology modeling of *Pf*Prx-1 using mammalian homologues has suggested that *Pf*Prx-1 possesses a redox-sensitive type of peroxidatic active-site structure (Kawazu *et al*. 2008) and this leads to the assumption that the enzyme can be

regulated similarly to other well-studied Prx proteins by factors such as changes in

phosphorylation state, redox state and possibly oligomerization state (Georgiou and

Masip, 2003, Woo *et al.*, 2003, Wood *et al.*, 2003a). *Pf*Prx-1 has a conserved

threonine residue (Thr88) similar to that of mammalian PrxI, PrxII, PrxIII and PrxIV

(Kawazu *et al.* 2008). This conserved threonine residue can be the target for

phosphorylation by cyclin-dependent kinases, which leads to the loss of peroxidase

activity (Chang *et al.*, 2002, Nickel *et al.*, 2005, Wood *et al.*, 2003b). With regards

to regulation of activity by oxidation, some Prx proteins are inactivated at high

concentrations of hydrogen peroxide and perhaps peroxynitrite, due to irreversible

oxidation of their peroxidatic cysteine (Cys_P) residue to sulfinic ($-SO_2H$) or sulfonic

($-SO_3H$) acid forms (Claiborne, 1999, Rabilloud, 2002, Woo *et al.*, 2003, Wood *et

al.*, 2003b). With regards to regulation via oligomerization, it has been shown that

the active sites of the typical 2-Cys Prx proteins are stabilized by the dimer–dimer

interface of the decamer, which may explain the greater enzymatic activity of the

decamer as compared with the dimer (Chauhan, 2001, Kitano *et al.*, 1999, Wood *et

al.*, 2003b).

Disruption of *Pf*Prx-1 gene expression (by gene knockout) in cultured *P. falciparum*

parasites led to a reduced growth rate compared with wild-type parasites (during the

erythrocytic stage), when the parasites were treated with paraquat or sodium

nitroprusside to generate either superoxide or nitric oxide, respectively. In the

absence of these compounds, however, the *Pf*Prx-1-knockout parasites grew

normally (Komaki-Yasuda *et al.*, 2003). These findings indicate that *Pf*Prx-1 is an

important, but not essential, component of the parasite's mechanism of defense

against oxidative and nitrosative stresses. Nevertheless, the enzyme may play an

important role in protecting the parasite under more severe oxidative or nitrosative stress conditions. *P. falciparum* develops in erythrocytes sequestered in the microvasculature. The observation of protein nitration in brain tissue from patients suffering cerebral malaria suggests that NO is elevated at the site of erythrocyte sequestration (Clark and Schofield, 2000). Thus the parasite may be exposed to more severe stresses in sequestered erythrocytes than in circulating erythrocytes (Kawazu, 2008). Further studies are needed to demonstrate the role of *Pf*Prx-1 under these severe stress conditions.

The expression of *Pf*Prx-1 mRNA and protein can be induced by oxidative stress (Krnajski *et al*., 2001b) and the levels of both *Pf*Prx-1 mRNA and protein were found to be increased when blood stage malaria parasites were subjected to exogenous or endogenous oxidative stress (Akerman and Müller, 2003). These results suggest that *Pf*Prx-1 is an important component of the antioxidant machinery of the *P. falciparum* parasite. Thus, inhibitors specifically targeting *Pf*Prx-1 might be promising leads for the development of new antimalarial drugs.

To develop an inhibitor of *Pf*Prx-1, detailed structural and functional data are vital. Previous studies using protein homology modelling with human Prxs revealed some insights into the structure and possible enzymatic mechanism of *Pf*Prx-1. However, in order to obtain more detailed information about the structure and function of *Pf*Prx-1, a crystal structure, preferably of an enzyme-substrate complex, would be valuable. Homology modelling predicts the structure of a protein based on its sequence alignment with a structurally-known template (Aszódi and Taylor, 1996).

This prediction is dependent on many factors such as the availability of homologous templates and the modelling method/program and does not guarantee a precise prediction of the novel protein's structure (Aszódi and Taylor, 1996). A *Pf*Prx-1 crystal structure would facilitate the study of enzyme-inhibitor complexes which is important in the development of new and specific drugs.

The aim of this study was to obtain a crystal structure for *Pf*Prx-1. Firstly, *Pf*Prx-1 was expressed at a high-level in *E. coli*. Then the recombinant *Pf*Prx-1 protein was purified, biochemically characterized and crystallized. The X-ray diffraction pattern of a crystal was then determined. The data obtained add to our understanding of the structure of the enzyme and they will also be useful for inhibitor studies aiding structure-based antimalarial drug design.

3.2 Materials and methods

3.2.1 Amplification of the *Pf*Prx-1 gene via polymerase chain reaction (PCR)

The *P. falciparum Pf*Prx-1 nucleotide sequence has been previously published (GenBank accession no. AF225977). The published sequence was used to design PCR primers which would amplify the 580 bp *Pf*Prx-1 open reading frame (ORF). In addition, the forward primer encoded a 6-Histidine (His$_6$) tag followed by a Factor Xa recognition site before the start codon. The His$_6$-tag was included to facilitate metal affinity purification of the recombinant protein and the Factor Xa

recognition site was added to enable the subsequent removal of the His$_6$-tag after protein purification. In the forward primer, a *Nco*I restriction enzyme site was situated directly before the His$_6$ -tag and in the reverse primer there was a BamHI site placed directly after the stop codon (Table 3.1).

Genomic DNA isolated from *P. falciparum* strain 3D7 (provided by Dr. Ian Menz, School of Biological Sciences, Flinders University, Australia) was used as the template to amplify the ORF of the *Pf*Prx-1 gene. Conveniently, the ORF contains no introns and therefore genomic DNA could be used as the template. All PCR reagents were purchased from Qiagen, Australia and PCR reactions were prepared according to the manufacturer's instructions. Approximately 0.5 μg of genomic DNA was added to a PCR master mix containing 1× Hotstar PCR buffer, 2.5 mM MgCl$_2$, 0.5 mM of each dNTP, 0.5 μM each of the forward and reverse primers and 2.5 U HotStarTaq DNA polymerase. The total reaction volume was 100 μl. The negative control was the PCR master mix without added DNA template. PCR was initiated by HotStarTaq DNA polymerase activation at 95ºC for 5 minutes, followed by 25 cycles of denaturation at 94ºC for 1 minute, annealing at 58ºC for 1 minute and extension at 65ºC for 3 minutes and then a final extension at 65ºC for 10 minutes. The extension temperature was kept rather low (65ºC) to avoid denaturation of the DNA template which was high in A+T content (~ 80%) (Su *et al*., 1996).

Table 3.1. Oligonucleotides used to amplify the *Pf*Prx-1 coding region. The *NcoI* and *BamHI* restriction enzyme sites mentioned in the text are shown in bold, the His$_6$-tag coding sequence is shown in italics and the Factor Xa protease cleavage site is underlined.

Primer name	Primer sequence
*Pf*Prx-1 forward	5'CAA**CCATGG**AA*CATCATCACCATCATCAT*<u>ATTGAGGGACGC</u>ATGGCATCATATGTAGGAAGAGAAGC-3'
*Pf*Prx-1 reverse	5'**GGATCC**TTACAACTTTGATAAATATTCACTAACACCTTCTTCTGATGGTTTCATGGCTACCTTTCCCTTTTCCAGTTTGC-3'

3.2.2   DNA electrophoresis

DNA fragments can be separated and purified from agarose gels for analytical and preparative purposes. One to 2% (w/v) agarose gels were made by adding the appropriate amount of agarose (Sigma, catalogue no. A4718)) to 1× TAE buffer (40 mM Tris-acetate, 1 mM ethylenediaminetetraacetate (EDTA), pH 8.0). The suspension was heated to dissolve all agarose and then poured into a get casting apparatus and left to polymerize.

DNA samples (PCR products, plasmid DNA) were prepared by mixing with 0.2 vol of 5× loading buffer (50% v/v glycerol, 0.04% w/v bromophenol blue) and loaded onto the agarose gel. The gel was then placed in an electrophoresis chamber, covered with 1× TAE buffer and electrophoresed at 80-100 V for 45-60 min. Next, the gel was stained in ethidium bromide solution (10 mg ml^{-1}) for 30 min and destained in water before visualization under UV light.

3.2.3   Purification of DNA from agarose gels

To ensure the highest purity of plasmid DNA and/or PCR fragments, they were purified from 1% (w/v) agarose gels using the Wizard® Plus SV Gel and PCR Clean-Up system (Promega catalogue no. A9281) according to the manufacturer's instructions. To avoid DNA damage, the gels were visualized on a UV transilluminator for the briefest time and the desired bands were excised with a sterile scalpel. Binding Buffer was added to the agarose gel in an appropriate ratio

(100 µg agarose gel corresponds to approximately 100 µl) and the mixture was

incubated at 50-65°C with occasional vortexing for 10 min or until the gel slices had

completely dissolved. The melted gel was applied to a SV Minicolumn and then

centrifuged at 16,000 *g* for 1 min. The column was then washed twice using

Membrane Wash Solution. Binding Buffer, Wash Solution and SV Minicolumns

were provided with the kits. Next the DNA was eluted with 50-100 µl of nuclease-

free water or TE buffer (10 mM Tris-HCl, pH 7.5; 1 mM EDTA, pH 8.0). The

purified DNA was store at 4°C or -20°C until use.

3.2.4   DNA Precipitation

To further purify and/or concentrate plasmid and insert DNA, ethanol precipitation

was performed following the method described by Sambrook *et al*. (1989). Firstly,

the DNA sample was mixed with 0.1 volumes of 3 M sodium acetate (pH 5.2)

followed by 2.5 volumes of cold absolute ethanol. The mixture was placed on ice or

at -20°C for 60 minutes and then it was centrifuged at maximum speed in a table top

centrifuge for 30 min at 4°C. The pellet was then rinsed with 1 ml 70% (v/v) ethanol

and re-centrifuged for 1 min (same conditions). The supernatant was removed and

after complete evaporation of the remaining ethanol, the DNA was dissolved in an

appropriate volume of nuclease-free water or TE buffer consisting of 10 mM Tris-

HCl (pH 7.5), 1 mM EDTA.

3.2.5   DNA Engineering Methods

3.2.5.1   Restriction of DNA by endonucleases

DNA plasmids (~3 μg of pET3d vector) and PCR products (0.5 μg) were digested at

37°C with two restriction endonucleases, i.e., 20 U *Bam*HI and 20 U *Nco*I (New

England Biolabs, catalogue no. R0136 and catalogue no. R0193, respectively) in 1 ×

NE Buffer 3 following the manufacturer's instructions. Completion of the digestions

(~3 h) was checked by agarose gel electrophoresis.

3.2.5.2   Dephosphorylation of DNA 5'-termini

Dephosphorylation of 3 μg of pET3d plasmid (~4 pmoles of 5-termini for a ~ 5 kb

plasmid when linearised by two restriction enzymes) was performed at 37°C for 30

min using 4 U Shrimp Alkaline Phosphatase (SAP) (Promega, catalogue no. M8201)

following the manufacturer's instructions. SAP was then heat inactivated at 65°C for

15 min. The dephosphorylated vector was then purified using the Promega Wizard$^{®}$

Plus SV Gel and PCR Clean-Up system.

3.2.5.3   DNA ligation

Two ligation reactions were set up with (i) 1:1 and (ii) 1:3 molar ratios of vector to

insert. The ligations were performed in a total volume of 20 μl containing 5 U of T4

DNA ligase (Promega, catalogue no. M1801) following the manufacturer's

instructions. The reactions were incubated at 16°C overnight. Constructs resulting

from successful ligation reactions were designated pET3d-Prx-1.

3.2.6   Microbiological methods

3.2.6.1   Growth media

Luria-Bertani (LB) broth: 1% (w/v) Bacto Tryptone; 0.5 % (w/v) Bacto Yeast

Extract; 1% (w/v) NaCl, pH 7.5.

LB agar: LB broth + 1.5% (w/v) agar.

SOC nutrient broth: 2% (w/v) Bacto Tryptone; 0.5 % (w/v) Bacto Yeast Extract; 10

mM NaCl; 2.5 mM KCl; 10 mM $MgCl_2$, 10 mM $MgSO_4$ and 20 mM glucose.

3.2.6.2   Growth and storage of bacterial strains

Strains (and plasmids) used in this chapter are listed in Table 3.2. *E.coli* DH5α and

BL21(DE3)pLysS strains were obtained from Dr. Ian Menz, School of Biological

Sciences, Flinders University, Australia. Bacteria were grown on LB plates or in LB

medium at 37°C unless stated otherwise. When required, appropriate antibiotics

were added to the growth media. All media and manipulation tools were sterilized

by autoclaving or, if heat labile, filtering through 0.22 μm filters. For long-term

storage, the cell culture in growth phase was mixed with 0.2% volumes of glycerol

and snap-frozen in liquid nitrogen, then stored at -80°C.

Table 3.2 . *E. coli* strains and plasmid vectors used for the cloning of *PfPrx-1* gene and the production of *Pf*Prx-1 recombinant protein

Cell strain	Genotype	Remark
DH5α	*F⁻, φ80dlacZΔM15, Δ(lacZYA-argF)U169, deoR, recA1, endA1, hsdR17(rk-, mk+), phoA, supE44, λ-, thi-1, gyrA96, relA1*	- Host for cloning vector (Invitrogen)
BL21(DE3) pLysS	F⁻, *omp*T, *hsd*S$_B$ (r$_B$⁻, m$_B$⁻), *dcm*, *gal*, λ(DE3), pLysS, *Cmʳ*.	- High stringency expression host (Novagen) - Containing a plasmid, pLysS, which carries the gene encoding T7 lysozyme that lowers the background expression level of target genes under the control of the T7 promoter (pET System Manual, 2002, Novagen). - Chloramphenicol resistance (34 μg/ml)

Vector	Origin	Remark
pET-3d	Novagen	- Expression vector with T7 lac promoter - *Amp^R* gene for ampicillin resistance
pET3d-*Pf*Prx1	This study	- pET3d with insert containing *Pf*Prx-1 - *Amp^R*

3.2.6.3   Preparation and transformation of competent cells

E. coli cells were made competent by the $CaCl_2$ method (Morrison, 1977). Briefly, 1 ml of an overnight culture (from a single colony) was used to inoculate 100 ml LB medium and grown at 37°C with vigorous shaking to an $OD_{600} = 0.4\text{-}0.6$. The cell culture was chilled on ice for 10 min then centrifuged at 4000 *g* for 10 min at 4ºC. The cell pellet was resuspended in 10 ml of ice-cold, sterile 0.1 M $CaCl_2$. The resuspended cells were chilled on ice for 1 h and then were pelleted again by centrifugation as above. The cell pellet was resuspended again in 2 ml of ice-cold, sterile 0.1 M $CaCl_2$. The cell suspension was chilled on ice for 1 h before transformation. The competent cells were stored at 4ºC for up to 48 h. For longer-term storage, 100-200 µl aliquots of competent cells were snap frozen in liquid nitrogen and stored at -80ºC.

To transform the *E. coli* competent cells, ~100 ng of plasmid DNA (10 µl of ligation reaction) was added to a 200 µl aliquot of competent cells (previously thawed on ice when using frozen competent cells). The mixture was flick mixed and chilled on ice for 30 min before being "heat-shocked" at 42°C for 90 s (in a water bath or a heating block). The cells were chilled on ice for 2 min, then 800 µl of nutrient broth (SOC) was added to the cells and they were incubated at 37ºC with gentle shaking for 1 h. Finally, 50 – 200 µl cells were plated onto LB plates (supplemented with 100 µg ml^{-1} ampicillin for the selection of the pET3d vector) and incubated at 37ºC overnight.

3.2.7   Colony PCR screening

The presence of *Pf*Prx-1 insert DNA in the vector was verified by direct colony PCR
screening following the method described by Hamilton *et al*. (1991) with some
modifications. Briefly, a single colony was suspended in 50 µl of sterile water and
the suspension was boiled at 99ºC for 5 min. After centrifugation at 12,000 *g* for 5
min to remove cell debris, 10 µl of the supernatant was used for PCR screening.
PCR reactions were set up and run as described in section 3.2.1 except that 10 µl of
cell lysate was used instead of genomic DNA as the template. In the negative
control, 10 µl of sterile water was used in place of the cell lysate. The products were
checked on 1% (w/v) agarose gels run at 80 V for 1.5 h.

Colonies that yielded PCR products of the expected size were cultured for the
production of plasmid DNA. Cells from each colony were transferred to 5 ml of
fresh LB liquid medium supplemented with 100 µg ml^{-1} ampicillin and incubated at
37°C with vigorous shaking overnight.

3.2.8   Plasmid Isolation

Plasmid preparation was performed using the Wizard$^{®}$ Plus SV Minipreps DNA
Purification System (Promega Catalogue no. A1330) following the manufacturer's
instructions. Briefly, cells from a 5 ml overnight culture were resuspended and lysed
in the provided Resuspension and Lysis solutions, respectively. Then 10 µl of
Alkaline Protease solution was added and the mixture was incubated for a further 5

min. After a Neutralization solution was added, the cell debris and precipitated

protein were separated by centrifugation at maximum speed (around 14,000 *g*) for

10 min. The clear supernatant was transferred into a Spin column which was then

centrifuged at 14,000 *g* for 1 minute and then washed twice using the Column Wash

solution. Last, the plasmid DNA was eluted by adding 50-100 µl of nuclease-free

water to the Spin column followed by centrifugation at maximum speed for 1

minute.

3.2.9   DNA sequencing

Plasmid DNA containing the *Pf*Prx-1 insert (named pET3d-Prx-1) was concentrated

to 200 ng µl^{-1} for sequencing purposes using the ethanol precipitation method as

described in section3.2.4. Plasmids containing inserts were sent for sequencing

using the T7 forward and reverse primers. The sequencing was done on an Applied

Biosystems 3100 Genetic Analyser with BigDye Terminator v3.1 chemistry at

SouthPath & Flinders Sequencing Facility (Adelaide, Australia). The sequencing

results were analyzed using SEQUENCHER 4.8 program

(http://www.genecodes.com).

3.2.10 Transformation of the pET3d-Prx-1 construct into expression host *E. coli* BL21 (DE3)pLysS cells

The pET3d-Prx-1 construct was transformed into the expression host *E. coli* BL21 (DE3)pLysS cells for the production of recombinant *Pf*Prx-1 protein as described in section 3.2.6.2. Control cells were transformed with the original pET3d vector without insert. Following transformation, the cells were plated onto LB medium containing 100 μg ml^{-1} ampicillin. Putative transformants were confirmed by colony PCR as described in section 3.2.7.

3.2.11 Recombinant protein production

Recombinant protein expression was performed following the method described in the pET System Manual (10th ed., Novagen). Briefly, a culture of *E. coli* BL21(DE3)pLysS cells containing pET3d-*Pf*Prx-1 (from a single colony) was grown in 50 ml of fresh LB medium containing 100 μg ml^{-1} ampicillin at 37°C until OD$_{600}$ reached 0.6-0.7. An aliquot was kept as the uninduced control and the remainder was induced by adding isopropyl β-D-1-thiogalactopyranoside (IPTG) to a final concentration of 0.5, 1 or 2 mM. The induced cells were grown at different temperatures (4°C, 20°C, 37°C) and samples (1 ml) were taken at 1, 2, 3, 4 and 5 h and after overnight culture. The cells were collected by centrifugation at 10,000 g for 5 min. The cell pellets were kept on ice or at -20°C for later analysis.

Larger scale production of the *Pf*Prx-1 protein was performed similarly to the test

expression above except that 5 ml of overnight culture was used to inoculate 1000

ml LB medium containing 100 μg ml^{-1} ampicillin. After induction with 1 mM IPTG

at 37°C for 4 hours, the cells were harvested by centrifugation at 5,000 *g* for 15 min,

washed in 1 × PBS (137 mM NaCl, 2.7 mM KCl, 10 mM sodium phosphate dibasic,

2 mM potassium phosphate monobasic and a pH of 7.4) and either processed

immediately or frozen in liquid nitrogen and stored at -80°C. All subsequent

experiments used cells which were cultured and harvested using exactly these

conditions.

3.2.12 Cell lysis

Cell pellets were lysed by sonication. Approximately, 1 ml of ice-cold extraction

buffer was added to 0.5 mg (wet weight) of cells and mixed by vigorous vortexing.

If using frozen cells, the cells were thawed on ice before the addition of extraction

buffer. The cells were then lysed by sonication (3 × 10 secs, kept on ice in between).

The lysate was centrifuged at 12,000 *g* for 30 min at 4°C and the supernatant was

retained for further analysis.

3.2.13 Determination of protein concentration

Total protein was determined using the Bradford assay with the Bio-Rad Coomassie

Blue dye reagent following the manufacturer's instruction (Bradford, 1976). Bovine

serum albumin (BSA) was used as the protein standard.

3.2.14 Peroxiredoxin enzyme assay

For the Prx enzyme assay, the extraction buffer was made up of 50 mM N-2-

hydroxyethyl-piperazine-N-2-ethanesulfonic acid (HEPES)-NaOH (pH 7.2), 1 mM

dithiothreitol (DTT), 0.2 mM EDTA and 1 mM phenylmethylsulfonyl fluoride

(PMSF). Cell extracts were prepared as described in section 3.2.12.

Prx enzyme activity was assayed as described by Kanzok *et al*. (2002). The reaction

mixture contained 50 mM HEPES-NaOH (pH 7.2), 100 μM β-nicotinamide adenine

dinucleotide 2′-phosphate (NADPH), 10 μM *E. coli* thioredoxin (Sigma, catalogue

no. T0910), 50 mU *E. coli* thioredoxin reductase (Sigma, catalogue no. T7915) and

200 μM H_2O_2. Assays were initiated by the addition of the cell extract after the

reaction mixture had been pre-incubated for 3 minutes at 25°C. Prx enzyme activity

was measured by following the decrease in absorbance at 340 nm, representing the

consumption of NADPH. One unit (U) of Prx enzyme activity is defined as the

amount required to oxidize one μmole NADPH per minute. The enzyme assay was

validated by (i) performing a "negative control" reaction in which the cell extract

(containing *Pf*Prx-1) was replaced with the same volume of the extraction buffer and

(ii) performing a "no substrate" reaction in which Trx was replaced with the same

volume of HEPES-NaOH buffer.

3.2.15 Sodium dodecyl sulfate polyacrylamide (SDS–PAGE) gel electrophoresis

The expression of recombinant *Pf*Prx-1 was analyzed using SDS–PAGE gel

electrophoresis following the method described by Sambrook *et al*. (1989). The

acrylamide concentration was 12% (w/v). The cell extracts were prepared as

described in section 3.2.12. Protein samples were prepared by mixing equal volumes

of the cell extracts and the sample loading buffer and then heating at 100°C for 1

min. The sample loading buffer contained 0.05 M Tris-HCl pH (6.8), 2% (w/v) SDS,

10% (v/v) glycerol, 2 mM EDTA, 50 mM DTT, 12 M urea and 0.0005% (w/v)

bromophenol blue. Gels were run at 170 V for 30-45 min. The proteins were stained

overnight in a solution containing 0.25% (w/v) Coomassie Brilliant Blue dye, 45%

(v/v) methanol and 10% (v/v) acetic acid and then destained in a solution containing

of 45% (v/v) methanol and 10% (v/v) acetic acid.

3.2.16 Immunodetection of *Pf*Prx-1

The presence of the His$_6$-tagged *Pf*Prx-1 protein was confirmed by western blotting

and immunodetection using a mouse Anti-Tetra His-Antibody (QIAGEN, catalogue

no. 34670) following the method specified by the manufacturer. Briefly, protein

extracts were run on SDS–PAGE gels as described in section 3.2.15 and then the

proteins were electroblotted to a nitrocellulose membrane. The membrane was blocked overnight at 4°C in 10 mM Tris-buffered saline (TBS, pH 7.4) containing 150 mM NaCl and 3% (w/v) BSA. After blocking, the membrane was incubated with the mouse Anti-Tetra His-Antibody at a dilution of 1:2000 in the blocking solution for 1 h at room temperature. The membrane was then washed in TBS-Tween/Triton buffer (20 mM Tris HCl , pH 7.5; 500 mM NaCl; 0.05% (v/v) Tween 20; 0.2% (v/v) Triton X-100) before being incubated with horseradish peroxidase conjugated Rabbit-Anti mouse IgG (Dako) at a dilution of 1: 1000 in 10% (w/v) skim milk powder in TBS for 1 h at room temperature. After four washes in TBS-Tween/Triton buffer, the membrane was incubated in a chemiluminescent substrate solution containing equal volumes of SuperSignal West Pico Luminol/Enhancer solution and SuperSignal West Pico Stable Peroxide (Progen). The membrane was then used to expose an X-ray film.

3.2.17 Purification of the recombinant *Pf*Prx-1 recombinant protein using Ni-affinity chromatograpthy

Transformed *E. coli* BL21 (DE3)pLysS cells giving high levels of expression of the *Pf*Prx-1 protein were used for protein purification. Approximately 5 g (wet weight) of cell pellet was used to prepare ~10 ml of cell extract as described in section 3.2.12. The extraction buffer consisted of 50 mM K_2HPO_4 + KH_2PO_4 (pH 8.0), 0.5 M NaCl, 10 mM imidazole, 1mM PMSF and 1 mM DTT. Cell debris was removed by ultracentrifugation at 45,000 g for 30 min at 4°C. The supernatant was filtered through a 0.2 or 0.45 µm membrane before being loaded onto the column.

The one-step metal affinity purification used a 5-ml HisTrap HP column prepacked with pre-charged Ni agarose medium (GE Health Science/Amersham, Catalogue no. 17-5248-01) following the manufacturer's instructions. The cell extract was loaded onto the column using a peristaltic pump at a flow rate of 0.5 ml min^{-1}. The column was then washed with 10 column volumes of lysis buffer followed by 10 column volumes of wash buffer (lysis buffer plus 20 mM imidazole). The His$_6$-tagged *Pf*Prx-1 protein was eluted from the column with elution buffer (lysis buffer plus 250 mM imidazole) at a flow rate of 1 ml min^{-1}. Peak A$_{280}$ fractions were saved for protein assays, Prx enzyme assays, SDS-PAGE and immunodetection.

For Prx enzyme assays, the fractions were buffer exchanged to remove the imidazole and concentrated to a protein concentration of ~0.5 mg/ml. The new buffer contained 50 mM HEPES-NaOH (pH 7.2), 0.2 mM EDTA, 1 mM DTT and 1 mM PMSF.

3.2.18 Protein concentration and/or buffer exchange

Buffer exchange was accomplished using PD-10 gel filtration columns (GE Healthcare) following the manufacturer's instructions. When required, protein samples were concentrated at 4°C using Amicon$^{®}$ ultra-centrifugation units fitted with 5 kDa-size exclusion ultracell membranes (Millipore, catalogueue no. UFC901024) following the manufacturer's instructions.

3.2.19 Gel filtration (GF) chromatography

To further purify and determine the molecular mass of the recombinant *Pf*Prx-1

protein, the fractions from the Ni-affinity column that contained the *Pf*Prx-1 protein

were pooled, buffer exchanged and concentrated to 10 mg protein ml^{-1} using the

same methods as described in section 3.2.18. The new GF column buffer contained

50 mM HEPES-NaOH (pH 7.2), 150 mM NaCl, 0.2 mM EDTA, 5 mM DTT and 1

mM PMSF. An aliquot (0.5 ml) of the concentrated protein sample was loaded at a

flow rate of 0.5 ml min^{-1} onto a Hiload 16/60 Superdex 200 prep grade gel filtration

column (GE Healthcare) attached to an FPLC system operated by UNICORN

software. The column was pre-equilibrated and eluted with the above GF column

buffer. Eluted proteins were collected in 2 ml fractions and their absorbance at 280

nm was monitored spectrophotometrically. Three fractions at each A_{280} peak were

analysed for the presence of the *Pf*Prx-1 protein by assaying them for Prx enzyme

activity and testing them by immunodetection using anti-His antibodies. Protein

samples were concentrated to a concentration of ~0.1 mg/ml as described in section

3.2.18 prior to enzyme assays and immunodetection. For molecular mass estimation,

standards of known M_r were used to calibrate the column (blue dextran 2,000,000;

β-amylase 200,000; alcohol dehydrogenase 150,000; albumin 66,000; carbonic

anhydrase 29,000 and cytochrome c 12,400; 500 μg of each).

3.2.20 Characterization of the recombinant *Pf*Prx-1 protein

3.2.20.1 Molecular mass determination using electrospray ionisation-mass

spectrometry

In order to obtain an accurate estimate of the molecular mass of the recombinant

*Pf*Prx-1 protein monomer, electrospray ionisation-mass spectrometry (ESI-MS) was

used. The Ni-affinity purified protein was treated with tributylphosphine (TBP) plus

iodoacetamide. TBP treatment was expected to reduce any disulfide bonds to form

sulphydryl groups. Iodoacetamide (IA) alkylates sulphydryl groups making the

reduction irreversible. The Ni-affinity purified *Pf*Prx-1 protein (concentration 5 mg

ml^{-1} in 50 mM HEPES-NaOH, 1 mM DTT, pH 7.2) was incubated for 1 h at room

temperature in a nitrogen-sparged airtight container with 5 mM TBP (Sigma,

catalogue no.T7567) and then 15 mM iodoacetamide (Sigma, catalogue no. A3221)

was added and the incubation was continued for another 1.5 h.

Following TBP treatment, the protein was desalted and buffer exchanged into sterile

deionized water as described in section 3.2.18. The protein sample was diluted into

sterile deionized water to a concentration of 0.185 mg ml^{-1} (~8 pmols per microlitre)

immediately prior to ESI-MS analysis. Electrospray ionisation (ESI) spectra were

recorded using a Quattro micro triple quadrupole mass spectrometer

(Waters/Micromass) fitted with an electrospray source. The spectra were scanned in

the positive ion mode, from m/z 1100 to m/z 1800, in 2 seconds. The cone voltage

was 60 V. The ESI capillary voltage was 3.0 kV and the source temperature was

80°C. The solvent was 50% (v/v) acetonitrile and the flow rate was 10 µl min^{-1}. The

mass scale for the instrument was calibrated by the separate analysis of a 5 pmol µl^{-1}

solution of horse heart myoglobin.

3.2.20.2 Determination of the effects of pH and urea concentration on the

oligomerization state of the recombinant PfPrx-1 protein

The effects of pH (5.4, 7.2, 7.5 and 8.5) and urea concentration (0 M, 1 M and 2.8

M) on the oligomerization state of the *Pf*Prx-1 protein were determined using the

same Superdex-200 gel filtration column and FPLC system as described in section

3.2.19. For the pH experiments, the gel filtration buffers used were 50 mM HEPES-

NaOH, 150 mM NaCl, 0.2 mM EDTA, 1 mM DTT and 5 mM PMSF adjusted to pH

5.4, 7.2, 7.5 or 8.5. For the urea experiments, the GF buffers used were 50 mM

HEPES-NaOH, 150 mM NaCl, 0.2 mM EDTA, 5 mM DTT, 1 mM PMSF with

either 0 M, 1 M or 2.8 M urea. The pH was adjusted to 7.2 after the addition of the

urea. In all cases, the column was equilibrated before the experiment with 2 column

volumes of the respective GF buffer. Ni-affinity purified *Pf*Prx-1 protein which had

been concentrated to 10 mg ml^{-1} (see above) was diluted to 1 mg ml^{-1} in the

respective GF buffer and incubated for approximately 1 h at room temperature prior

to loading onto the gel filtration column. The sample volume loaded onto the

column for each run was 0.5 ml (~0.5 mg protein). The loading and running of the

gel filtration column was the same as described in section 3.2.19.

3.2.20.3 Determination of the effect of the His$_6$-tag on Prx activity

In order to determine whether the presence of the N-terminal His$_6$-tag had any effect on the enzyme activity of the recombinant *Pf*Prx-1 protein, the protein was treated with Factor Xa to cleave off the His$_6$-tag. To do this, 1.6 U of Factor Xa (Promega) was added to 0.25 mg of the Ni-affinity purified *Pf*Prx2 in a reaction buffer containing 20 mM Tris-HCl (pH 7.4), 100 mM NaCl and 1 mM CaCl$_2$. The reaction was left at room temperature overnight. The treated sample was then applied to a Ni-affinity HisTrap column using the same protocol as described above. It was expected that the column would bind the His$_6$-tag. Thus, the *Pf*Prx-1 protein without the His$_6$-tag was collected in the flow-through from the column. Prx assays were performed as described in section 3.2.14.

3.2.21 Crystallization

3.2.21.1 Preparation of protein samples

The recombinant *Pf*Prx-1 protein was purified by Ni-affinity chromatography followed by gel filtration chromatography as previously described and the fractions containing the dimeric form of the protein (elution volume ~80 ml) were exchanged into a new buffer containing 20 mM HEPES-NaOH (pH 7.2) and 1 mM DTT and then concentrated to 12 mg ml^{-1} as described in section 3.2.18. The concentrated protein was stored at -20°C or used immediately. Prior to setting up the crystallization trials, the *Pf*Prx-1 protein solution was thawed on ice and filtered

using a Millex®-filter unit (pore size 0.22 μm) (Millipore) to remove any

precipitated protein.

3.2.21.2   *Initial screening of crystallization conditions*

The initial screening of crystallization conditions used the microbatch method. The

reagents to be tested were from the Crystal Screen (Hampton Research, catalogue

no. HR2-110) and Crystal Screen 2 (Hampton Research, catalogue no. HR2-112)

kits. There were 50 reagents in the Crystal Screen, named CS 1→ 50 and 48

reagents in the Crystal Screen 2, named CSII 1 → 48. The initial screens were set up

in micro-plates pre-treated with N-decane (Merck, catalogue no. S37079312) and

then filled with paraffin oil (BDH, catalogue no. 630024N). Each well was loaded

with 1.5 μl of the protein sample and 1.5 μl of the appropriate reagent. The samples

were loaded into each well through the paraffin oil and then mixed well with a

pipette tip. The plates were observed under a microscope after preparation and then

they were daily screened.

3.2.21.3 *Optimization of the initial screening*

The first optimization used the vapour diffusion method achieved by the sitting drop

technique using 24-well Chryschem plates (Hampton Research). In the vapour

diffusion method, the difference in concentration between the reservoir and the drop

drives the system to equilibrium via the vapour phase. This process concentrates the

protein in the drop until saturation is reached, when conditions may be suitable for the protein to come out of solution. Vapour diffusion usually allows slower formation of crystals and therefore may lead to better crystal formation compared to the microbatch method. In the vapour diffusion method, supersaturation is achieved gradually as the crystallization progresses. In contrast, in the microbatch method, supersaturation is achieved at the beginning of the experiment.

The first optimization used the crystallization reagents that gave promising results from the initial screen (Table 3.3). Protein samples (1 µl) were mixed with an equal volume of the crystallization reagent and then placed on a bridge in the middle of a well and the well was filled with 0.5 ml of the same crystallization reagent (Fig. 3.1). The plate was carefully sealed with crystal tape and incubated at 20°C. The plates were examined after preparation, then every day during the first week, then once or twice a week thereafter.

After the first optimization, all subsequent experiments used self-made crystallization reagents instead of those from the Crystal Screen kits. A summary of all reagents used for crystallization optimization is shown in Table 3.3. All crystallization optimization plates were set up, incubated, and examined in the same way as for the first optimization.
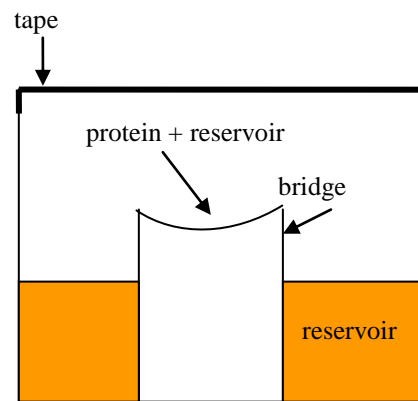
Figure 3.1: **Sitting drop vapour diffusion method of crystallization**

3.2.21.4 Microseeding

Microseeding is a way to control the crystallization process by separating the nucleation phase from the growth phase. It can sometimes lead to the formation of larger crystals. The small crystals from one of the previous optimizations (fifth optimization) were chosen. A well with a well-formed crystal was selected and the crystal was crushed with a glass fiber and then resupended in 100 µl of the well solution in a sterile microfuge tube. The tube was vortexed to break the crystals into seeds. Several seed dilutions (1:10, 1:50 and 1:100) were made with the well solution. Sitting drop diffusion was performed. The drop consisted of 0.5 µl seed crystals mixed with 1 µl protein sample and 0.5 µl reservoir solution.

3.2.22 X-ray Analysis of Crystal Structure

3.2.22.1 Harvesting crystals

Crystals were visually inspected for quality and their dimensions were measured using a Leica microscope. Selected crystals were transferred to a solution containing 20% (v/v) glycerol in mother liquor prior to flash-cooling by plunging directly into liquid nitrogen.

3.2.22.2 *X-ray analysis of the crystals*

X-ray data were collected on X-ray diffraction equipment located at the University

of Queensland (Australia). The X-ray diffraction equipment consisted of a Rigaku

FR-E X-ray generator operated at 45 kV and 45 mA. The images were recorded

using a Rigaku R-AXIS IV$^+$ imaging-plate detector. A native data set was collected

from a single crystal. The crystal-to-detector distance was 150 mm. A total of 240

rotation images were collected with an oscillation angle of 0.5°. Data for the

complex were integrated, scaled and merged using the program *CrystalClear* 1.3.6

and later using *MOSFLM*.

3.3 Results

3.3.1   Cloning and sequencing of the *Pf*Prx-1 gene

A single product of approximately 600 bp was obtained for the amplification of the

*Pf*Prx-1 protein coding region by PCR from *P. falciparum* strain 3D7 genomic DNA

(Fig. 3.2). The ~ 600 bp product was ligated into the pET3d vector and the ligation

products were used to transform *E. coli* DH5α cells. Fig. 3.3 shows the PCR

products obtained from colony screening for the presence of the *Pf*Prx-1 insert in

four putatively positive colonies. All had prominent bands of the expected size

(~600 bp) plus another unidentified band of ~1200 bp. Plasmid DNA was isolated

from these colonies and the *Pf*Prx-1 insert plus the flanking regions were sequenced.

The *Pf*Prx-1 coding region was identical to the published sequence (GenBank

accession no. AF225977) and it was in frame. The His$_6$-tag was also present and in

frame (see Appendix B).

3.3.2   Expression of the recombinant *Pf*Prx-1 protein

*Pf*Prx-1 was expressed as a His$_6$-tagged protein in *E. coli* BL21(DE3)pLysS cells.

Different IPTG concentrations (0.5 M, 1 M, 2 M) did not seem to affect the level of

expression (data not shown). Fig. 3.4 shows the effects of induction temperature and

duration of induction on *Pf*Prx-1 expression. For the induced samples (except at

4°C), there were two prominent protein bands (Fig. 3.4, lanes 4, 6 and 8). The

molecular mass of the upper band was approximately 23 kDa which is the calculated

size for the recombinant *Pf*Prx-1 monomer and the molecular mass of the lower

band was around 21 kDa. These prominent protein bands were completely absent

from the 'no insert' control (i.e. cells transformed with the pET3d vector without the

*Pf*Prx-1 insert) (Fig. 3.4, lane 9) suggesting that they both belong to *Pf*Prx-1.

From Fig. 3.4, it can be seen that the abundance of these two protein bands increased

with duration of induction from 4 h (lane 8) to overnight (lane 6). An induction

temperature of 37°C (lane 6) yielded more *Pf*Prx-1 protein compared to the other

lower induction temperatures (lanes 2 and 4). While the prominent protein bands

were absent in the uninduced sample after 4 h at 37°C (lane 7), they started to

appear when the cells were left overnight at either 15°C or 37°C (lanes 3 and 5).

This suggested that there was some 'leaky' expression.
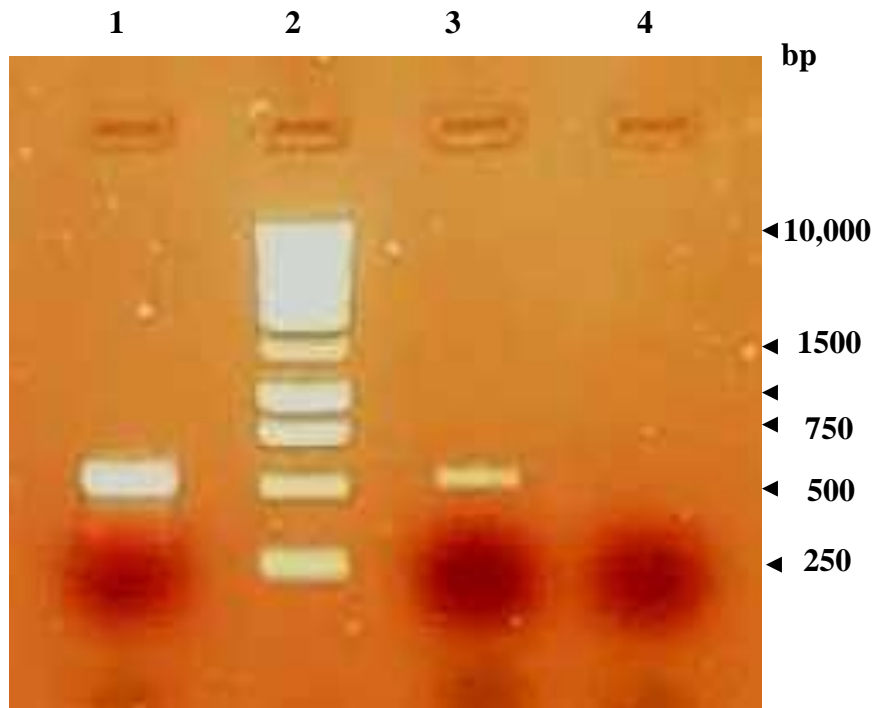
Figure 3.2: **PCR amplification of the *Pf*Prx-1 protein coding region using *P.
falciparum* (strain 3D7) genomic DNA as the template**. Lane 1: 5 μl (~2.5 μg
DNA) of the PCR products obtained from the reaction with 0.5 mg genomic DNA;
Lane 2: 0.5 μg of a 1 kb DNA ladder (Promega, catalogue no. G5711); Lane 3: 1 μl
(~0.5 μg DNA) of PCR products obtained from the reaction with 0.5 mg genomic
DNA; Lane 4: 5 μl of the the PCR products obtained from the reaction without the
genomic DNA template (negative control). The sizes of the molecular markers (bp)
are shown with the arrows on the right.
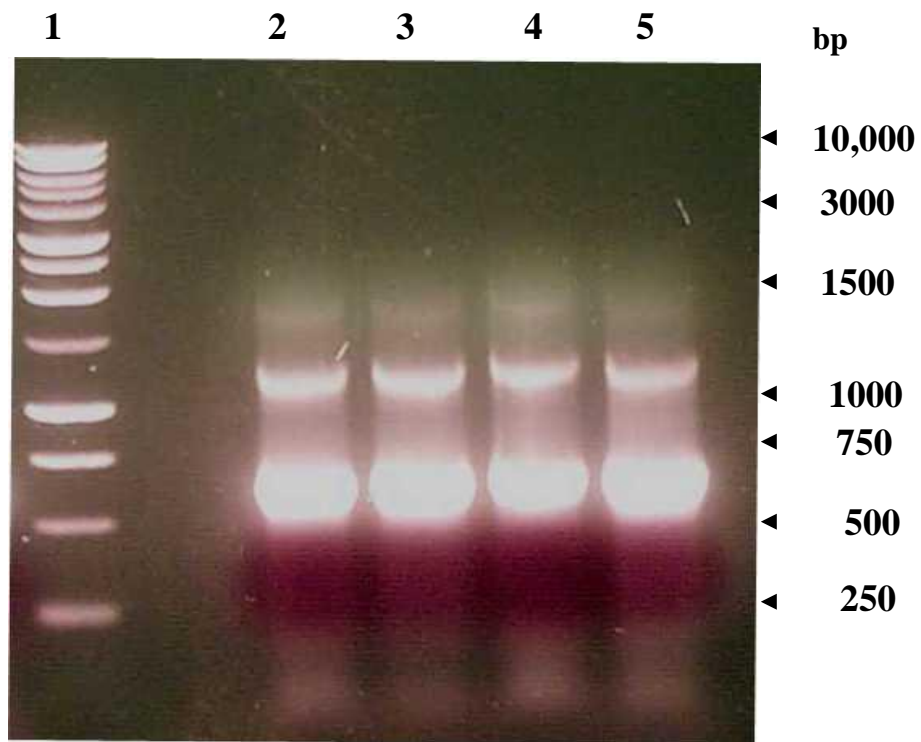
Figure 3.3: PCR screening for the presence of the *Pf*Prx-1 insert in four independent colonies of *E. coli* BL21(DE3)pLysS cells transformed with the pET3d-*Pf*Prx-1 construct. Lane 1: DNA size marker (Promega). Lanes 2-5: PCR products from four independent colonies. The sizes of the molecular markers (bp) are shown with the arrows on the right.
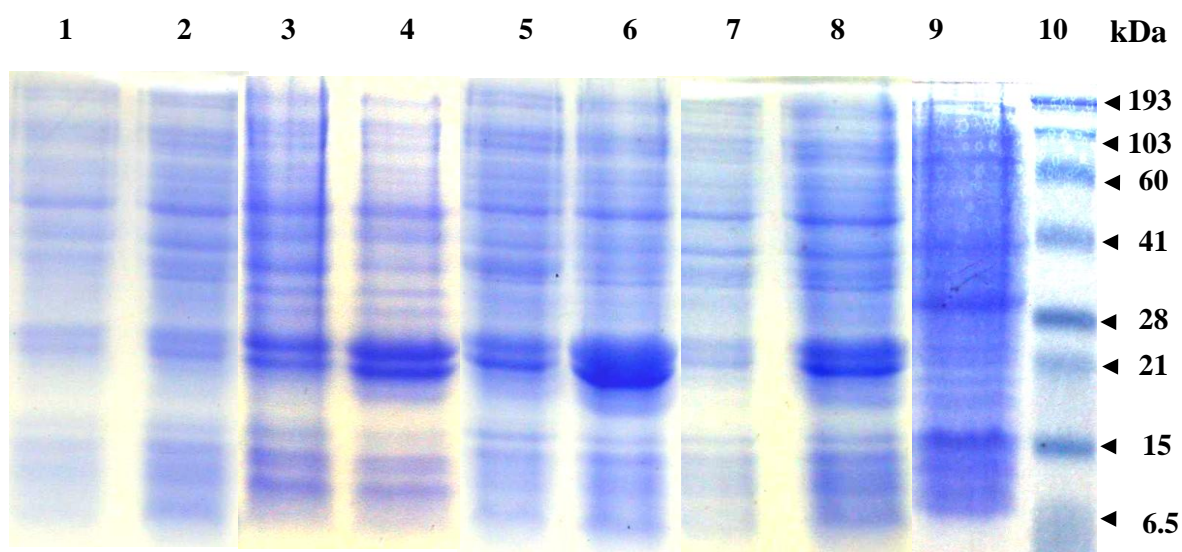
Figure 3.4: SDS-PAGE analysis of recombinant *Pf*Prx-1 protein expression in *E. coli* BL21(DE3)pLysS cells. Lane 1, uninduced, overnight at 4°C (10 μg protein); lane 2, induced, overnight at 4°C (12 μg protein); lane 3, uninduced, overnight at 20°C (14 μg protein); lane 4, induced, overnight at 20°C (15 μg protein); lane 5, uninduced, overnight at 37°C (14 μg protein); lane 6, induced, overnight at 37° C (20 μg protein); lane 7, uninduced, 4 h at 37°C (12 μg protein); lane 8, induced, 4 h at 37°C (14 μg protein); lane 9, empty vector control, induced, overnight at 37°C (20 μg protein); lane 10: 5μl pre-stained SDS-PAGE broad range marker (Bio-Rad). The sizes of the molecular markers (kDa) are shown with the arrows on the right. All cell cultures were grown at 37°C before being induced with 1 mM IPTG. After induction, the cultures were incubated at appropriate induction temperatures and harvested after appropriate time intervals. Proteins were extracted from the cells as described in section 3.2.12 and soluble extracts were loaded onto the gel.

As the level of *Pf*Prx-1 protein expression was reasonably high after 4 h at 37°C, this induction time and temperature were used for all other experiments in this study. These conditions yielded approximately 168 mg of soluble protein per litre of culture.

3.3.3   Purification of the recombinant *Pf*Prx-1 protein

The recombinantly expressed *Pf*Prx-1 protein with the His_6-tag attached was purified using HisTrap HP Ni-affinity column chromatography. Fig. 3.5A shows that the recombinant *Pf*Prx-1 protein was eluted from the Ni-affinity column with 250 mM imidazole. Immunodetection using an anti-His antibody showed that some of the *Pf*Prx-1 protein was eluted with the 20 mM imidazole wash as well (Fig. 3.5B). The *Pf*Prx-1 protein obtained with the 250 mM imidazole wash was highly purified but it was decided to follow the Ni-affinity purification step with a gel filtration purification step to further purify the protein and to obtain information about its native molecular mass. The yield of Ni-affinity purified *Pf*Prx-1 protein was approximately 12.5 ± 0.33 mg protein per litre of culture and its Prx activity was approximately 0.75 ± 0.21 U mg^{-1} protein.

A

B
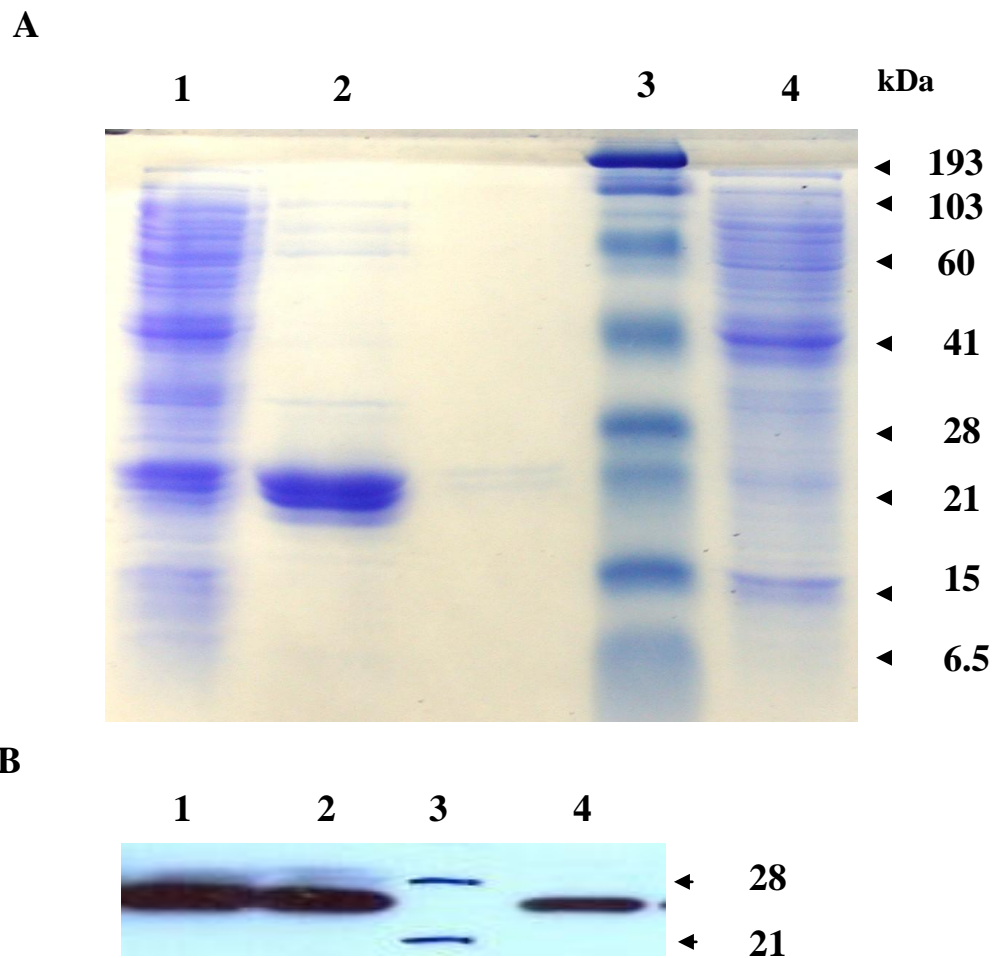
Figure 3.5: **SDS-PAGE (A) and Immunoblot detection (B) analysis of Ni-affinity chromatography purification of recombinant *Pf*Prx-1.** Lane 1, crude extract (20 μg protein); lane 2, peak fraction from the elution of the column with 250 mM imidazole (~10 μg soluble protein); lane 3, prestained SDS-PAGE broad range marker (Bio-Rad); lane 4, peak fraction from the 20 mM imidazole wash of the column (~15 μg soluble protein). The sizes of the molecular markers (kDa) are shown with the arrows on the right. For Immunoblot detection, the amounts of protein used were half those used for SDS-PAGE.

3.3.4   Prx enzyme activity

The Ni-affinity purified *Pf*Prx-1 possessed Prx enzyme activity as it efficiently catalyzed the reduction of H_2O_2 in the presence of NADPH, Trx and TrxR (as a thioredoxin regenerating system). At 25°C and in the presence of 10 μM Trx and 200 μM H_2O_2, the specific activity of the Ni-affinity purified Prx protein was 0.75 U $\pm$ 0.21 mg^{-1} protein. Negative-control assays included (i) a reaction in which the *Pf*Prx-1 protein sample was replaced with the buffer and (ii) a reaction without the reducing partner Trx. Neither of the negative controls showed any Prx activity. These results demonstrate that the protein was indeed a thioredoxin-dependent peroxidase. Following His$_6$-tag removal, the Ni-affinity purified *Pf*Prx-1 protein had a specific activity of 0.46 ± 0.15 U mg^{-1} protein which was approximately half of its activity before tag removal (0.75 ± 0.21 U mg^{-1} protein).

3.3.5   Molecular mass determination by ESI-MS

The molecular mass of the Ni-affinity purified *Pf*Prx-1 protein after treatment with TBP+IA to irreversibly reduce any disulphide bonds was determined by ESI-MS. The results showed that there was a major peak corresponding to 23586 ± 3 Da and five minor peaks corresponding to 23457 Da, 23534 Da, 23645 Da, 23683 Da, 23851 Da.

3.3.6   Analysis of the native molecular mass of the Ni-affinity purified *Pf*Prx-1 protein using gel filtration chromatography

Fig. 3.6 shows two major peaks and one minor peak. The peak at 58 ml (A) corresponded to a size of 222 kDa and the peak at 80 ml (B) corresponded to a size of 44 kDa. Both peaks contained recombinant *Pf*Prx-1 protein as confirmed by SDS-PAGE and immunodetection (Fig. 3.7). Given that the calculated molecular mass of the recombinant *Pf*Prx-1 monomer is ~ 23 kDa, the first peak (222 kDa) corresponds closely to a decamer and the second peak corresponds closely to a dimer. Both forms of the protein exhibited Prx enzyme activity with specific activities of 0.83 ± 0.16 and 0.10 ± 0.03 U mg^{-1} protein for the decameric and dimeric forms, respectively. The minor peak (C) corresponding to an intermediate (tetramer) form also had similar enzyme activity to the dimer form.

Fig. 3.8 illustrates the effects of pH on the oligomerization state of the recombinant *Pf*Prx-1 protein. At pH 5.5, a major peak (A) was observed corresponding to the decamer size and a minor peak (D) corresponding to a larger size (501 kDa corresponding to approximately 20 subunits). At pH 7.2 and pH 7.5 the results were similar to those at pH 5.5 in that there was a major peak (A) corresponding to the decamer size. However, there was also a minor peak corresponding to the dimer size (B). In contrast, at pH 8.5, there was a major peak (B) corresponding to the dimer size but only minor peaks (C) corresponding to the larger sizes (tetramer and hexamer). Thus, the recombinant *Pf*Prx-1 eluted mainly as a decamer at lower pH values (5.5, 7.2 and 7.5) and mainly as dimer at higher pH values (8.5).
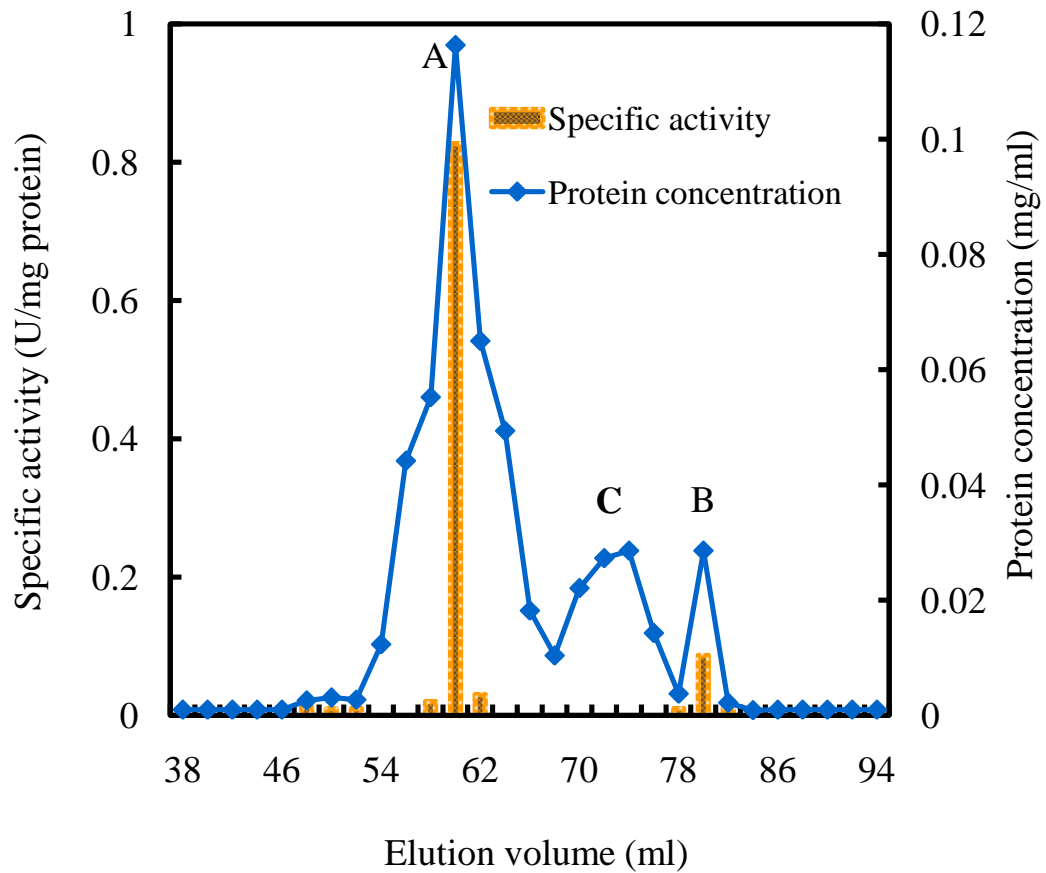
Figure 3.6: **Gel filtration column chromatography of the *Pf*Prx-1 fractions from the Ni-affinity column**. The total amount of protein loaded onto the gel filtration column was 5 mg in a volume of 0.5 ml.

A

B
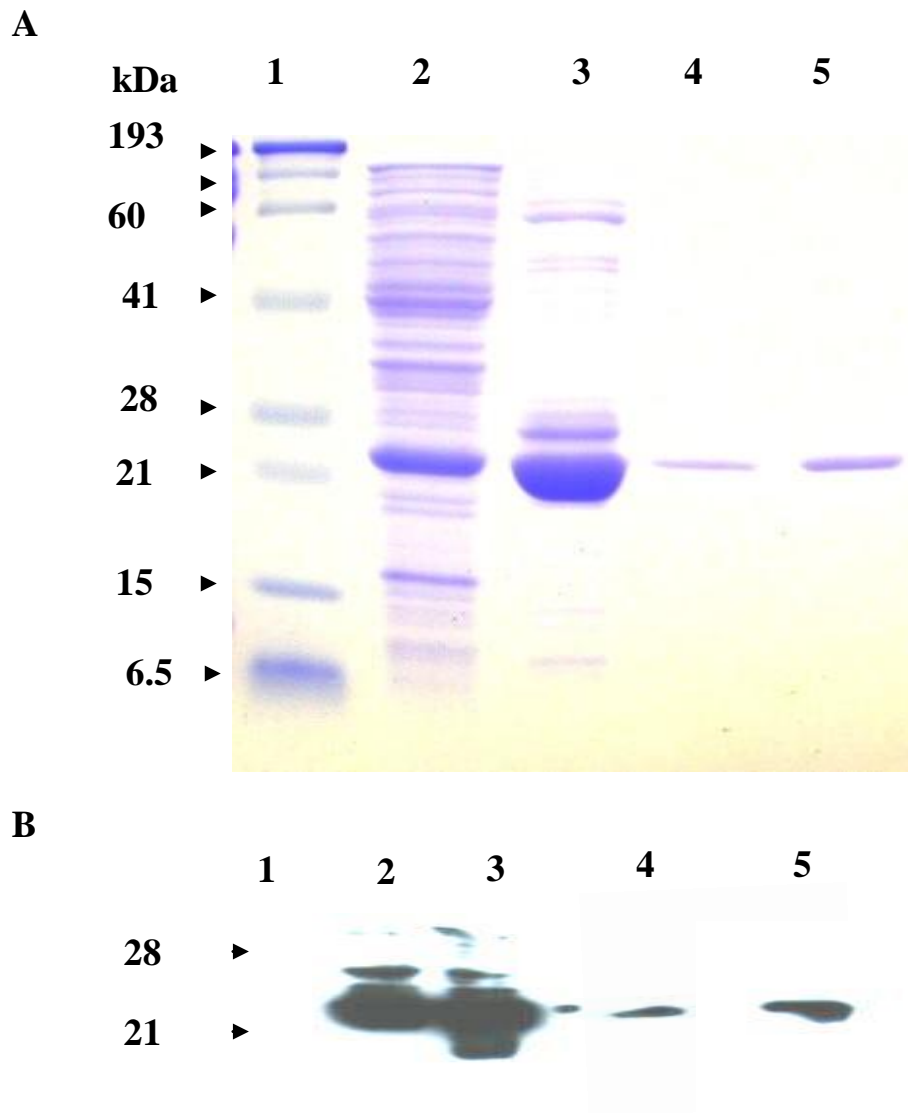
Figure 3.7: **SDS-PAGE (A) and Immunodetection (B) analysis of the fractions obtained before and after gel filtration chromatography** (see Figure 6). Lane 1, 5 µl of the prestained SDS-PAGE broad range marker (Bio-Rad); Lane 2, crude extract (~18 µg protein); lane 3, concentrated sample eluted with 250 mM imidazole from Ni-affinity column (refer to Fig. 3.6:~15 µg soluble protein); lanes 4, peak fraction eluted at 58 ml from gel filtration column (refer to Fig. 3.6; ~2 µg soluble protein); lane 5, peak fraction eluted at 80 ml from gel filtration column (refer to Fig. 3.6; ~4 µg soluble protein). The sizes of the molecular markers (kDa) are shown with the arrows on the left.
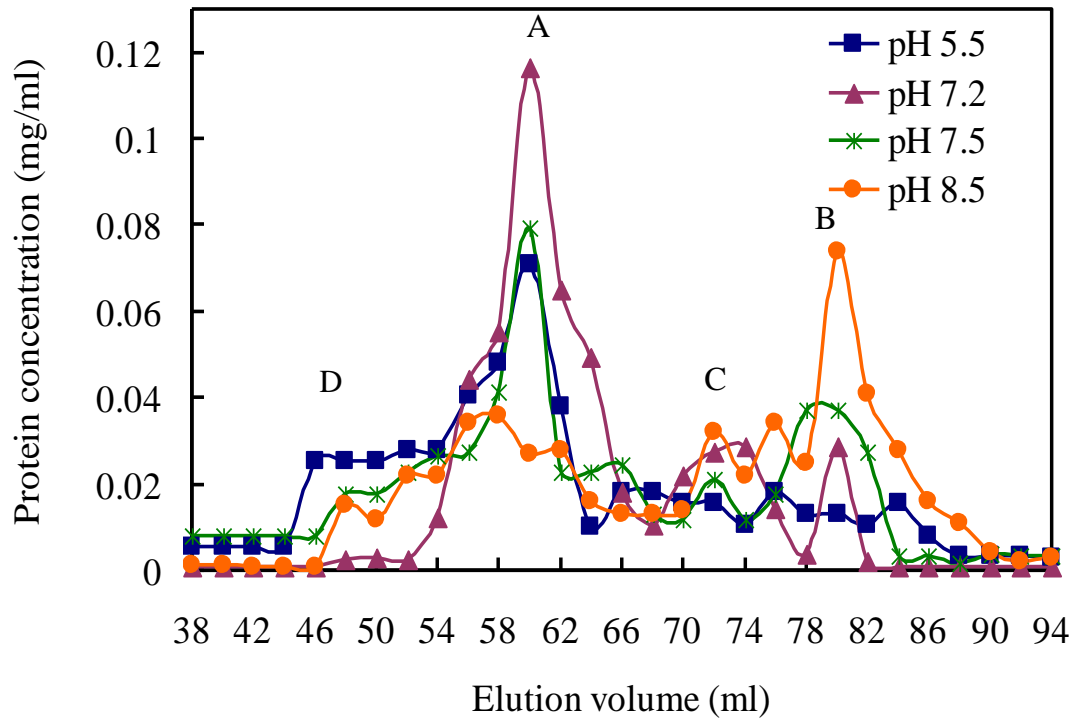
Figure 3.8: **Gel filtration chromatography analysis of the effect of pH on the oligomeric state of the Ni-affinity purified *Pf*Prx-1 protein**. Total amount of protein loaded for each of the four gel filtration runs was ~0.5 mg in a volume of 0.5 ml. A, B, C and D are the peak elution fractions

The effect of urea on the oligomerization state of the recombinant *Pf*Prx-1 protein was also studied (Fig. 3.9). Increasing the concentration of urea decreased the abundance of the supposed decameric form (peak A) of the enzyme and possibly also increased the abundance of the dimeric form (peak B) although the latter was not particularly clear. The intermediate form (peak C) was present in all three conditions. There was a small peak corresponding to the decamer size for the protein treated with 2.8 M urea suggesting that dissociation to dimers was mostly complete at this urea concentration.

3.3.7   Crystallization

3.3.7.1   Initial crystallization screen

The crystallization screen was set up with the supposed dimeric form of the *Pf*Prx-1 protein purified using Ni-affinity chromatograph followed by gel filtration chromatography. The protein was kept in a solution containing 1 mM DTT which was presumed to maintain it in its reduced form. Initial screens were set up using the Crystal Screen and Crystal Screen II kits (Hampton Research). After 7 days, observations were recorded and the most promising conditions are summarised in Table 3.3.
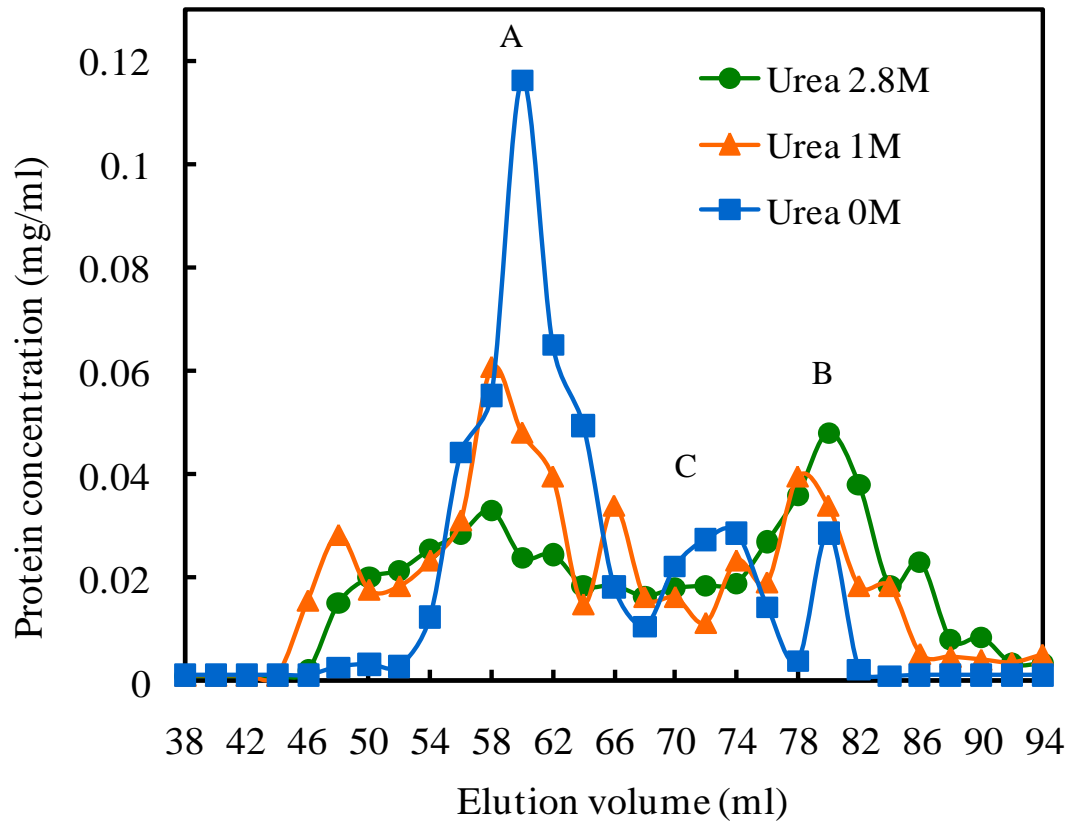
Figure 3.9: Gel filtration chromatography analysis of the effect of urea concentration on the oligomeric state of the Ni-affinity purified *Pf*Prx-1 protein. Total amount of protein loaded for each of the four gel filtration runs was ~0.5 mg in a volume of 0.5 ml. A, B and C are the peak elution fractions

Table 3. 3. Summary of initial crystal screen and optimizations of protein crystallization

	Crystallizing conditions tested	**Results**
Initial screen Microbatch method	All reagents from CS and CSII kits Protein concentrations 10 mg/ml	Crystalline precipitates Phase separation Some crystal-like formation (Figure 10A)
1st optimization Sitting drop vapour diffusion	Selective reagents from CS and CS II kits - CS kit: CS 1, 2, 8, 12, 13, 14, 16, 17, 24, 32, 34, 44 - CSII kit2: CSII 5, 8, 14, 15, 20, 24, 25, 29, 32, 37, 39, 42 Protein concentrations 10 mg/ml	CSII 39 consisting of 3.4 M 1,6 Hexanediol, 0.1 M Tris-Cl pH 8.5, 0.2 M magnesium chloride (MgCl$_2$) gave the best result of crystal formation Crystal had needle-like shape, size ~ 500 μm × 25 μm) (Figure 10B)
2nd optimization Sitting drop vapour diffusion	*Varying protein concentrations, 1,6-Hexanediol concentrations and pHs* - 1,6 Hexanediol concentrations: 40, 45, 50, 55, 60 % (w/v) - pHs: 8.0, 8.5, 8.8 - Protein concentrations: 8, 10 and 12 mg/ml - 0.1M Tris-Cl and 0.2 M MgCl$_2$ were kept the same. There were total of 45 conditions Note: Original concentration of 1,6 Hexanediol was 3.4 M equipvalent to 40.18% w/v)	pHs 8.0 and 8.5 gave bigger crystals Protein concentrations 12 mg/ml gave bigger crystals Crystals were very small, had cubic-like shape, size < 10 μm × 10 μm
3rd optimization Sitting drop vapour diffusion	*Varying 1,6 Hexanediol concentrations and pHs* - 1,6 Hexanediol concentrations: 40, 50, 60, 67 % (w/v) - pHs : 7.5, 8.0, 8.5 - 0.1 M Tris-Cl and 0.2 M MgCl$_2$ were kept the same - Protein concentration 12 mg/ml There were total of 12 conditions	1,6 Hexanediol concentration ~ 50%(w/v) and pH 8.5 gave biggest crytals Crystals were small and had column-like shape size ~ *20* μm × *30* μm

Table 3.3 (Continued)	Crystallizing conditions tested	Results
4th optimization Sitting drop vapour diffusion	*Varying MgCl$_2$ and 1,6 Hexanediol concentrations* - MgCl$_2$ concentrations: 2, 4, 6, 8 % (w/v) - 1,6 Hexanediol concentrations: 48, 48.5, 49.5, 50, 50.5, 51, 51.5% (w/v) - 0.1 M Tris-Cl, pH 8.5 was kept the same - Protein concentration 12 mg/ml There were total of 28 conditions Note: Original concentration MgCl$_2$.6H$_2$O of used was 0.2 M equivalent to 4.07 % (w/v)	1,6 Hexanediol concentration between 49- 50%(w/v) and MgCl$_2$.6H$_2$O concentration around 4% w/v gave best results Crystals were small and had column-like shape size ~ *20* μm × *30* μm
5th optimization Sitting drop vapour diffusion	*Varying MgCl$_2$.6H$_2$O and 1,6 Hexanediol concentrations* - MgCl$_2$.6H$_2$ O concentrations: 3.5, 4, 4.5, 5, 5.5, 6 % (w/v) - 1,6 Hexanediol concentrations: 48.5, 49, 49.5, 50 (w/v) - 0.1 M Tris-Cl, pH 8.5 was kept the same - Protein concentration 12 mg/ml There were total of 24 conditions	1,6 Hexanediol concentration ~ 50%(w/v) and MgCl$_2$.6H$_2$O concentration ~4% w/v gave best results Crystals were small and had column-like shape size ~ *20* μm × *50* μm (Figure 10C)
6th optimization Sitting drop vapour diffusion	*Microseeding* Conditions used for microseeding was - 50% w/v 1,6 Hexanediol and 4% w/v MgCl$_2$.6H$_2$O 0.1 M Tris-Cl, pH 8.5	Crystals were small and had column-like shape size ~ *10* μm × *20* μm

During the initial screening, several different conditions resulted in some kind of precipitate, phase separation, micro crystals or salt crystals. Certain precipitants within certain concentration ranges were observed to give a high frequency of some sort of precipitate, phase separation or micro-crystals. Optimisation of the initial trials took advantage of this trend.

3.3.7.2   Optimization of the initial crystallization screen

Crystallization was optimized by varying the pH of the buffer or by varying the concentration of one or more of the precipitating agents. Results of the optimization process are shown in Table 3.3. Most drops produced very small crystals with either cubic shape (smaller in size) or columnar shape (bigger in size) two weeks after setup. Figs. 3.10B and C show promising protein crystals and they are contrasted with the lithium sulphate salt crystal shown in Fig. 3.10A. Microseeding was tried but it did not improve the size of the crystals. There were three crystals at around 20 $\mu m \times 50$ μm obtained 4 weeks after setup. A photo of one of the three crystals is shown in Fig. 3.10C. The rest of the crystals were smaller in size. The three bigger crystals were subjected to X-ray diffraction analysis.
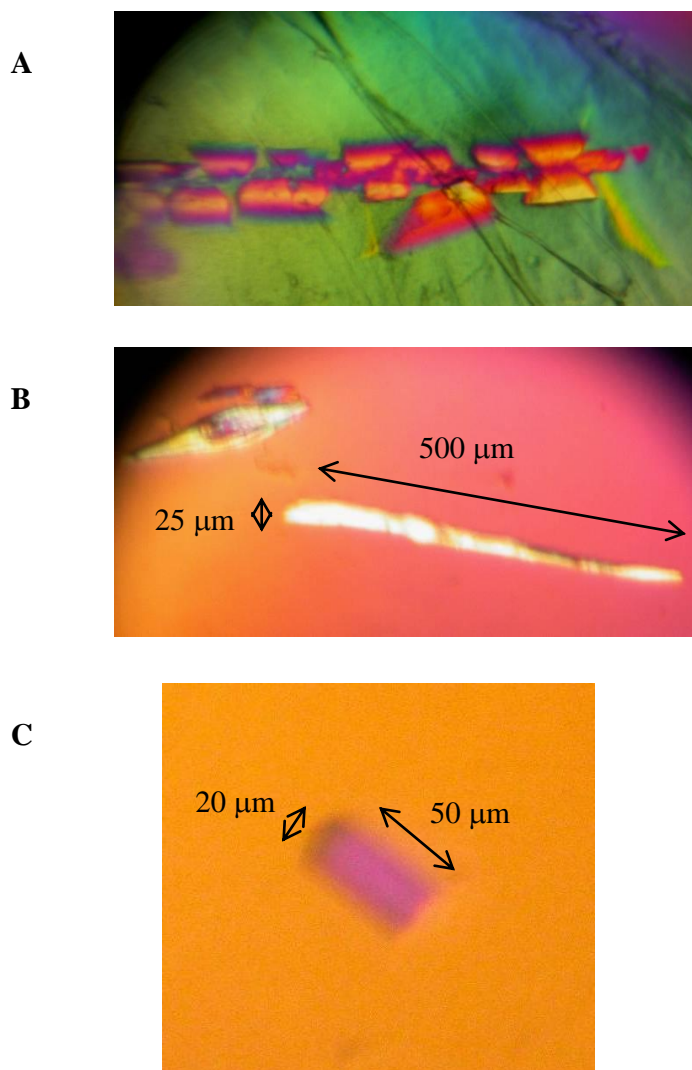
Figure 3.10: Crystal photos. (A) Salt crystals obtained with 1.5 M lithidium sulfate and 0.1 HEPES-NaOH (pH 7.5) after 8 days (initial screen); (B) Protein crystals obtained with 3.4 M 1,6 Hexanediol, 0.2 M MgCl$_2$, 0.1 M Tris-Cl (pH 8.5) and 1 µg recombinant *Pf*Prx-1 after 4 weeks (first optimization, refer to Table 3.3); (C) Protein crystal obtained with 50% (w/v) 1,6 Hexanediol, ~4% w/v MgCl$_2$, 0.1 M Tris-Cl (pH 8.5) and 1.2 µg recombinant *Pf*Prx-1 after 4 weeks (fifth optimization, refer to Table 3.3)

3.3.8   X-ray diffraction analysis

One out of the three crystals diffracted to 6-7 Å. All diffraction images show a dark ring around the beam stop (Fig. 3.11A). However, when the contrast was adjusted to a smaller range (between 200 to 500), the diffraction pattern could be viewed (Fig. 3.11B). It was not possible to integrate and merge all data. However, indexing of selected images revealed that the crystal belongs to space group P2, with unit-cell parameters a= 117.37; b= 67.11; c= 118.36; α=90.00°; β= 119.53°; γ= 90.00° (Table 3.4). The space group describes the symmetry of the crystal. A crystal is a periodic arrangement of a motif (i.e. a protein molecule in this case) in a lattice (Malkin and Thorne, 2004). Often, the motif is subjected to a number of symmetry operations yielding differently oriented copies that are packed in one unit cells. The crystal is built from the unit cells arranged into a three dimensional lattice. The combination of all available symmetry operations is represented by the Space group.

Schematically, a crystal can be described with the aid of a grid of lattice, defined by three axes and the angles between them. Along each axis a point will be repeated at distances referred to as the unit cell constants, labelled a, b and c. The angles between b and c, a and c and a and b are denoted α, β and γ, respectively.
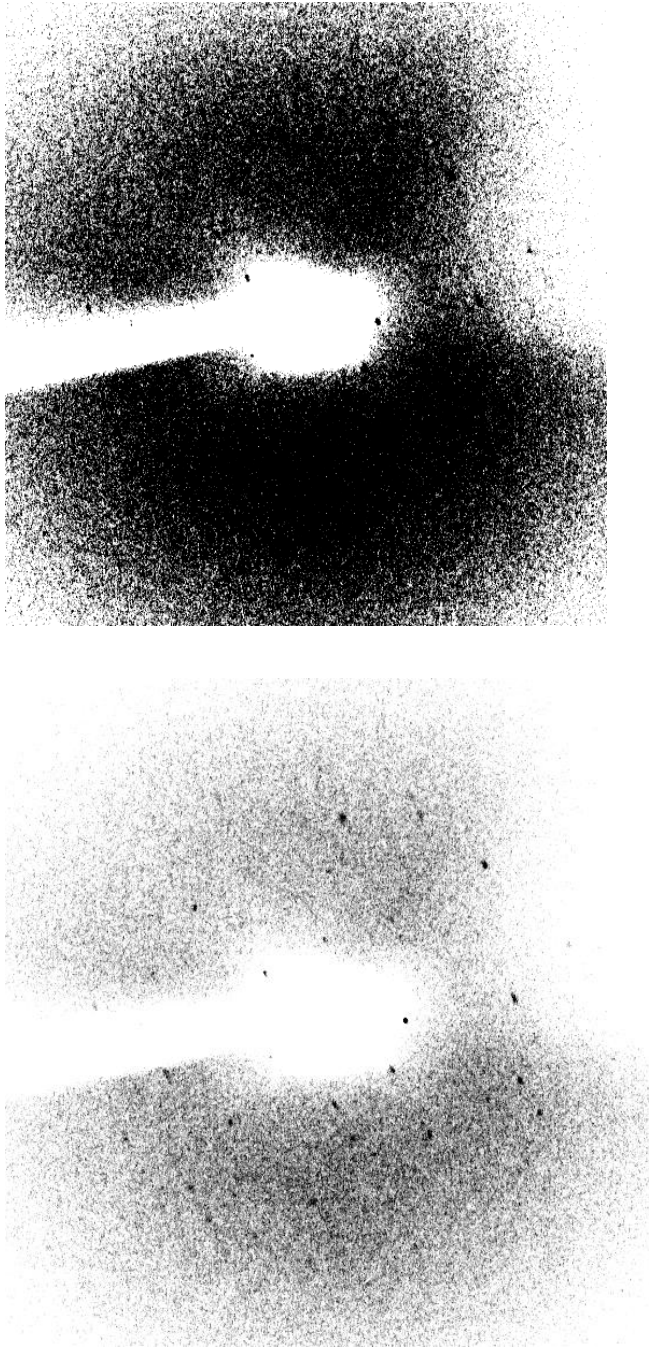
Figure 3.11. Diffraction pattern of the *Pf*Prx-1 protein crystal. (A) Before contrast adjustment, (B) After contrast adjustment

Table 3.4. Summary of data collection and statistics for *Pf*Prx-1 X-ray data

Space group	**P2**
Unit cell dimensions (units)	
unit cell lengths	a = 117.37; b = 67.11; c = 118.36
unit cell angles	α = 90.00; β = 119.53; γ = 90.00
unit cell volume	8110.560.77
Resolution range (Å)	6-7
Total number of unique reflections	250
Mosaicity	0.5
I/σ (cut off)	5

3.4 Discussion

3.4.1   Cloning and recombinant expression of *Pf*Prx-1

The cloning and recombinant expression of *Pf*Prx-1 in *E. coli* was first reported by Kawazu *et al*. (2001), Krnajski *et al*. (2001) and Ralfhs and Becker (2001). The results of this study are broadly similar to those previously reported. The recombinant *Pf*Prx-1 was expressed as a His$_6$-tagged protein in *E. coli* and purified to near homogeneity using a combination of Ni-affinity and gel filtration chromatography. The yield of the recombinant *Pf*Prx-1 was approximately 12.5 mg protein per litre of culture. This yield is higher than the 2-5 mg protein per litre of culture previously obtained by Krnajski *et al*. (2001).

The recombinant *Pf*Prx-1 reacted with H$_2$O$_2$ using *E. coli* Trx as the reducing partner confirming that it was functional. The presence of the His$_6$-tag did not affect enzyme activity as the *Pf*Prx-1 after His$_6$-tag cleavage did not show any increase but in fact a decrease in specific activity. The reason for this activity decrease might be due to the fact that cleaving the His-tag can change the protein conformation. As reported in previous studies, the presence of an N-terminal His$_6$-tag in a recombinant 2-Cys Prx (mammalian PrxIII) markedly enhanced the stability of high molecular weight forms (decamer, dodecamer) which had higher activity than the dimer (Cao *et al*., 2007). The process of His$_6$-tag cleavage (FactorXa treatment) might also have affected the Prx activity. This theory, however, has not been tested.

As in the previous studies, the recombinant *Pf*Prx-1 protein appeared as two prominent bands on SDS-PAGE gels (Fig. 3.4). The upper band had the size expected for the *Pf*Prx-1 monomer, i.e., approximately 23 kDa whereas the lower band was slightly smaller. Other authors have suggested that this size difference could be due to different conformations of the *Pf*Prx-1 monomer (Kawazu *et al*. 2001, Rahlfs and Becker 2001). For example, there could be intramolecular interactions between Cys residues within a single monomer to form intra-monomer-disulfide bonds as described for the 2-Cys Prx proteins from yeast and *E. coli* (Choi *et al*., 2003, Chae *et al*., 1994). Rahlfs and Becker (2001) obtained the protein species representing the lower band after prolonged storage at 4°C and found that its enzyme activity was similar to other Prx proteins in that it was reduced by *Pf*Trx and it was able to reduce H_2O_2, *tert*-butylhydroperoxide and cumene hydroperoxide. These results suggest that the smaller form of *Pf*Prx-1 is also functional.

Another possibility for the presence of the lower band could be partial proteolytic degradation of the *Pf*Prx-1 protein. Cha *et al*. (2000) reported that the human erythrocyte plasma membrane Prx, also known as human thiol-specific antioxidant protein 1 (hTSA1), fragmented to form a smaller protein species during the purification process. This smaller protein species was found to be the result of cleavage of a C-terminal fragment which did not affect either the typical 2-Cys Prx Cys motifs or Prx enzyme activity. In this study, the second, smaller band was absent after the gel filtration step suggesting it is more likely the case of changing protein conformation rather than protein degradation. If an intra-monomer-disulfide bond were involved, the high concentration of reducing reagent DTT (5mM) in the gel filtration buffer seemed to reduce this bond. Due to the fact that high

concentrations of DTT can affect the performance of Ni-affinity columns, the DTT concentration was kept at 1 mM. This might not have been enough to remove all intramolecular disulfide bonds.

The purified recombinant *Pf*Prx-1 had a specific activity of 0.75 ± 0.21 U mg^{-1} protein following Ni-affinity chromatography and 0.83 ± 0.16 U mg^{-1} protein (in the decameric form) following gel filtration chromatography. This small increase in specific activity is consistent with the conclusion that the enzyme was already highly purified following Ni-affinity chromatography. This conclusion is supported by the SDS-PAGE results shown in Fig. 3.5A. The specific activity of this enzyme preparation is lower than the specific activity of the enzyme prepared by Rahlfs and Becker (2001). Their recombinantly expressed *Pf*Prx-1 had a specific activity of 3.1 U mg^{-1} protein. The difference could be due to the fact that Rahlfs and Becker (2001) used recombinantly expressed *P. falciparum* Trx and TrxR to assay their *Pf*Prx whereas we used *E. coli* Trx and TrxR. Even though it has been demonstrated that *Pf*Prx-1 is capable of using *E.coli* Trx and TrxR to reduce H_2O_2 (Kawazu *et al.*, 2001), it is likely that *Pf*Prx-1 has a lower affinity for the *E. coli* Trx than for *P. falciparum* Trx. Substrate specificity has also been studied for other members of the 2-Cys Prx family. *Pf*Prx-2, a mitochondrial *P. falciparum* 2-Cys Prx, clearly prefers mitochondrial *Pf*Trx as its substrate ($K_m = 11.6$ μM) compared to cytosolic *Pf*Trx ($K_m = 130.4$ μM) (Boucher *et al.*, 2006). Also, a mitochondrial 2-Cys Prx from pea (*Ps*PrxIIF) reacted with the pea mitochondrial Trx/TrxR but not with thioredoxins from either wheat or *Arabidopsis thaliana* (Barranco-Medina *et al.*, 2007).

3.4.2   Structural analysis of *Pf*Prx-1

3.4.2.1   *Molecular mass determination by ESI-MS*

The ESI-MS results showed that the Ni-affinity purified *Pf*Prx-1 protein had a molecular mass of ~23586.16 ± 2.92 Da after treatment with TBP + IA. The calculated molecular mass for the *Pf*Prx-1 monomer including the His$_6$-tag and the Factor Xa recognition site but without the start methionine residue is approximately 23,319 Da. A *Pf*Prx-1 monomer has 3 Cys residues and each Cys residue has one sulphydryl group (Wood *et al*., 2003). Treatment with iodoacetamide (IA) adds an acetamide group (58 Da) to the sulphydryl group. Thus, the calculated molecular mass of the recombinant *Pf*Prx-1 protein after treatment with TBP+IA is 23,435 Da. Thus, the molecular mass obtained by ESI-MS is consistent with the calculated monomer size allowing for experimental errors due to the presence of impurities in the protein samples.

3.4.2.2   *Oligomerization*

Several members of the Prx family are known to exist in different oligomeric states, usually dimers and larger oligomeric forms such as tetramers hexamers, octamers decamers or dodecamers (Barranco-Medina *et al*., 2008b, Boucher *et al*., 2006, Guimaraes *et al*., 2005, Li *et al*., 2005, Schröder *et al*., 2000, Smeets *et al*., 2008, Wood *et al*., 2002)

In this study, the purified *Pf*Prx-1 existed in both decameric and dimeric forms at a protein concentration of ~ 10 mg ml^{-1} and a pH value of 7.2 and in the presence of 1 mM DTT. These oligomeric states for *Pf*Prx-1 are similar to those reported for the *P. falciparum* mitochondrial *Pf*Prx-2 and the human 2-Cys Prx II (Schröder *et al.* 2000; Boucher *et al.* 2006). Akerman and Müller (2003), however, showed that the native *Pf*Prx-1 purified from *P. falciparum* cultures existed only as oligomers (decamers in the presence of DTT and larger oligomers in the absence of DTT). The difference between the recombinant *Pf*Prx-1 and the native *Pf*Prx-1 purified by Akerman and Müller (2003) could be due to the presence of the N-terminal His$_6$-tag in the recombinant protein. It has been demonstrated in a recent study that the presence of a N-terminal His$_6$-tag can have a marked effect on the oligomeric state of recombinant mammalian PrxIII (Cao *et al.*, 2007). In their study, however, Cao *et al.* (2007) found that the N-terminal His$_6$-tag favoured the formation of larger oligomers (dodecamers) of the oxidized PrxIII and did not have much effect on the oligomerization state of the reduced PrxIII.

The type of buffer used and/or the concentration of NaCl are factors that can influence the dimer-decamer transition as well. For example, Bernier-Villamor *et al.* (2004) studied the oligomerization of a recombinant 2-Cys Prx from pea and found that the decamer was the predominant species in phosphate buffer at pH 7.5 with 1.5 M NaCl whereas in Tris buffer the amounts of the dimer and decamer were similar to one another. By contrast, at pH 8.0 in Tris buffer, there was only the dimer, whereas in phosphate buffer the amounts of the two species were similar. In this study the recombinant *Pf*Prx-1 existed as both decamer (predominant) and dimer

(minor) in 50 mM HEPES-NaOH buffer at pH 7.2 with 150 mM NaCl and 1 mM

DTT.

The solution pH has been shown to affect the oligomeric state of several Prx

proteins (Barranco-Medina *et al*., 2008a, Kristensen *et al*., 1999, Wood *et al*.,

2003b). In this study, the effects of pH on *Pf*Prx-1 oligomerization were investigated

at four different pH values, 5.5, 7.2, 7.5 and 8.5. These pH values were selected

because (a) it had been shown that pH 5.5 stabilized calpromotin (a human Prx) in

the decameric form whereas pH 8.5 and above caused dissociation to dimers and (b)

it was estimated that *Pf*Prx-1 had pI values of 7.2 and 7.5 without and with the His$_6$-

tag, respectively. Our results showed pH values of 5.5, 7.2 and 7.5 favoured the

decameric form whereas pH 8.5 favoured the dimeric form. These results are similar

to the findings of Kristensen *et al*. (1999) and Barranco-Medina *et al*. (2008a) with

Prx proteins from human red blood cells and pea mitochondria, respectively.

It is interesting to note that the gel filtration elution profiles for *Pf*Prx-1 differed

depending on the amount of protein loaded on the column (compare Figs. 3.6 and

3.8). When the protein amount loaded was 5 mg (Fig. 3.6), there were only two

elution peaks at decamer and dimer sizes. When the protein amount loaded was

decreased to 0.5 mg (Fig. 3.8), there was another elution peak appearing at around

70-72 ml corresponding to tetramer size (86-98 kDa). Thus it seems that lowering

the concentration of *Pf*Prx-1 favours the dissociation of decamers to smaller forms.

This result agrees with the findings of Matsumura *et al*. (2008) who studied a rat

type I 2-Cys Prx (HBP23/Prx I) and found that the protein existed as a mixture of

various forms with the decamer being favoured at higher protein concentrations, lower salt concentrations and in the presence of DTT.

Our recombinant *Pf*Prx-1 protein was dissociated into dimers by urea treatment at both concentrations tested (1.0 and 2.8 M). These results are similar to those of Kristensen (1999) who showed that urea caused the dissociation of calpromotin, a 2-Cys PrxII from erythrocytes, into a dimer at a concentration of 2.8 M.

Although the biochemical properties of *Plasmodium* 2-Cys Prx proteins have been well studied, their cellular functions remain unclear. In other organisms, the oligomerization of Prx proteins has been shown to be associated with the modulation of their functions under oxidative stress conditions. In yeast exposed to oxidative stress, cytosolic PrxI and II can associate further into higher-order structures, so-called super-chaperone complexes, which exert protective effects on cells such as enhancing yeast resistance to heat shock in conjunction with displaying reduced peroxidase activity (Jang *et al*., 2004). Similar results were reported for human PrxII (hPrxII), a cytosolic human 2-Cys Prx (Moon *et al*., 2005). Upon exposure to oxidative stress, hPrxII formed a high molecular weight structure that had highly efficient chaperone function. The subsequent removal of the stressors induced the dissociation of the protein to low molecular weight forms (Moon *et al*., 2005). The authors concluded that oligomerization triggers a chaperone-to-peroxidase functional switch. It is possible that the oligomerization of *Pf*Prx-1 could play similar chaperone-like roles in protecting the parasites under oxidative stress conditions. However, this theory needs further studies to clarify.

3.4.3 Crystallization

In order to design specific inhibitors of target proteins, it is necessary to have a detailed understanding of their three-dimensional structure. Once a structure is available for *Pf*Prx-1, comparisons can be made with the already known structure for the human red blood cell Prx (Schröder *et al.*, 2000) and any structural differences can be used to design antimalarial drugs that work by specifically inhibiting the enzyme from the parasite without affecting the enzyme from the human host. This protein crystal structure is also essential for inhibitor screening. An alternative but less desirable option to obtaining protein crystal structures is to build the protein structure based on known structures (template) with high amino acid sequence similarity. Recently, the crystal structures of 2-Cys Prxs from *P. vivax* and *P. yoelii* have been published (Protein Data Bank). Since these *Plasmodium* 2-Cys Prxs share high amino acid sequence identities to the *Pf*Prx-1(approximately 80%), they can be used as templates for homology modelling of *Pf*Prx-1. As stated in Section 3.1, this method does not always give the most precise protein structure (Aszódi and Taylor, 1996).

The *Pf*Prx-1 protein crystallized in space group P2, thus sharing the same crystallization space group with a 2-Cys Prx from *P. vivax* (Vedadi *et al.*, 2007). These two proteins share approximately 80% identity in their amino acid sequences. The crystal structures of the other crystallized 2-Cys Prx proteins from other *Plasmodium* species, however, have different space groups. The *P. falciparum* mitochondrial *Pf*Prx-2 was crystallized in the space group C2 (Boucher el al., 2006)

and the 2-Cys Prx from *P. yoelii* was crystallized in space groups P 4 2 2 (RCSB

Protein Data Bank).

However, at this low resolution (6-7 Å), the data are insufficient to solve the

structure of the protein (Delabarre and Brunger, 2006). The most likely explanations

for the low resolution data are the small size and/or the poor quality of the analysed

*Pf*Prx-1 crystal. Generally, crystal sizes of around 100-300 μm are required for

satisfactory X-ray diffraction (Bergfors, 1999) but the largest size obtained for the

*Pf*Prx-1 crystal was only 20-50 μm. With regard to the quality of the *Pf*Prx-1 crystal,

Fig. 3.11A shows a diffraction image with a dark ring around the beam spot which

likely represented small angle X-ray scattering (Malkin and Thorne, 2004). When

the contrast was adjusted, diffraction patterns or spots could be observed underneath

the small angle X-ray scattering (Fig. 3.11B). The results indicated that there were

ordered crystals stacked within a disrupted lattice. In a perfect crystal, molecules

would be packed in a perfectly periodic arrangement and each molecule would be

identical (Malkin and Thorne, 2004). In the case of *Pf*Prx-1, however, there is a

chance that the *Pf*Prx-1 molecules in the solution use for crystallization were not

identical or there were some impurities present.

As discussed above, *Pf*Prx-1 can exist in different oligomeric states. It is possible

that the dimeric protein used in the crystallization experiments underwent structural

transitions during storage or during the crystallization process, resulting in different

forms of larger oligomers. In that case, these large *Pf*Prx-1 oligomers could be

packed in a high-order-oligomerisation formation but not forming true crystals.

These non-crystalline forms of *Pf*Prx-1 might lead to the small angle X-ray scattering problem as discussed above. The presence of different oligomeric structures might also interfere with protein packing of the identical dimeric *Pf*Prx-1 molecules preventing the dimeric *Pf*Prx-1 crystallising in a single unique conformation. Poorly ordered or disrupted crystals lead to disorder in diffraction patterns as stated above. In order to solve this problem, it is necessary to make sure that the *Pf*Prx-1 is present in only one oligomeric state (dimer) during storage and crystallization. In the future, gel filtration chromatography could be carried out for *Pf*Prx-1 solutions stored for different times and under different conditions to establish the best conditions to obtain *Pf*Prx-1 as a homogeneous dimer.

In order to solve any problems with impurities, future experiments could focus on obtaining higher purity of *Pf*Prx-1. Extra steps such as ion-exchange chromatography or additional gel-filtration chromatography could be used in order to improve the purity of the protein for crystallization.

Some of the X-ray diffraction images had much better diffraction patterns than others. The reason might be that in some parts of the crystal, the protein molecules (dimeric form) were packed in a highly ordered way due to the low interference from any highly oligomeric molecules. As the crystal rotated around and exposed its different angles to the X-ray beam, different qualities of diffraction pattern could be achieved. The images with good diffraction patterns were those selected for indexing.

Though the complete structure of the *Pf*Prx-1 protein could not be solved, some structural information could still be obtained. Using the International Tables for Crystallography (http://it.iucr.org/) all symmetry operations of Space group P2 can be determined. Also the bond length and bond angles of the cells are determined. Thus, low-resolution models can provide important insights into macromolecular function and, more importantly, provide the basis for further experimentation.

References

Akerman, S. E. & Müller, S. (2003) 2-Cys peroxiredoxin *Pf*Trx-Px1 is involved in the antioxidant defence of *Plasmodium falciparum. Molecular and Biochemical Parasitology,* 130**,** 75-81.

Aszódi, A. and Taylor, W.R. (1996)Homology modelling by distance geometry, Folding and Design, 1, 325–334.

Barranco-Medina, S., Kakorin, S., Lazaro, J. J. & Dietz, K. J. (2008a) Thermodynamics of the dimer-decamer transition of reduced human and plant 2-Cys peroxiredoxin. *Biochemistry.,* 47**,** 7196–7204.

Barranco-Medina, S., Krell, T., Bernier-Villamor, L., Sevilla, F., Lázaro, J. J. & Dietz, K. J. (2008b) Hexameric oligomerization of mitochondrial peroxiredoxin PrxIIF and formation of an ultrahigh affinity complex with its electron donor thioredoxin Trx-o. *Journal of Experimental Botany,* 59**,** 3259-3269.

Barranco-Medina, S., Krell, T., Finkemeier, I., Sevilla, F., Lázaro, J. J. & Dietz, K. J. (2007) Biochemical and molecular characterization of the mitochondrial peroxiredoxin PsPrxIIF from *Pisum sativum. Plant Physiology and Biochemistry,* 45**,** 25-39.

Bergfors, T. M. (Ed.) (1999) *Protein Crystallization: Techniques, Strategies and Tips. A Laboratory Manual*, Internat'l University Line.

Bernier-Villamor, L., Navarro, E., Sevilla, F. & Lazaro, J.-J. (2004) Cloning and characterization of a 2-Cys peroxiredoxin from *Pisum sativum. Journal of Experimental Botany,* 55**,** 2191-2199.

Boucher, I. W., McMillan, P. J., Gabrielsen, M., Akerman, S. E., Brannigan, J. A., Schnick, C., Brzozowski, A. M., Wikinson, A. J. & Müller, S. (2006) Structural and biochemical characterization of a mitochondrial peroxiredoxin from *Plasmodium falciparum. Molecular Microbiology,* 61**,** 948-959.

Bradford, M. M. (1976) A rapid and sensitive method for the quantitation of microgram quantities of protein utilizing the principle of protein-dye binding. *Analytical Biochemistry,* 72**,** 248-254.

Cao, Z., Bhella, D. & Lindsay, J. G. (2007) Reconstitution of the mitochondrial PrxIII antioxidant defence pathway: General properties and factors affecting PrxIII activity and oligomeric state *Journal of Molecular Biology*, 372**,** 1022-1033.

Cha, M. K., Yun, C. H. & Kim, I. H. (2000) Interaction of human thiol-specific antioxidant protein 1 with erythrocyte plasma membrane. *Biochemistry,* 39**,** 6944-6950.

Chae, H. Z., Chung, S. J. & Rhee, S. G. (1994) Thioredoxin-dependent peroxide reductase from yeast. *Journal of Biological Chemistry,* 269**,** 27670-27678.

Chang, T. S., Jeong, W., Choi, S. Y., Yu, S., Kang, S. W. & Rhee, S. G. (2002) Regulation of peroxiredoxin I activity by Cdc2-mediated phosphorylation. *Journal of Biological Chemistry,* 277**,** 25370–25376.

Chauhan, R. & Mande, S. C. (2001) Characterization of the *Mycobacterium tuberculosis* H37Rv alkyl hydroperoxidase AhpC points to the importance of ionic interactions in oligomerization and activity. *Biochemical Journal,* 354**,** 209-215.

Choi, H. J., Kang, S. W., Yang, C. H., Rhee, S. G. & Ryu, S. E. (1998) Crystal structure of a novel human peroxidase enzyme at 2 Å resolution. *Nature Structural Biology,* 5 (5)**,** 400-406.

Choi, J., Choi, S., Choi, J., Cha, M. K., Kim, I. H. & Shin, W. (2003) Crystal structure of *Escherichia coli* thiol peroxidase in the oxidized state: insights into intramolecular disulfide formation and substrate binding in atypical 2-Cys peroxiredoxins. *Journal of Biological Chemistry,* 278**,** 49478-49486.

Choi, J., Choi, S., Chon, J. K., Choi, J., Cha, M.-K., Kim, I.-H. & Shin, W. (2005) Crystal structure of the C107S/C112S mutant of yeast nuclear 2-Cys peroxiredoxin. *Proteins: Structure, Function, and Bioinformatics,* 61**,** 1146 - 1149.

Clark, I.A., Schofield, L.(2000), Pathogenesis of malaria, *Parasitology Today*, 16, 451–4.

Claiborne, A. e. a. (1999) Protein-sulfenic acids: diverse roles for an unlikely player in enzyme catalysis and redox regulation. *Biochemistry,* 38, **,** 15407–15416.

DeLaBarre, B. & Brunger, A. T. (2006) Considerations for the refinement of low-resolution crystal structures. *Acta Crystallographica Section D,* D62**,** 923-932.

Echalier, A., Trivelli, X., Corbier, C., Rouhier, N., Walker, O., Tsan, P., Jacquot, J.-P., Aubry, A., Krimm, J. & Lancelin, J.-M. (2005) Crystal structure and solution NMR dynamics of a D (type II) peroxiredoxin glutaredoxin and thioredoxin dependent: a new insight into the peroxiredoxin oligomerism. *Biochemistry,* 44**,** 1755-1767

Georgiou, G. & Masip, L. (2003) Biochemistry. An overoxidation journey with a return ticket. *Science,* 300**,** 592–594.

Guimaraes, B. G., Souchon, H., Honore, N., Saint-Joanis, B., Brosch, R., Shepard, W., Cole, S. T. & Alzari, P. M. (2005) Structure and mechanism of the alkyl hydroperoxidase AhpC, a key element of the *Mycobacterium tuberculosis* defense system against oxidative stress. *Journal of Biological Chemistry,* 280**,** 25735–25742.

Hamilton, B. A., Palazzolo, M. J. & Meyerowitz, E. M. (1991) Rapid isolation of long cDNA clones from existing libraries. *Nucleic Acids Research,* 19**,** 1951-1952.

Jang, H. H., Lee, K. O., Chi, Y. H., Jung, B. G., Park, S. K., Park, J. H., Lee, J. R., Lee, S. S., Moon, J. C., Yun, J. W., Choi, Y. O., Kim, W. Y., Kang, J. S., Cheong, G.-W., Yun, D.-J., Rhee, S. G., Cho, M. J. & Lee, S. Y. (2004) Two enzymes in one: Two yeast peroxiredoxins display oxidative stress-dependent switching from a peroxidase to a molecular chaperone function. *Cell,* 117**,** 625-635.

Kanzok, S. M., Rahlfs, S., Becker, K. & Schirmer, R. H. (2002) Thioredoxin, thioredoxin reductase, and thioredoxin peroxidase of malaria parasite *Plasmodium falciparum*. *Methods in Enzymology,* 347**,** 370-381.

Kawazu, S., Komaki-Yasuda, K., Oku, H. & Kano, S. (2008) Peroxiredoxins in malaria parasites: Parasitologic aspects. *Parasitology International,* 57**,** 1-7.

Kawazu, S., Komaki, K., Tsuji, N., Kawai, S., Ikenoue, N., Hatabu, T., Ishikawa, H., Matsumoto, Y., Himeno , K. & Kano, S. (2001) Molecular characterization of a 2-Cys peroxiredoxin from the human malaria parasite *Plasmodium falciparum*. *Molecular and Biochemical Parasitology,* 116**,** 73-79.

Kitano, K., Kita, A., Hakoshima, T., Niimura, Y. & Miki, K. (2005) Crystal

structure of decameric peroxiredoxin (AhpC) from *Amphibacillus xylanus*.

Proteins: Structure, Function, and Bioinformatics, 59**,** 644-647.

Kitano, K., Niimura, Y., Nishiyama, Y. & Miki, K. (1999) Stimulation of peroxidase

activity by decamerization related to ionic strength: AhpC protein from

Amphibacillus xylanus. *J. Biochem.,* 126**,** 313-319.

Komaki-Yasuda, K., Kawazu, S. & Kano, S. (2003) Disruption of the *Plasmodium

falciparum* 2-Cys peroxiredoxin gene renders parasites hypersensitive to reative

oxygen and nitrogen species. *FEBS Letters,* 547**,** 140-144.

Kristensen, P., Rasmusssen, D. E. & Kristensen, B. (1999) Properties of thiol-

specific antioxidant protein or calpromotin in solution. *Biochemical and

Biophysical Research Communications,* 262**,** 127-131.

Krnajski, Z., Gilberger, T. W., Walter, R. D. & Müller, S. (2001a) The malaria

parasite *Plasmodium falciparum* possesses a functional thioredoxin system.

Molecular and Biochemical Parasitology, 112**,** 219-228.

Krnajski, Z., Walter, R. D. & Müller, S. (2001b) Isolation and functional analysis of

two thioredoxin peroxidases (peroxiredoxins) from *Plasmodium falciparum*.

Molecular and Biochemical Parasitology, 113**,** 303-308.

Li, S., Peterson, N. A., Kim, M.-Y., Kim, C.-Y., Hung, L.-W., Minmin, Y., Lekin,

T., Segelke, B. W., Lott, J. S. & Baker, E. N. (2005) Crystal structure of AhpE

from *Mycobacterium tuberculosis*, a 1-Cys peroxiredoxin. *Journal of Molecular

Biology,* 346**,** 1035-1046.

Malkin, A. J. and Thorne, R. E. (2004) Growth and disorder of macromolecular crystals: Insights from atomic force microscopy and X-ray diffraction studies. *Methods*, 34, 273-299.

Matsumura, T., Okamoto, K., Iwahara, S., Horis, H., Takahashi, Y., Nishino, T. & Abe, Y. (2008) Dimer-oligomer interconversion of wild-type and mutant rat 2-Cys peroxiredoxin. *Journal of Biological Chemistry,* 283**,** 284-293.

Moon, J. C., Hah, Y. S., Kim, W. Y., Jung, B. G., Jang, H. H., Lee, J. R., Kim, S. Y., Lee, Y. M., Jeon, M. G. & Kim, C. W., Cho, M.J. and Lee SY. (2005) Oxidative stress-dependent structural and functional switching of a human 2-Cys peroxiredoxin isotype II that enhances HeLa cell resistance to H_2O_2-induced cell death. *Journal of Biological Chemistry,* 280**,** 28775-28784.

Nickel, C., Trujillo, M., Rahlfs, S., Deponte, M., Radi, R. & Becker, K. (2005) *Plasmodium falciparum* 2-Cys peroxiredoxin reacts with plasmoredoxin and peroxynitrite. *Biological Chemistry,* 386**,** 1129-1136.

Rabilloud, T., Heller, M., Gasnier, F., Luche, S., Rey, C., Aebersold, R., Benahmed, M., Louisot, P. & Lunardi, J. (2002) Proteomics analysis of cellular response to oxidative stress: Evidence for in vivo over-oxidation of peroxiredoxins at their active site. *Journal of Biological Chemistry,* 277**,** 19396–19401.

Rahlfs, S. & Becker, K. (2001) Thioredoxin peroxidases of the malarial parasite *Plasmodium falciparum. European Journal of Biochemistry,* 268**,** 1404-1409.

Sarma, G. N., Nickel, C., Rahlfs, S., Fischer, M., Becker, K. & and Karplus, P. A. (2005) Crystal structure of a novel *Plasmodium falciparum* 1-Cys peroxiredoxin. *Journal of Molecular Biology,* 346**,** 1021-1034.

Schröder, E., Littlechild, J. A., Lebedev, A. A., Errington, N., Vagin, A. A. & Isupov, M. N. (2000) Crystal structure of decameric 2-Cys peorxiredoxin from human eruthrocytes at 1.7 Å resolution. *Structure,* 8**,** 605-615.

Smeets, A., Evrard, C., Landtmeters, M., Marchand, C., Knoops, B. & Declercq, J.-P. (2005) Crystal structures of oxidized and reduced forms of human mitochondrial thioredoxin 2. *Protein Science,* 14**,** 2610-2621.

Smeets, A., Loumaye, E., Clippe, A., Rees, J.-F., Knoops, B. & Declercq, J.-P. (2008) The crystal structure of the C45S mutant of annelid *Arenicola marina* peroxiredoxin 6 supports its assignment to the mechanistically typical 2-Cys subfamily without any formation of toroid-shaped decamers. *Protein Science,* 17**,** 700-710.

Su, X. Z., Wu, Y., Sifri, C. D. & Wellems, T. E. (1996) Reduced extension temperatures required for PCR amplification of extremely A+ T-rich DNA. *Nucleic Acids Research,* 24**,** 1574.

Vedadi, M., Lew, J., Artz, J., Amani, M., Zhao, Y., Dong, A., Wasney, G. A., Gao, M., Hills, T., Brokx, S., Qiu, W., Sharma, S., Diassiti, A., Alam, Z., Melone, M., Mulichak, A., Wernimont, A., Bray, J., Loppnau, P., Plotnikova, O., Newberry, K., Sundararajan, E., Houston, S., Walker, J., Tempel, W., Bochkarev, A., Kozieradzki, I., Edwards, A., Arrowsmith, C., Roos, D., Kain, K. & Hui, R. (2007) Genome-scale protein expression and structural biology of *Plasmodium falciparum* and related Apicomplexan organisms. *Molecular & Biochemical Parasitology,* 151**,** 100-110

Woo, H. A., Chae, H. Z., Hwang, S. C., Yang, K. S., Kang, S. W., Kim, K. & Rhee, S.G. (2003) Reversing the inactivation of peroxiredoxins caused by cysteine sulfinic acid formation. *Science,* 300**,** 653-656.

Wood, Z. A., Poole, L. B., Hantgan, R. R. & Karplus, P. A. (2002) Dimers to doughnuts: Redox-sensitive oligomerization of 2-cysteine peroxiredoxins. *Biochemistry,* 41**,** 5493– 5504.

Wood, Z. A., Poole, L. B. & Karplus, P. A. (2003a) Peroxiredoxin evolution and the regulation of hydrogen peroxide signaling. *Science,* 300**,** 650–653.

Wood, Z. A., Schroder, E., Harris, J. R. & Poole, L. B. (2003b) Structure, mechanism and regulation of peroxiredoxins. *Trends in Biochemical Sciences,* 28**,** 32-40.

Yano, K., Komaki-Yasuda, K., Kobayashi, T., Takemae, H., Kita, K., Kano, S. & and Kawazu, S. (2005) Expression of mRNAs and proteins for peroxiredoxins in *Plasmodium falciparum* erythrocytic stage. *Parasitology International,* 54**,** 35-41.

Chapter 4 Expression, purification and characterisation of a recombinant *Plasmodium falciparum* mitochondrial 2-Cys peroxiredoxin in *Pichia pastoris*

Abstract

A *Pichia pastoris* expression system has been developed for the production of recombinant *Plasmodium falciparum* mitochondrial peroxiredoxin-2 (*Pf*Prx-2). The AT rich native full-length *Pf*Prx-2 coding sequence was cloned into the pPICZ B vector under the transcriptional control of the AOX promoter and this construct was successfully integrated into the *P. pastoris* genome. The recombinant protein was found to be functionally active and localised to the mitochondria, indicating that *P. pastoris* is capable of recognising and processing the *P. falciparum* mitochondrial targeting sequence. Evidence for the production by *P. pastoris* of the *Pf*Prx-2 protein as an oligomer (decamer and larger) was obtained by gel filtration chromatography, SDS-PAGE and immunodetection. It was found that purification of the functionally active *Pf*Prx-2, by Ni-affinity chromatography, resulted in the protein being "locked" in the dimeric state and it could not be converted to the monomer by a variety of reducing agents as indicated by SDS-PAGE.

4.1 Introduction

P. falciparum peroxiredoxin-2 (*Pf*Prx-2) has been proposed as a potential target for the development of novel anti-malarial drugs because of its function as a peroxiredoxin (Boucher et al., 2006, Kawazu et al., 2008, Rahlfs and Becker, 2001, Yano et al., 2005). However, in order to design such drugs, large quantities of the protein are needed to produce protein crystals and elucidate their structure using X-ray crystallography. Both *P. falciparum* 2-Cys peroxiredoxins (*Pf*Prx-1 and *Pf*Prx-2) have been expressed as recombinant proteins in *E. coli* (Boucher et al. 2006, Rahlfs and Becker 2001). Rahlfs and Becker (2001) found that recombinantly-expressed *Pf*Prx-1 exhibited typical peroxiredoxin activity whereas *Pf*Prx-2 did not. They hypothesized that this was due to incorrect folding of the *Pf*Prx protein because of the presence of a predicted mitochondrial targeting sequence. Boucher et al. (2006) subsequently supported this hypothesis by recombinantly-expressing a truncated form of *Pf*Prx-2 missing the first 19 amino acids predicted to be the mitochondrial targeting sequence. The truncated protein expressed by Boucher et al. (2006), exhibited greater affinity for mitochondrial *P. falciparum* thioredoxin than it did for cytosolic *P. falciparum* thioredoxin adding further evidence for the conclusion that *Pf*Prx-2 is mitochondrial. In a separate study, Yano et al. (2005) double-stained *P. falciparum* cells with an anti-*Pf*Prx-2 antiserum and Mito Tracker[®] (a stain specific for mitochondria) and provided further evidence that *Pf*Prx-2 is located in the *P. falciparum* mitochondrion. This was subsequently confirmed by Boucher et al. (2006) using *Pf*Prx-2 fused to green fluorescent protein (GFP). Boucher et al. (2006) produced large quantities of the truncated *Pf*Prx-2 protein missing the mitochondrial targeting sequence in *E. coli* and were able to produce protein crystals and examine

their structure using X-ray crystallography. They found that the crystallized protein existed as a dimer and they identified the Cys residues holding the monomers together via disulphide bridges. Thus, *Pf*Prx-2 has been successfully recombinantly expressed in *E. coli* and a crystal structure has been determined. However, the possibility exists that post-translational processing of the *Pf*Prx-2 protein in a prokaryote (i.e. *E. coli*) is different than it is in a eukaryote. Thus, this study aims to recombinantly express *Pf*Prx-2 in the methylotrophic yeast *Pichia pastoris* and characterise its biochemical properties.

4.2 Materials and methods

4.2.1   DNA/RNA methods

4.2.1.1   *Amplification of PfPrx-2 and construction of the pPICZ B-PfPrx-2 vector*

The *P. falciparum Pf*Prx-2 nucleotide sequence (GenBank accession no. **AF225978**) was used to design PCR primers to amplify the 648 bp *Pf*Prx-2 protein coding sequence from *P. falciparum* strain 3D7 genomic DNA. Conveniently, the *Pf*Prx-2 gene has no introns. For subsequent procedures, a *XhoI* restriction enzyme site followed by the yeast consensus translation start sequence was included in the forward primer and a *NotI* restriction enzyme site followed by the Factor Xa protease cleavage site was included in the reverse primer (Table 4.1). The pPICZ B

vector adds a c-*myc* and a His$_6$-tag to the expressed proteins for subsequent detection and purification by metal ion affinity chromatography (see Appendix C for pPICZ B vector map). The Factor Xa protease cleavage site was engineered into the construct to permit subsequent removal of these tags.

The PCR reactions were set up and run as described in section 3.2.1 using *Pf*Prx-2 forward and reverse primers to amplify the *PfPrx-2* gene. PCR products of the expected size (~700bp) were purified from agarose gels as described in section 3.2.3 and then they were digested using *XhoI* and *NotI* before being ligated into the similarly digested pPICZ B expression vector (as described in section 3.2.5).

4.2.1.2   *Confirmation of complete gene transcription by RNA extraction and reverse-transcriptase PCR from transformed yeast cells*

This step was done to confirm that the *Pf*Prx-2 gene was completely transcribed in the expression host. The reason is because of the fact that the *Plasmodium* genome is extremely A+T rich (Brocchieri 2001). A+T rich regions can cause premature termination of transcription in *Pichia* and other yeast expression hosts (Romanos et al., 1992). To confirm that the *Pf*Prx-2 gene was completely transcribed, total RNA was isolated from yeast cells induced to express the *Pf*Prx-2 gene and reverse transcriptase-PCR (RT-PCR) was performed.

Table 4.1

Oligonucleotides used to amplify the *Pf*Prx-2 coding region. The *XhoI* and *NotI* restriction enzyme sites are shown in bold, the yeast consensus translation start sequence is shown in italics and the Factor Xa protease cleavage site is underlined.

Primer name	Primer sequence
*Pf*Prx-2 forward	5'-**GTACTCGAG***ACAATAATGTCT*TTTTTAAAAAAACTGTGCAGGAGCAATTTTTTCGG-3'
*Pf*Prx-2 reverse	5'-GAA**GCGGCCGC**GCGTCCCTCAATATTTTTATTTGCATTATTC-3'

Total RNA isolation was done using a RiboPure^{TM} kit (Ambion, catalogue no. 1924)

following the manufacturer's instructions. The cells were first subjected to

mechanical disruption via grinding in liquid nitrogen. One ml of TRI reagent

(provided with the kit) was added to 100 mg of pulverized cells to completely lyse

the cells and inactivate any nucleases. To extract the RNA, 100 μl of

bromochloropropane (BCP) was mixed with the cell homogenate and the mixture

was incubated for 5 min. The aqueous phase containing the RNA was separated

from the mixture after a centrifugation at 12,000 *g* for 10 min at 4°C. To purify the

RNA, 99% (v/v) ethanol was added to the aqueous phase (ethanol: aqueous phase

volume ratio = 1:2) and the mixture was applied to a filter cartridge. After

centrifugation at 12,000 *g* for 30 s at room temperature, the RNA bound to the filter

cartridge was washed twice with the provided wash solution. Finally, the RNA was

eluted with 100 μl of TE buffer (pH 8.0,). All samples were subjected to on-column

DNase digestion using the Qiagen RNase free DNase treatment (Qiagen) during

RNA isolation. The isolated RNA was used as template in the reverse transcriptase

reaction.

RT-PCR analysis was conducted in two parts. The first part was cDNA synthesis.

First strand cDNA synthesis was performed using the Omniscript Reverse

Transcriptase kit (Qiagen catalogueue no. 205111) as specified by the manufacturer,

using 2 μg of RNA as the template. The cDNA produced from this RT reaction was

then used as template for amplification by PCR. The second part, i.e, the PCR

reaction was performed as described in section 3.2.1 using the *Pf*Prx-2 forward and

reverse primers (Table 4.1). PCR controls included PCR mix without added cDNA

template (negative control), and the pPICZ B vector containing the gene insert

(positive control). Both induced and un-induced samples were analyzed. The

products of the RT-PCR reactions were purified from agarose gels and sequenced

with *PfPrx-2* forward and reverse primers as described in sections 3.2.3 and 3.2.9.

4.2.2   Microbiological methods

4.2.2.1   Growth media

- Low Salt LB broth: 1% (w/v)Tryptone, 0.5% (w/v) Yeast Extract and 0.5% (w/v)

  NaCl, pH 7.5.

- Low Salt LB agar: same as Low Salt LB broth + 1.5% (w/v) agar.

- YDP broth: 1% (w/v) yeast extract, 2% (w/v) peptone, 2% (w/v) dextrose

  (glucose)

- YPDS Agar: 1% (w/v) yeast extract, 2% (w/v) peptone, 2% (w/v) dextrose

  (glucose), 1 M sorbitol, 2% (w/v) agar

- BMGY: 1% (w/v) yeast extract, 2% (w/v) peptone, 100 mM potassium phosphate,

  pH 6.0, 1.34% (w/v) Yeast Nitrogen Base with ammonium sulfate but without

  amino acids, 4×10^{-5}% (w/v) biotin,1% (w/v) glycerol for BMGY

- BMMY: same as for BMGY except 0.5% methanol was used in place of 1% (w/v)

  glycerol

4.2.2.2   *Growth of bacteria and yeast strains*

Bacteria and yeast strains and plasmid vectors used in this chapter are listed in Table 4.2. They were all supplied by Invitrogen™ as components of the EasySelect™ *Pichia* Expression Kit.

The *E. coli* TOP10F′ cells were used as the host for cloning vectors to produce plasmid DNA for both DNA sequencing and subsequent transformation of yeast. These cells were grown in low-salt LB supplemented with tetracycline (10 μg/ml). When required for the selection of positive clones, the growth medium was supplemented with zeocin (25 μg/ml).

The *P. pastoris* X-33 and KM71H were the two strains of *P. pastoris* used as the expression host for *Pf*Prx-2. The *P. pastoris* X-33 and KM71H cells were routinely grown in YPD or YPDS agar. When required for the selection of positive clones, the growth media were supplemented with various concentrations of Zeocin® (0.2 – 1.0 mg/ml). For protein production, the yeast cells were first grown in BMGY medium and then transferred to BMMY medium which contained methanol to induce the expression of recombinant protein.

Table 4.2: *E. coli* and *P. pastoris* strains and plasmid vectors used for the cloning of *PfPrx-2* gene and the production of *Pf*Prx-2 recombinant protein.

Cell strain	Genotype	Remark
E. coli TOP10F'	F′ {*pro*AB, *lac*Iq, *lac*ZΔM15, Tn*10* (TetR)} *mcr*A, Δ(*mrr-hsdRMS-mcr*BC), φ80*lac*ZΔM15, Δ*lac*X74, *deo*R, *rec*A1, λ–*ara*D139, Δ(*ara-leu*)7697, *gal*U, *gal*K, *rps*L(StrR), *end*A1, *nup*G λ–	Host for cloning vector (Invitrogen) Tetracycline resistance (10 μg/ml)
P. pastoris X-33	Wild-type	Methylotrophic yeast, capable of metabolizing methanol as its sole carbon source using enzyme called by the enzyme alcohol oxidase (AOX1 and AOX2). The promoter regulating the production of alcohol oxidase (*AOX1*) is the one used to drive heterologous protein expression in *Pichia* as linearized vector with containing AOX1 promoter sequence are able to integrate into the host genome in the region containing the wild-type AOX1 promoter.
P. pastoris KM71H	*his4, aox1: ARG4;arg4*	Disrupted *AOX1* gene, thus the cells rely on the alcohol oxidase enzyme being produced from an alternative gene called *AOX2*. The AOX2 enzyme has the same specific activity as AOX1 but has a much lower expression level (weaker promoter) and can only consume methanol slowly, hence the phenotype of these strains are termed 'methanol utilization slow' (Mut^s). Defective in histidine dehydrogenase gene (His⁻)
Plasmid vector	**Origin**	**Remark**
pPICZ B	Invitrogen	*AOX1* promoter that allows methanol-inducible, high-level expression in *Pichia* C-termnial myc epitope tag and polyhistidine tag Zeocin™ resistance gene for selection in *E. Coli*
pPICZ B-*Pf*Prx-2	This study	pPICZ B vector with insert containing *PfPrx-2* Resistance to Zeocin 25 μg/ml

4.2.3   Transformation of *E. coli* and confirmation of the presence of the *Pf*Prx-2 protein coding sequence

The ligation products were used to transform *E. coli* TOP10F′ cells (TOP10F′ cells were made competent and transformed with plasmid vectors following the method described in 3.2.6.2). Transformed colonies were selected on Low Salt LB medium supplemented with 25 μg/ml Zeocin™. The transformed colonies were screened for the presence of the *Pf*Prx-2 insert using direct colony PCR screening (as described in section 3.2.7) with the 5' and 3' *AOX1* sequencing primers. Plasmid DNA was isolated and purified from the positive colonies and sent for sequencing (as described in sections 3.2.8 and 3.2.9). The construct that contained the correct coding sequence for the *Pf*Prx-2 protein and the c-*myc* and His$_6$-tags, in the correct orientation and reading frame with respect to the *AOX1* promoter was named pPICZ B-*Pf*Prx-2 and used to transform *P. pastoris*.

4.2.4   Transformation of *P. pastoris* and confirmation of the presence of the *Pf*Prx-2 protein coding sequence.

Theoretically, linear DNA can generate stable transformants of *P. pastoris* via homologous recombination between the transforming DNA and regions of homology within the genome (Romanos et al., 1992). Here, the gene insertion events expected at the AOX1 (X-33) or aox1::ARG4 (KM71H) loci resulted from a single crossover event between the loci and either of the two AOX1 regions; the AOX1 promoter or the AOX1 transcription termination region (TT). This results in the

insertion of one or more copies of the vector upstream or downstream of the AOX1 or the aox1::ARG4 genes.

Prior to transformation, the pPICZ B-*Pf*Prx-2 construct was linearized using the *SacI* restriction enzyme. Ten μg of the linearized construct was used to transform the *P. pastoris* cells by electroporation using a GenePulser (Bio-Rad). Both X-33 and KM71H strains were grown overnight at 30$^{\text{o}}$C in YPD medium and prepared for transformation by electroporation according to the manufacturer's instructions. Multicopy transformants were selected by plating on YPDS agar medium supplemented with increasing concentrations of Zeocin$^{\circledR}$ (0.1, 0.2, 0.5 and 1.0 mg/ml). It was expected that the higher the number of copies of the insert gene integrated into the host genome, the higher the zeocin resistance capacity conferred to the host cells. *P. pastoris* X-33 and KM71H cells transformed with the pPICZ B vector without the *Pf*Prx-2 insert were used as controls for endogenous Prx enzyme activity in the yeast host cells.

To test for the presence of the *Pf*Prx-2 insert, transformed cells were lysed (10 min incubation at 30$^{\text{o}}$C with 25 U lyticase per 10 μl cells followed by 1 min freezing in liquid nitrogen) and then screened by PCR as described in section 3.2.7.

4.2.5   Expression of the recombinant *Pf*Prx-2 protein in *P. pastoris*

4.2.5.1   Test expression

Six *P. pastoris* X-33 and six *P. pastoris* KM71H colonies containing pPICZ B-*Pf*Prx-2 constructs were tested for *Pf*Prx-2 expression. Cells from a single colony were used to inoculate 25 ml BMGY medium which was then incubated at 30°C with vigorous shaking until OD_{600}~2-6 was reached. The cells were then harvested and resuspended to OD_{600}~1 in BMGY to induce protein expression. To maintain inducing conditions, the cultures were supplemented with 1% (v/v) methanol every 24 h. Aliquots were removed at various times and analysed for Prx enzyme activity. The strain and conditions that produced the highest level of Prx expression were chosen for large-scale production of the *Pf*Prx-2 protein.

4.2.5.2   Large-scale expression

Cells were grown in a 25 ml culture as above to obtain OD_{600}~2-6. This 25 ml culture was then used to inoculate 1 L BMGY and the culture was let grown to OD_{600}~2-6 again. The cells were then harvested and induced for protein expression in BMGY as above. Cells were harvested 72 h after induction by centrifugation at 3000 *g* for 5 min and store at -80°C until use.

4.2.6 Cell lysis and protein extraction

The cells were separated from the culture medium by centrifugation at 3,000 *g* for 5 minutes. Disruption of the cell wall was achieved by repeated vortexing of the cell pellet with acid-washed glass beads in an extraction buffer. Soluble proteins and cell debris were separated from one another by centrifugation at 12,000 *g* for 10 min at 4°C. Both the supernatant and the pellet were stored at -70°C for later analysis.

4.2.7 Prx enzyme assay

To assay for Prx activity, proteins were extracted as above in an ice-cold extraction buffer containing 50 HEPES-NaOH (pH 7.2), 1 mM DTT, 0.2 mM EDTA and 1 mM PMSF. Usually, 1 ml of extraction buffer was added to 0.5 g (wet weight) of yeast cells. Prx enzyme activity was assayed as described in section 3.2.14.

4.2.8 SDS–PAGE and immunodetection

Protein samples were analyzed under denaturing conditions using SDS–PAGE as described in section 3.2.15. His$_6$-tagged proteins were identified by western blotting and immunodetection using a mouse Anti-Tetra His-Antibody (Qiagen) and a Rabbit-Anti mouse Ig/HRP (Dako) together with a chemiluminescent substrate (Pierce). The chemiluminescence was detected by using X-ray film. The immunodetection procedure was as described in section 3.2.16.

4.2.9   Isolation of yeast mitochondria

Yeast mitochondria were prepared as described by González-Barroso et al. (2006) with some modifications. Cells were grown and protein expression was induced as described above. The cells were harvested 3 d after induction. Cells (1 g wet weight) were washed twice with cold distilled water. The washed cells were suspended in 20 ml of 0.1 M Tris-HCl (pH 9.3), 0.5 M 2-mercaptoethanol, and incubated for 10 min at 30°C with shaking. Cells were collected by centrifugation for 2 min at 5,800 g and washed twice in buffer containing 10 mM Tris-HCl (pH 7.0) and 0.5 M KCl. Spheroplasts were formed by enzymatic digestion of the cell wall with 400 U lyticase enzyme (Sigma, Australia) in 14–16 ml digestion buffer (10 mM citrate-phosphate, 1.35 M sorbitol, 1 mM ethylene glycol-bis(2-aminoethylether)-N,N,N,N-tetra acetic acid (EGTA), pH 5.8) with shaking at 30°C for 60 min. The spheroplast suspension was centrifuged for 10 min at 1,600 g and washed twice in spheroplast buffer (10 mM Tris-maleate, 0.4 M mannitol, 0.75 M sorbitol, 0.1% (w/v) bovine serum albumin (BSA), pH 6.8). After washing the spheroplasts, they were gently homogenized in mitochondrial buffer (0.6 M mannitol, 2 mM EGTA, 10 mM Tris-maleate, 0.5 mM Na$_2$HPO$_4$, 2% (w/v) BSA, pH 6.8) in a Wesley Coe homogenizer. The cell lysate was centrifuged at 1,300 g for 8 min. The resulting pellet, containing unbroken cells, was re-homogenized and centrifuged for 8 min at 1,300 g. The two resulting supernatants were centrifuged at 12,500 g for 8 min. The pellets were combined and gently homogenized. Cellular debris was removed by centrifugation at 1,300 g for 8 min. Mitochondrial pellets obtained after 8 min centrifugation at 12,500 g were resuspended in 0.4 ml mitochondrial buffer. This mitochondrial suspension was then analysed for mitochondrial respiration activity.

Immediately after isolation of the yeast mitochondria, mitochondrial respiration was measured using a Hansatech oxygen electrode set at 20°C following the method described by González-Barroso et al.(2006). Ten μl of mitochondrial suspension (0.25 mg protein ml^{-1}) was mixed with 1.5 ml of respiration medium containing 70 mM sucrose, 220 mM mannitol, 20 mM HEPES, 5 mM MgCl$_2$, 5 mM K$_2$HPO$_4$ + KH$_2$PO$_4$ (pH 7.4), 1 mM EDTA and 0.1% (w/v) BSA. After 3 min, 20 μl of 1 M succinate and 5 μl of 100 mM adenosine triphosphate (ATP) were added. After a further 5 min, 5 μl of 100 mM adenosine diphosphate (ADP) was added. The rate of oxygen consumption after each substrate addition was monitored.

To determine whether *Pf*Prx-2 was located in the yeast mitochondria, the mitochondria were lysed by sonication (4×15 s, on ice in between). The soluble proteins were extracted from the mitochondria in a buffer containing 50 HEPES-NaOH (pH 7.2), 1 mM DTT, 0.2 mM EDTA and 1 mM PMSF. Membranes were removed by centrifugation at 12,000 *g* for 15 min at 4°C. The supernatant was then used for Prx enzyme assays, protein quantification and immunodetection.

4.2.10 Purification of the recombinant *Pf*Prx-2 protein using Ni-affinity column chromatography

P. pastoris X33-4 cells expressing the *Pf*Prx-2 protein were harvested by centrifugation. The cells (5 g wet weight) were disrupted in 10 ml of ice-cold lysis buffer by repeated vortexing with acid-washed glass beads. The cell debris was removed by ultracentrifugation at 45,000 *g* for 30 min at 4º C. All buffers including

lysis buffer were prepared and the Ni-affinity column chromatography was run as described in section 3.2.17. The fractions obtained with the elution buffer were buffer exchanged and concentrated to 5 mg protein ml^{-1} as described in section 3.2.18. All subsequent analyses were performed with this concentrated protein sample.

4.2.11 Treatment of the Ni-affinity purified *Pf*Prx-2 protein with various reducing agents

The Ni-affinity purified *Pf*Prx-2 protein was treated with DTT, β-mercaptoethanol or tributylphosphine (TBP) to assess the effects on its molecular mass as determined by SDS-PAGE and immunodetection. For the DTT and β-mercaptoethanol treatments, the purified protein (concentration 1.25 mg ml^{-1}) was incubated overnight at 4°C with either 50 mM DTT or 0.5 M β-mercaptoethanol in 50 mM HEPES-NaOH (pH 7.2). For the TBP treatment, the purified protein (concentration 5 mg ml^{-1}) was incubated for 1 h at room temperature in a nitrogen-sparged airtight container with 5 mM TBP and then 15 mM iodoacetamide was added to make the reduction irreversible and the incubation was continued for another 1.5 h.

4.2.12 Factor Xa protease treatment to remove the His$_6$-tag from the Ni-affinity purified *Pf*Prx-2 protein

The Ni-affinity purified *Pf*Prx-2 protein, diluted to 0.25 mg ml^{-1} in 20 mM Tris-HCl (pH 7.4), 100 mM NaCl and 1 mM CaCl$_2$, was incubated overnight at room temperature with Factor Xa protease (16 U ml^{-1}) to remove the His$_6$-tag. To ensure that the His$_6$-tag had been removed, the protein was subsequently re-loaded onto a Ni-affinity column and collected in the flowthrough.

4.2.13 Gel filtration column chromatography to determine the native molecular mass of the recombinant *Pf*Prx-2 protein

In order to determine the native molecular mass of the recombinant *Pf*Prx-2 protein, one ml of a *P. pastoris* X33-4 crude cell extract (prepared as described in section 4.2.4) containing approximately 8 mg of protein was fractionated at a flow rate of 0.5 ml min^{-1} on a 1.6 x 60 cm Hiload 16/60 Superdex 200 Prep Grade gel filtration column. The gel filtration chromatography procedure was described in section 3.2.19. The separation was performed in the presence of various concentrations of reducing agent (DTT) to determine the effects on the oligomerisation state of the *Pf*Prx-2 protein. Peak A$_{280}$ fractions were analysed for the presence of *Pf*Prx-2 by measuring Prx enzyme activity and by immunodetection using anti-His antibodies.

4.3 Results

4.3.1   Cloning and expression of *Pf*Prx-2

The *Pf*Prx-2 protein coding region was amplified by PCR from *P. falciparum* strain 3D7 genomic DNA (Fig. 4.1) and ligated into the pPICZ B vector. The resulting construct (pPICZ B-*Pf*Prx-2) was sequenced using 5'- and 3'-AOX1 sequencing primers to confirm that the *Pf*Prx-2 protein coding sequence was identical to the published sequence in the GenBank database and in the correct orientation and reading frame for expression (Appendix D).

The expression construct (pPICZ B-*Pf*Prx-2) was transformed into *P. pastoris* X33 and KM71H competent cells. After 3 d, 35 *P. pastoris* X33 and 20 *P. pastoris* KM71H colonies were obtained on YPDS agar plates supplemented with zeocin. The presence of the *Pf*Prx-2 insert was confirmed by PCR analysis in 25 *P. pastoris* X33 and 18 *P. pastoris* KM71H transformants. Six of the transformants from each strain were used to test for *Pf*Prx-2 protein expression by assaying Prx enzyme activity after various times of induction. Prx enzyme activity increased up to 3 d after induction in the case of the *P. pastoris* X-33 transformants and up to 8 d in the case of the *P. pastoris* KM71H transformants (data not shown). Fig. 4.2 shows the highest Prx enzyme activities for all of the transformants tested. The activities ranged from 1.0 to 3.8 U per 50 mL culture. The highest activity was obtained for *P. pastoris* strain X33-4. Low levels of Prx enzyme activity were obtained for the uninduced control, the host cell only control and the host cell transformed with the

pPICZ B vector lacking the *Pf*Prx-2 insert (<0.5 U per 50 mL culture). Generally,

multiple insertions of the target gene lead to higher levels of protein expression

compared to single insertions (Romanos et al., 1992). Thus, it is likely that X-33-4

had more copies of the insert sequence containing the *PfPrx-2* gene than the other

transformants. Thus, subsequent experiments were performed with the *P. pastoris*

X33-4 cells.

Fig. 4.3 shows SDS-PAGE and immunodetection analysis of the expression of the

*Pf*Prx-2 protein in crude extracts of the *P. pastoris* X-33-4 cells. Immunodetection

using anti-His antibodies, revealed that the recombinant *Pf*Prx-2 protein had a

molecular mass of approximately 28 kDa (Fig. 4.3B). This agreed well with the 25

kDa size previously reported for the *Pf*Prx-2 monomer expressed without its

mitochondrial targeting sequence in *E. coli* (Boucher et al., 2006). The extra ~3 kDa

is likely contributed by the His_6-tag, the myc epitope tag and the Factor Xa

recognition site at the C-terminal end. The abundance of the 28 kDa protein

increased with duration of induction (Fig. 4.3B). Very small amounts were also

detectable in the uninduced control indicating some 'leaky' expression.
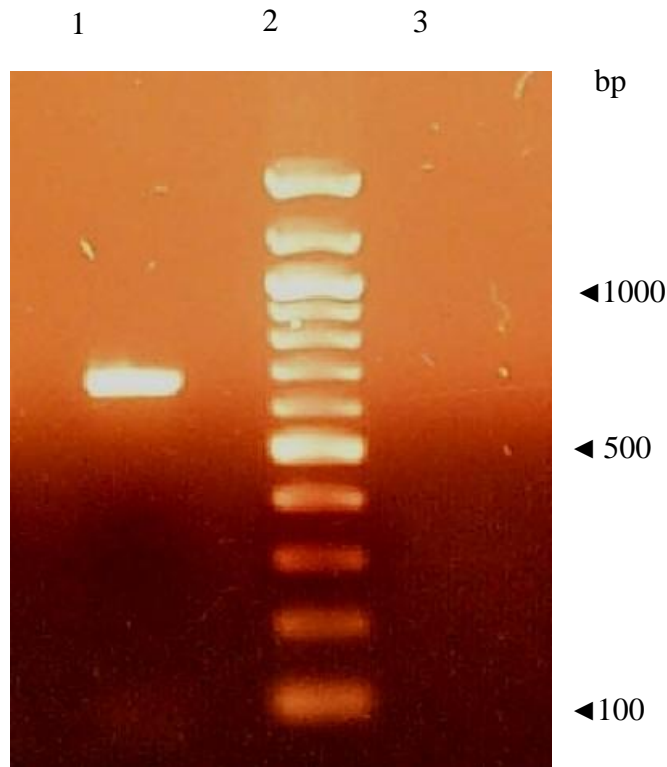
**Figure 4.1. PCR amplification of the *Pf*Prx-2 protein coding region using *P.
falciparum* (strain 3D7) genomic DNA as the template**. Lane 1, 5 μl of the PCR
products obtained from reaction with the DNA template; lane 2, 100 bp DNA ladder
(New England Biolabs); lane 3, 5 μl of the PCR products obtained from reaction
without the DNA template (negative control). The sizes of the molecular markers
are shown with the arrows on the right.
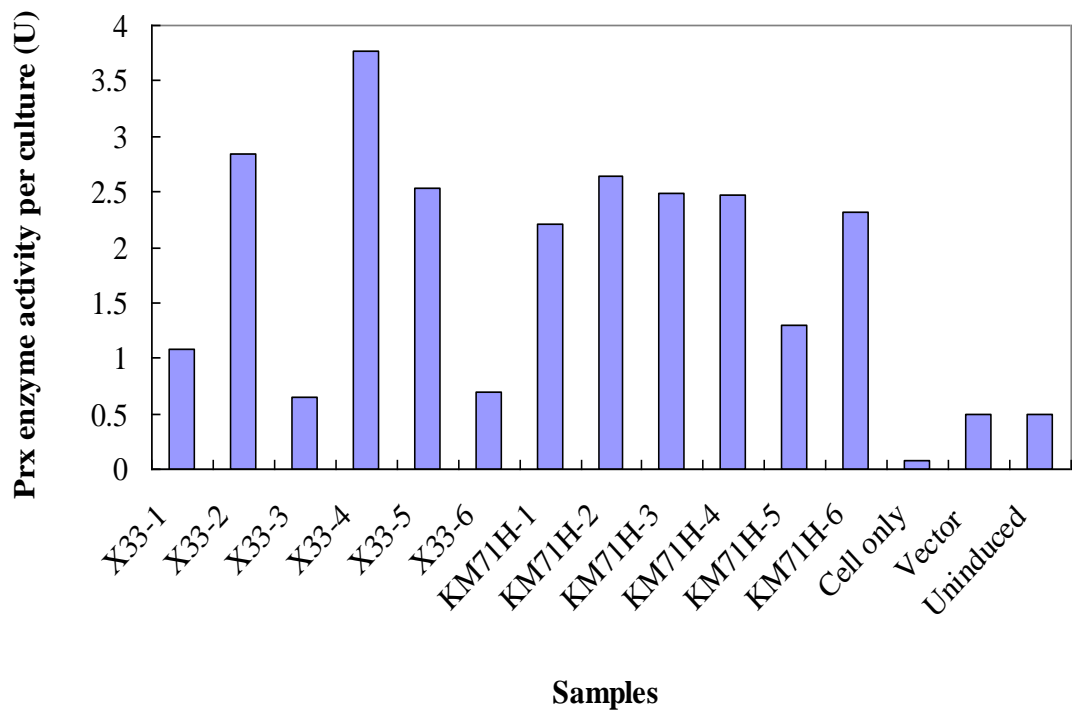
Figure 4.2. Prx enzyme activity of transformed *P. pastoris* X33 and KM71H cells following 3 and 8 d, respectively, of induction. Cell only refers to untransformed *P. pastoris* cells. Vector refers to X-33 cells transformed with the vector lacking the *Pf*Prx-2 insert. Uninduced refers to X-33 cells transformed with the *Pf*Prx-2 construct grown in BMGY medium, i.e, growth medium with glycerol instead of methanol. Culture volumes were 50 ml for all samples. Cell density was similar for all samples as determined by OD_{600}.
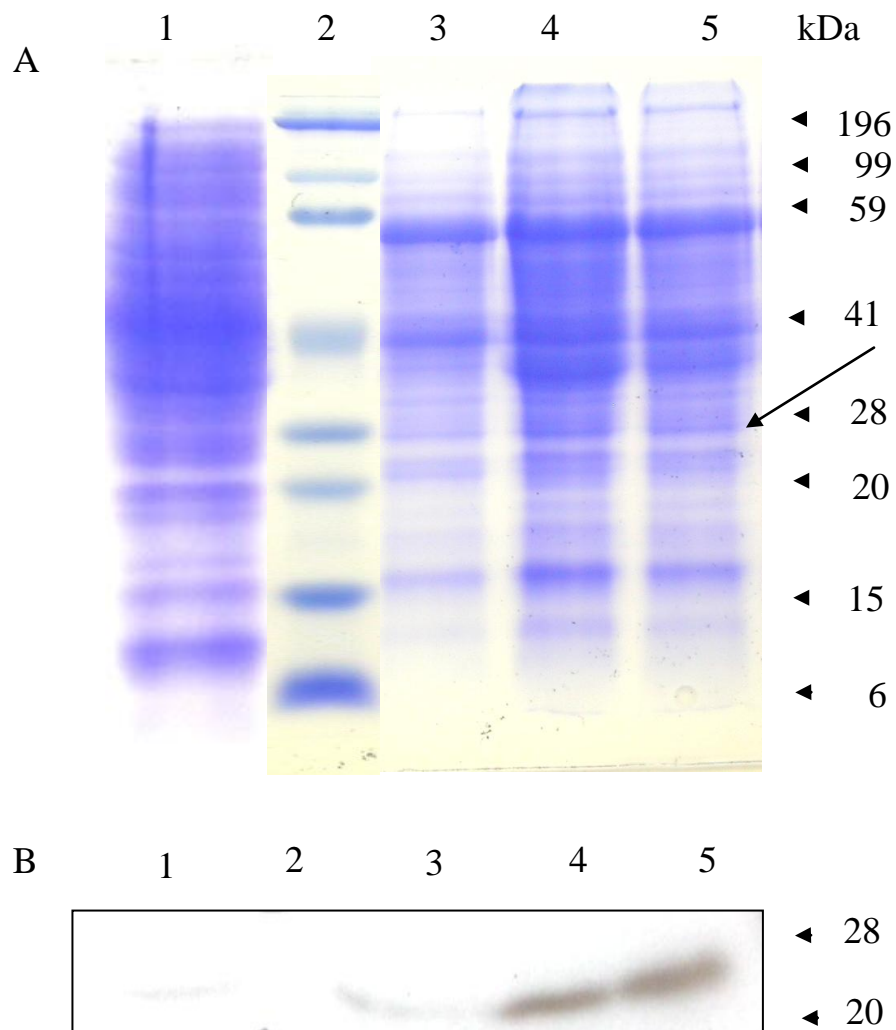
Figure 4.3. SDS-PAGE (A) and Immunodetection (B) analysis of proteins extracted from *P. pastoris* X33-4 cells at various times after induction for protein expression. Approximately 25 μg of soluble protein was loaded in each lane. Lane 1, uninduced sample; lane 2, pre-stained SDS-PAGE broad range marker (Bio-Rad); lanes 3, 4 and 5, samples taken 24, 48 and 72 h after induction. The sizes of the molecular markers are shown on the right. The big arrow indicates the protein band that increases in intensity with increasing induction time.

4.3.2   Confirmation of the complete transcription of the *Pf*Prx-2 protein coding region

It has been reported that AT-rich genes, such as those of *P. falciparum*, are not well expressed in yeast and that this AT-richness leads to premature termination of transcription (Romanos et al. 1992). Thus, RT-PCR analysis was carried out to prove that the complete *Pf*Prx-2 protein coding region had been transcribed in the *P. pastoris* host cells. *P. pastoris* X33-4 cells were harvested following 3 d of induction and uninduced *P. pastoris* X33-4 cells were used as the negative control. The results shown in Fig. 4.4 and the sequencing of RT-PCR products indicate that transcription of the *Pf*Prx-2 gene was indeed complete. The expected RT-PCR products of approximately 700 bp with the *Pf*Prx-2 primers and approximately 900 bp with the *AOX1* primers were obtained for the induced *P. pastoris* X33-4 cells. No PCR products were obtained for the uninduced cells.

Subsequent DNA sequencing of the RT-PCR products confirmed that the *Pf*Prx-2 protein coding region plus the nucleotides encoding the c-*myc* and His$_6$-tags were completely transcribed and in the correct reading frame for translation.
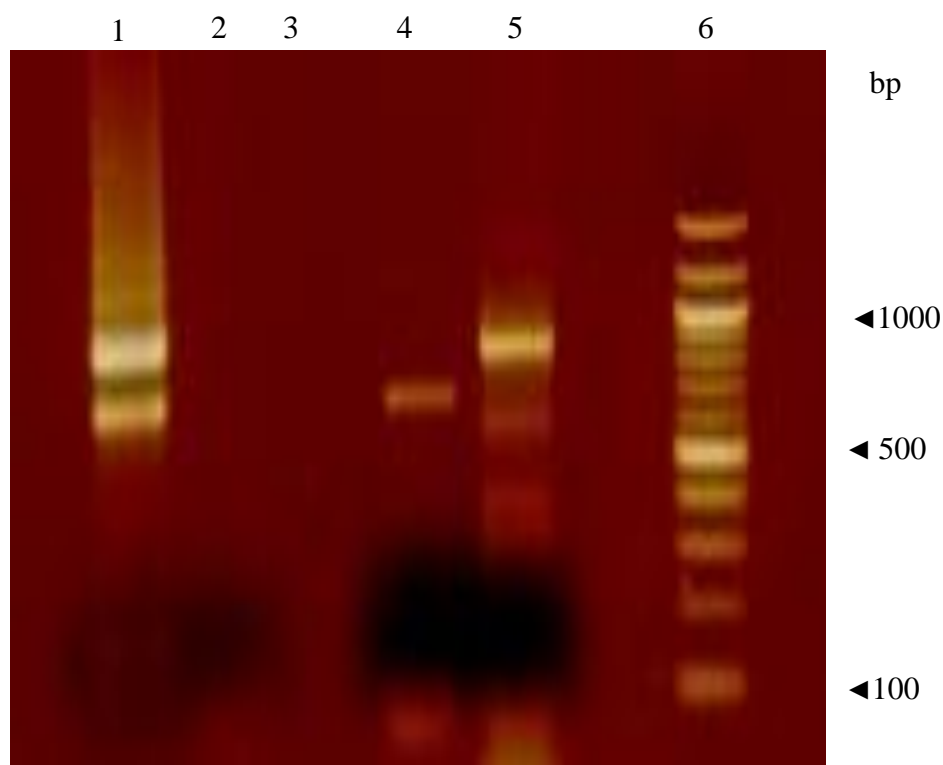
Figure 4.4. RT-PCR amplification of *Pf*Prx-2 mRNA from *P. pastoris* X33-4 cells either induced for 3 d or uninduced. Lane 1, 1.7 µg of total RNA from induced *P. pastoris* X33-4 cells; lane 2, 10 µl of the RT-PCR reaction with the *Pf*Prx-2 primers but without any RNA template; lane 3, 10 µl of products from the RT-PCR reaction with the *Pf*Prx-2 primers and with the RNA template from uninduced *P. pastoris* X33-4 cells; lane 4, 10 µl of the products from RT-PCR reaction with the *Pf*Prx-2 primers and with the RNA template from induced *P. pastoris* X33-4 cells; lane 5, 10 µl of the products of RT-PCR reaction with the *AOX1* primers and with the RNA template from induced *P. pastoris* X33-4 cells; Lane 6, 100 bp DNA ladder (New England Biolabs). The sizes of the marker are shown on the right.

4.3.3 Purification of the recombinant *Pf*Prx-2 protein using Ni-affinity column chromatography

The recombinant *Pf*Prx-2 protein was purified from extracts of *P. pastoris* X33-4 cells using Ni-affinity column chromatography. The *Pf*Prx-2 protein eluted from the column with the 250 mM imidazole wash as shown by Prx enzyme activity (Fig. 4.5) and immunodetection with Anti-Tetra His antibodies (Fig. 4.6B).

Prior to Ni-affinity chromatography, the *Pf*Prx-2 protein had a molecular mass of 28 kDa whereas after Ni-affinity chromatography this had approximately doubled to 59 kDa (Fig. 4.6). We hypothesized that this may have been due to oxidation of the protein and consequent formation of disulphide bonds between Cys residues leading to dimerization of the 28 kDa monomers. Therefore, various reducing conditions were tested to determine whether they could reverse this apparent conformational change (Fig. 4.7). An overnight incubation of the Ni-affinity purified *Pf*Prx-2 with either 50 mM DTT or 0.5 M β-mercaptoethanol had no effect. Similarly, incubation for 1 h with tributylphosphine to reduce any disulphide bonds to sulphydryl groups, followed by incubation for 1.5 h with iodoacetamide to alkylate the sulphydryl groups thus making the reduction irreversible also had no effect.
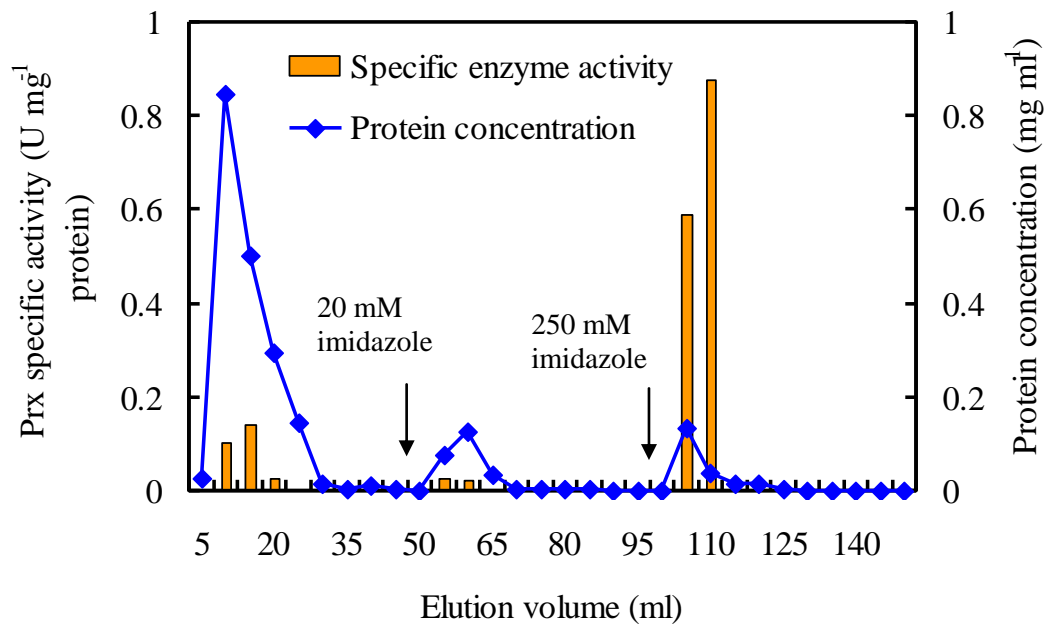
Figure 4.5: **Ni-affinity purification of recombinant *Pf*Prx-2 from a *P. pastoris* X33-4 crude cell extract**. The total amount of protein loaded onto the column was approximately 12 mg in a total volume of 5 ml. Three peak fractions from each wash (0 mM, 20 mM and 250 mM imidazole) were assayed for Prx activity. The fractions were buffer exchanged and concentrated (as described in sections 3.2.18) before the Prx assays.
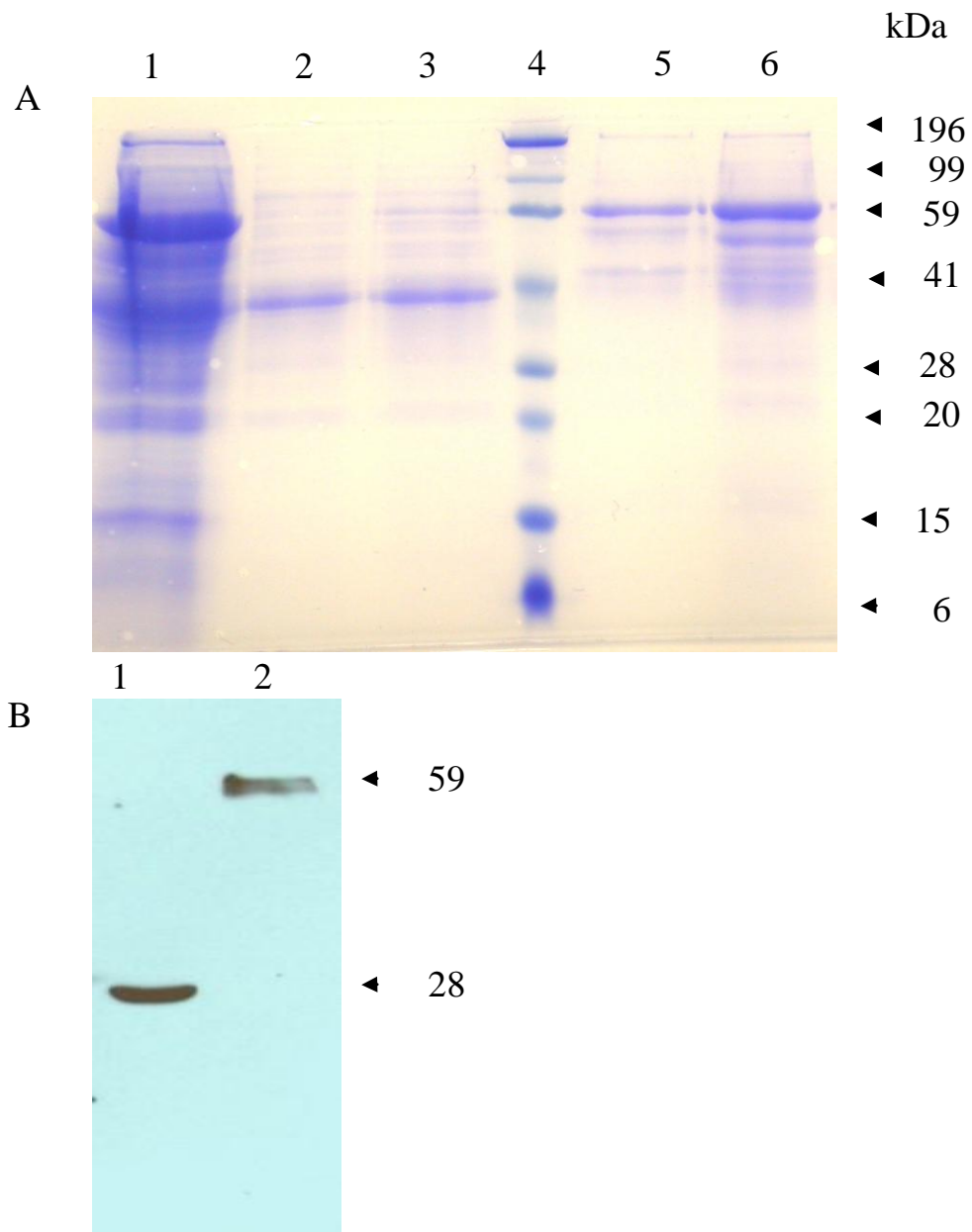
Figure 4.6. SDS-PAGE (A) and Immunodetection (B) analysis of Ni-affinity chromatography purification of recombinant *Pf*Prx-2 from *P. pastoris* X33-4 cells. (A) Lane 1, crude extract (20 µg soluble protein); lanes 2 and 3, peak fractions from the 0 mM and 20 mM imidazole washs of the column respectively (~3-4 µg soluble protein); lane 4, prestained SDS-PAGE broad range marker (Bio-Rad); lanes 5 and 6, peak fractions from the elution of the column with 250 mM imidazole (~3-4 µg soluble protein). (B) Lane 1, crude extract (20 µg soluble protein); lane 2, peak fraction from the elution of the column with 250 mM imidazole (~3-4 µg) soluble protein.
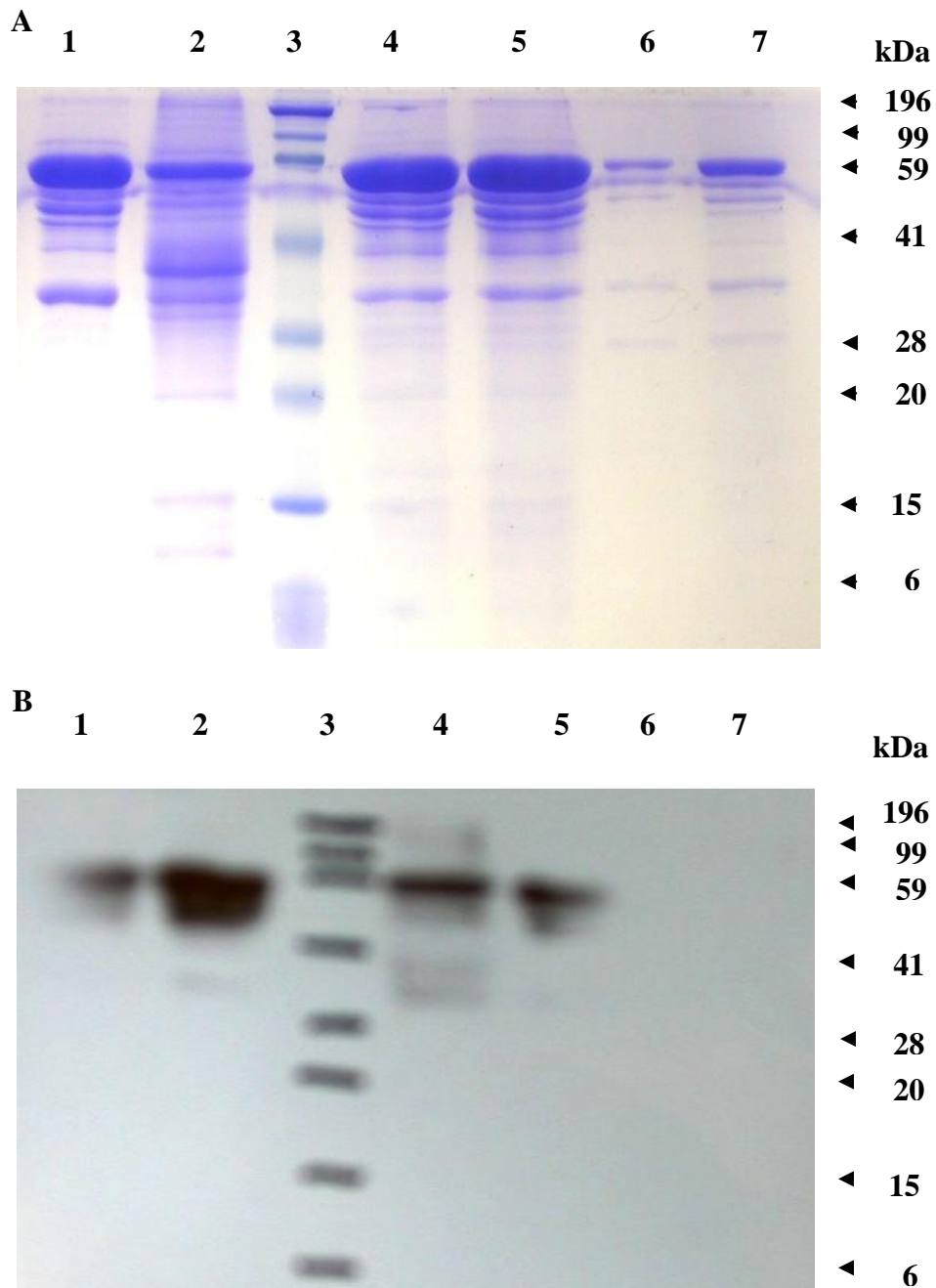
Figure 4.7. SDS-PAGE (A) and Immunodetection analysis (B) of the size of the Ni-affinity purified recombinant *Pf*Prx-2 following various treatments. Lane 1, untreated sample (10 µg protein); lane 2, 5 mM TBP treatment (8 µg protein); lane 3, 5 µl of prestained SDS-PAGE broad range marker (Bio-Rad); lane 4, 50 mM DTT treatment (10 µg protein); lane 5, 0.5 M β-mercaptoethanol treatment (10 µg protein); Lanes 6 & 7, Factor Xa treatment (2.5 and 5 µg protein, respectively). For Immunodetection analysis, the amount of protein loaded were 5 µg for all lanes except the marker.

The conformation of the recombinant *Pf*Prx-2 protein may also have been affected by the presence of the c-*myc* and His_6 tags. Thus, the Ni-affinity purified *Pf*Prx-2 protein was treated with Factor Xa protease to remove these tags and then re-purified using Ni-affinity chromatography (Fig. 4.7). As expected, the *Pf*Prx-2 protein with the His_6-tag removed failed to bind to the Ni-affinity column and was collected in the flow-through. Figure 4.7B confirms that the His_6-tag was successful removed because there was no binding of the anti-His antibody in lanes 6 and 7. Removal of the His_6-tag resulted in a loss of activity from 0.088 to 0.020 U mg^{-1} protein but it did not affect the molecular mass of the *Pf*Prx-2 protein, i.e., the molecular mass was still approximately 59 kDa, equivalent to a dimer (Fig. 4.7A).

4.3.4 Determination of the native molecular mass of the recombinant *Pf*Prx-2 protein

To determine the native molecular mass of the recombinant *Pf*Prx-2 protein, a crude extract of the *P. pastoris* X33-4 cells was fractionated on a gel filtration column in the presence of 1, 5 or 10 mM DTT (Fig. 4.8A). At all three DTT concentrations, Prx enzyme activity was detected only in the fractions corresponding to elution volumes of 50 and 52 ml and protein sizes of 382 and 334 kDa. Immunodetection using anti-His antibodies confirmed the presence of the *Pf*Prx-2 protein in these fractions (Fig. 4.8B). Thus, the native molecular mass of the recombinant *Pf*Prx-2 protein was very large, approximately 12-14 times the size of the 28 kDa monomer.

A
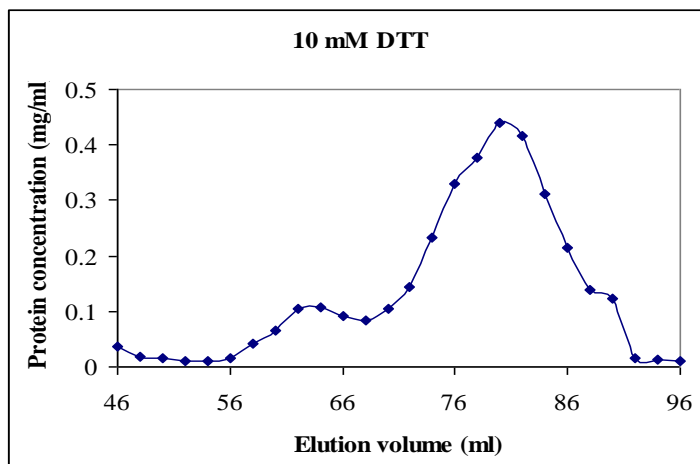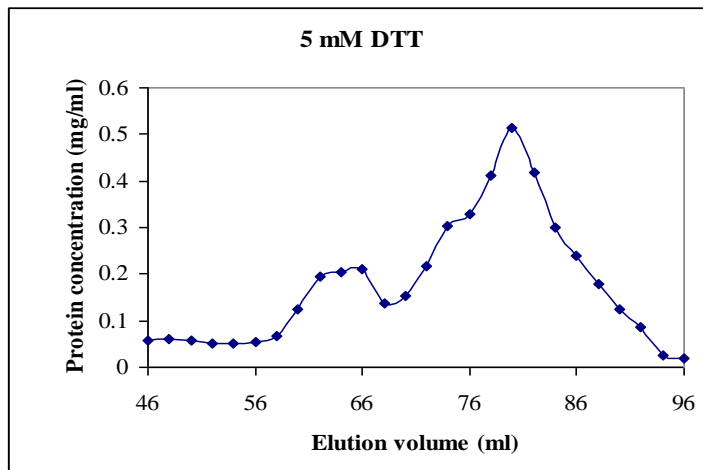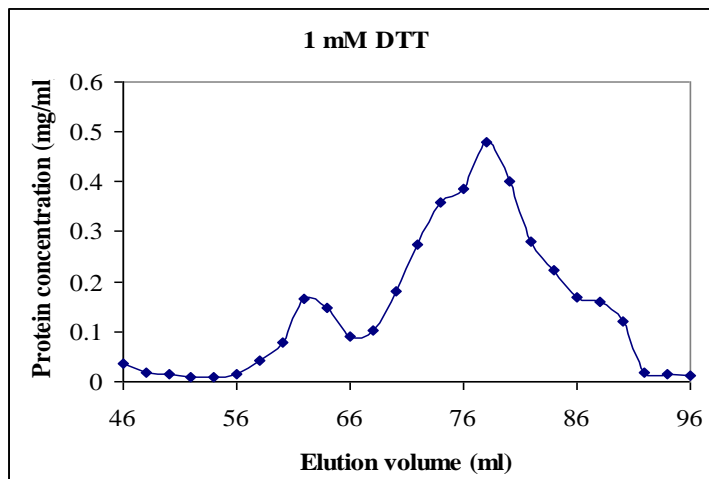
B
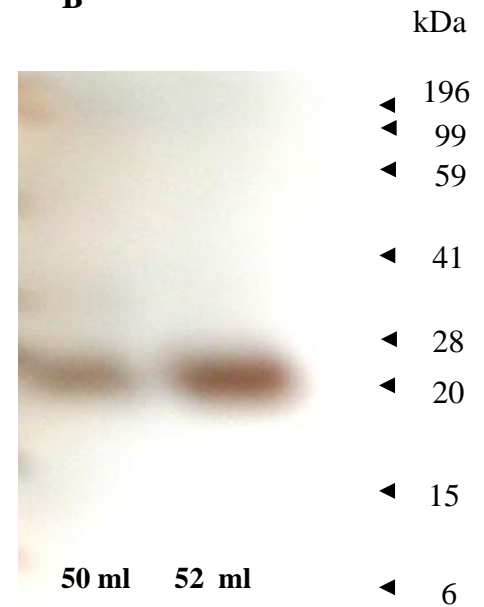
Figure 4.8. The effect of increasing concentrations of reducing agent (DTT) on the native molecular mass of recombinant *Pf*Prx-2 (A) Gel filtration column chromatography elution profiles and (B) Immunodetection analysis of fractions from the column. The column was loaded with 8 mg of protein in 1.0 ml of a crude extract of *P. pastoris* X33-4 cells that had been induced for 3 d.

4.3.5   Subcellular localization of the recombinant *Pf*Prx-2 protein expressed in *P. pastoris*

To investigate the subcellular localization of the recombinant *Pf*Prx-2 protein expressed in *P. pastoris*, mitochondria were isolated following 3 days of induction of *P. pastoris* X33-4 cells and *P. pastoris* cells transformed with the pPICZ B vector lacking the *Pf*Prx-2 insert (vector-only control). Mitochondrial respiration measurements confirmed that the isolated mitochondria were intact (data not shown). Figure 4.9 shows SDS-PAGE and immunodetection analysis of protein extracts from cells and mitochondria. Immunodetection using the anti-His antibody showed that the *Pf*Prx-2 protein was present in the mitochondria isolated from the *P. pastoris* X33-4 cells but not in the mitochondria isolated from the vector-only control cells. In addition, Prx enzyme activity was detected in the mitochondria isolated from the *P. pastoris* X33-4 cells (0.039 U mg^{-1} protein) but not in the mitochondria isolated from the vector-only control cells. Thus, the *Pf*Prx-2 protein is likely to localize to the mitochondria in *P. pastoris* and it was enzymatically active.
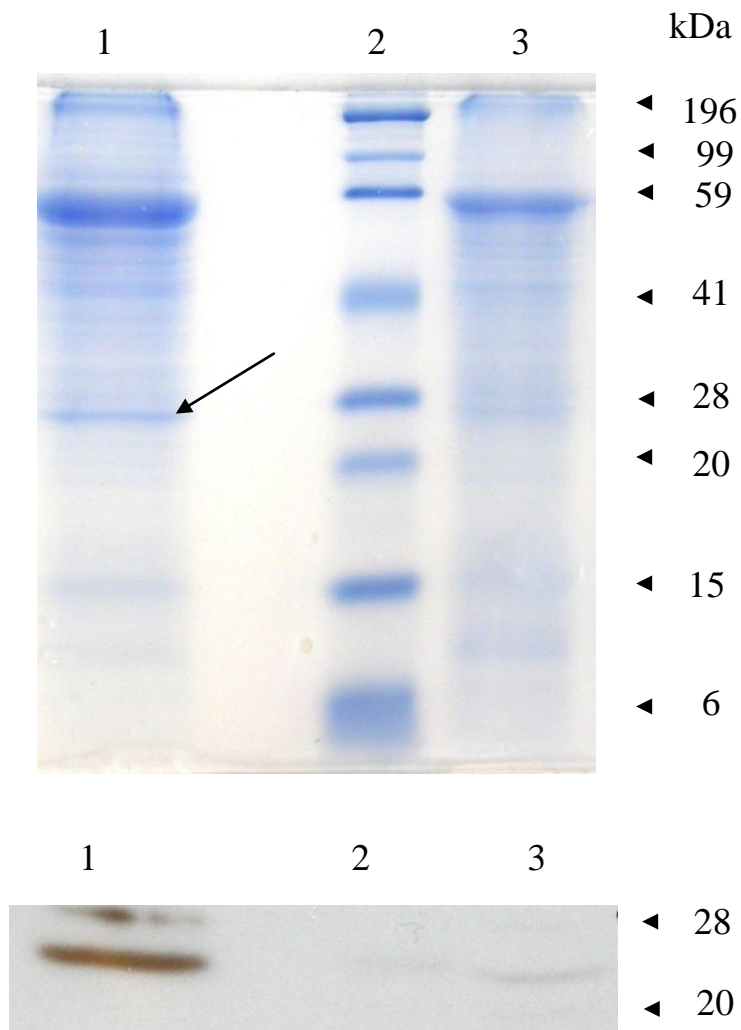
Figure 4.9. SDS-PAGE (A) and Immunodetection (B) analysis of proteins extracted from *P. pastoris* cells and mitochondria following 3 d induction for protein expression. Approximately 30-40 μg soluble protein was loaded in each lane. Lane 1, mitochondria isolated from *P. pastoris* X33-4 cells transformed with the *Pf*Prx-2 construct; lane 2, prestained SDS-PAGE broad range marker (Bio-Rad); lanes 3 mitochondria isolated from *P. pastoris* cells transformed with the empty pPICZ B vector.

4.4 Discussion

The antioxidant defence system of *P. falciparum* has received considerable attention as an antimalarial drug target because of its vital role in protecting the parasite against oxidative stress during the erythrocytic stage of its life cycle inside the human host (Atamna and Ginsburg, 1993). In particular, it was shown that *Pf*Prx-1, which occurs in the *P. falciparum* cytosol and is closely related to *Pf*Prx-2, has an important role to play in protecting the parasite against oxidative and nitrosative stress (Komaki-Yasuda et al., 2003). Several *P. falciparum* antioxidant proteins have been investigated in detail as potential anti-malarial drug targets. For example, inhibitor studies have been done using *P. falciparum* thioredoxin reductase (Andricopulo et al., 2006) and *P. falciparum* glutathione reductase (Sarma et al., 2003). In contrast, relatively few functional studies have been done with *Pf*Prx-2. As a mitochondrial enzyme, *Pf*Prx-2 is likely to be important in protecting this organelle against oxidative damage. In other organisms, mitochondrial Prx enzymes and thioredoxins have been identified and it has been suggested that they play crucial roles in defence against oxidative stress (Miranda-Vizuete et al., 2000, Smeets et al., 2005, Wheeler and Grant, 2004). Recently it was reported that the overexpression of a mitochondrial Prx gene in *Leishmania donovani* protects this parasite against H_2O_2-induced cell death (Harder et al., 2006).

The ultimate aim of this study was to produce sufficient quantities of recombinant *Pf*Prx-2 protein to enable structural and functional studies for structure-based antimalarial drug design. These studies typically require large quantities of highly

purified proteins (McRee, 1993). Our results showed that up to 0.5 mg of recombinant *Pf*Prx-2 protein per 1 L shake flask culture could be obtained with this expression system. Although the amount of the *Pf*Prx-2 protein produced is modest, it is adequate for targeted experimental use and the total yield could be further improved using a large-volume fermentation system.

The *Pf*Prx-2 protein has been previously expressed, but only in *E.coli* (Boucher et al., 2006, Rahlfs and Becker, 2001). As a prokaryotic expression host, *E.coli* has the disadvantage that it cannot carry out post-translational processing of eukaryotic proteins. When *Pf*Prx-2 was expressed in *E.coli* as a full-length protein, it was found to be enzymatically inactive when assayed with various hydroperoxide substrates in the presence of *Pf*Trx and *Pf*TrxR (Rahlfs and Becker, 2001). It was hypothesized that the lack of enzymatic activity was due to incorrect folding of the recombinant protein as a result of the presence of a mitochondrial targeting sequence which could not be processed by the prokaryotic *E. coli* expression host. Here *P. pastoris* was used as an expression host because it is a eukaryote and as such may be able to perform essential post-translational modifications. To confirm that the *P. pastoris* host was able to recognise and cleaved off the mitochondrial targeting sequence, further study using amino acid sequencing of the N-terminus of the recombinant *Pf*Prx-2 protein should be done.

The results presented here demonstrate that functionally active *Pf*Prx-2 was produced by *P. pastoris* transformants, indicating that the correct folding of the protein had occurred. It has been shown in previous studies that another yeast

expression system, *Saccharomyces cerevisiae*, is capable of recognizing other

eukaryotic mitochondrial targeting sequences. For example, the uncoupling protein

(UCP) from rat brown adipose tissue, an integral component of the mitochondrial

inner membrane, has been expressed in *S. cerevisiae* and found to target to the yeast

mitochondria and display the same bioenergetic properties as in rat brown adipose

tissue mitochondria (Bathgate et al., 1992). In this study, both enzyme activity

assays and immunodetection showed the presence of *Pf*Prx-2 protein in the

mitochondrial fraction purified from the transformed yeast indicating that the

recombinant protein was localised to the yeast mitochondria. However, it is possible

that the recombinant *Pf*Prx-2 protein co-incidentally co-purified with the yeast

mitochondria. To eliminate this possibility and confirm the localisation of the

recombinant protein, future experiments could be done such as double staining of

the mitochondria (using a yeast mitochondria staining dye) and the *Pf*Prx-2 protein

(using antibody staining).

With regards to enzyme activity, the recombinant *Pf*Prx-2 protein was shown to

possess typical Prx activity as it had the capacity to reduce H_2O_2 in the presence of

thioredoxin, thioredoxin reductase and NADPH. It is important to mention here that

E. coli thioredoxin was used as the substrate in the Prx enzyme assay in this study.

Recently, there was an interesting publication on the substrate specificity of the

recombinant *Pf*Prx-2 expressed without the putative mitochondrial targeting

sequence in *E. coli* (Boucher et al., 2006). These authors compared the kinetics of

their recombinant *Pf*Prx-2 using either the cytosolic or the mitochondrial thioredoxin

from *P. falciparum* (*Pf*Trx1 and *Pf*Trx2, respectively). Their results showed that

their recombinant *Pf*Prx-2 clearly preferred *Pf*Trx2 to *Pf*Trx1 as a reducing partner,

with K_m values of 11.6 μM and 130.4 μM, respectively. It would be interesting to test these two alternative substrates using the recombinant *Pf*Prx-2 produced in yeast in this study. A comparison of the enzyme kinetics of the recombinant *Pf*Prx-2 with those of the wild-type enzyme is another area for future study.

The results obtained here demonstrate the successful purification of the recombinant *Pf*Prx-2 (Figs. 4.5 and 4.6). Higher Prx specific activity was obtained in the elution fractions (250 mM imidazole) compared to other wash fractions (0 and 20 mM imidazole) (Fig. 4.5) indicating that most of the recombinant *Pf*Prx-2 successfully bound to the column and was eluted out in the 250 mM imidazole wash. The presence of Prx activity in the other wash fractions could be due to the host's endogenous Prx activity. It was shown that the *Pf*Prx-2 was the predominant protein in the elution fractions from the Ni-affinity column (Fig. 4.6). However, there were other proteins present. Further purification steps employing other techniques such as ion-exchange or size-exclusion chromatography might be used if a higher degree of purity is required for future study.

In the present study, recombinant *Pf*Prx-2 was detected as a monomer on SDS-PAGE gels prior to Ni-affinity chromatography purification but as a dimer after Ni-affinity chromatography purification. None of the reducing agents tested (DTT, β-mercaptoethanol, tributylphosphine plus iodoacetamide) could reverse this size change. These results suggest disulphide bond formation was not the explanation for the conversion of the monomer to a dimer. An alternative hypothesis is that Ni^{2+} ions leaking from the Ni-affinity column may have caused the irreversible

aggregation of the monomers to form dimers. Metal ions are known to affect the

structure and stability of many proteins (Petsko and Ringe, 2004). For example, a

study of the zinc protein PerR from *Bacillus subtilis* showed that a $Zn(Cys)_4$ site

"locks" the protein in its dimeric form (Traoré et al., 2006). Further experiments are

required to test the hypothesis that Ni interacts in this way with the recombinant

*Pf*Prx-2 protein. However, to avoid this problem, future experiments should employ

different methods to purify *Pf*Prx-2 protein. One of the methods to try is using a

TALON affinity column which uses Cobalt instead of Ni.

To eliminate the possibility that the prominent bands in Fig. 4.7A were from some

other proteins with high Prx activity, the specificity of the immunodetection needs to

be clarified. Fig. 4.7 shows that after treatment with Factor Xa, the proteins (seen in

lanes 6 & 7 in Fig. 4.7A) did not appear following immunodetection using the Anti-

His antibody (lanes 6 & 7 in Fig. 4.7B). The Factor Xa cleavage site was engineered

into the recombinant protein immediately after the *Pf*Prx-2 protein coding sequence

and before the C-terminal His_6-tag (refer to Appendix D). Treatment with Factor Xa

was therefore expected to separate *Pf*Prx-2 proteins with the C-terminal His_6-tag.

The results in Fig. 4.7 indicate the high specificity of the immunodetection (the

Anti-His antibody in particular) towards His_6-tagged proteins as the removal of this

tag led to the total disappearance of the immunodetected bands.

We also characterized the *Pf*Prx-2 protein expressed in *P. pastoris* with respect to its

molecular mass. The native molecular mass as determined by gel filtration

chromatography was 330 to 380 kDa. This corresponds to approximately 12-14

times the molecular mass of the monomer as determined by SDS-PAGE and as

reported by others (Rahlfs and Becker, 2001; Boucher et al., 2006). These results are

consistent with those of Boucher et al. (2006) who found that recombinant *Pf*Prx-2

expressed without its mitochondrial targeting sequence in *E. coli*, was mostly in the

form of a decamer with only a small proportion in the form of a dimer. Another

member of the *P. falciparum* 2-Cys Prx family, the *Pf*Prx-1 protein, has also been

shown to exist mostly as a decamer with only a small proportion existing as a dimer

(Akerman and Müller, 2003).

Oligomers larger than dimers have also been observed for 2-Cys Prx proteins from

other species such as bacteria, plants, rats and humans (Choi et al., 2003, König et

al., 2003, Kitano et al., 2005, Matsumura et al., 2008, Nagahara et al., 2007,

Schröder et al., 2000, Seo et al., 2000, Wood et al., 2002). As a member of the 2-Cys

peroxiredoxin family, *Pf*Prx-2 possesses two conserved Cys residues that form

typical interchain disulphide linkages (Wood et al., 2003, Boucher et al., 2006).

Wood et al. (2002) proposed a detailed catalytic cycle for 2-Cys Prx proteins in

which the enzymes undergo structural transitions between dimers, decamers and

higher molecular mass oligomers. The catalytic mechanism of typical 2-Cys Prx

proteins involves cycling of the active site pair of Cys residues between the reduced

form and the disulphide-linked oxidized form. During the catalytic cycle it is

believed that the protein undergoes structural transitions, typically resulting in the

formation of an $(\alpha_2)_5$ decamer in the reduced state which resolves partially into

homodimers at lower protein concentrations in the oxidized state (Alphey et al.,

2000, Wood et al., 2002, Kawazu et al., 2008).

The factors that regulate the oligomeric assembly of 2-Cys Prx proteins are complicated and still not well understood (Wood et al., 2003). Kitano et al. (1999) reported that high ionic strength favours the oligomerization of a bacterial 2-Cys Prx, whereas Chauhan and Mande (2001) suggested the opposite, i.e., that high ionic strength leads to dissociation of the decamer. Other reports have indicated that oligomerization is dependent on pH (with lower pH values favouring oligomerization) or on redox state (with reduction of the enzyme resulting in oligomerization) (Kristensen et al., 1999, Schröder et al., 1998). A recent study of a rat 2-Cys Prx combined the above factors and found that in the presence of a reducing agent (DTT), the only form found was the decamer whereas in the absence of DTT, decamers were found at high protein concentrations but they tended to dissociate into tetramers or dimers as the protein concentration was decreased or as the ionic strength was increased (Matsumura et al., 2008). Thus it can be concluded that redox state, protein concentration, pH and ionic strength all influence the oligomeric state but their effects differ between different 2-Cys Prx proteins from different species.

In this study, the effects of redox state (by varying the concentration of the reducing agent DTT) were tested. The results agree with those of Matsumura et al. (2008) in that *Pf*Prx-2 existed as decamers when DTT was present. However, the recombinant *Pf*Prx-2 was also detected as decamers in the absence of DTT. The reason might be because of the high protein concentration of the *Pf*Prx-2 (8 mg ml^{-1}) applied onto the gel filtration column in this study. In their study, Matsumura et al. (2008) also reported that the rat 2-Cys Prx I was detected as only a decamer when the protein

concentration was 1 mg ml^{-1} and dissociation into tetramers or dimers occurred when the protein concentration was decreased to 0.23 mg ml^{-1} or lower.

The oligomerization of 2-Cys Prx proteins is believed to affect their Prx enzyme activity and their binding efficiency with their electron donor protein (Rhee et al., 2005, Wood et al., 2002). The decameric form of the enzyme has been shown to have higher activity than the dimeric form (Rhee et al., 2005, Wood et al., 2002). For example, the dimeric form of *Salmonella typhimurium* 2-Cys Prx exhibited lower binding efficiency with Ah*Pf* (electron donor) and lower peroxidase activity than the decameric form (Parsonage et al., 2005). However, a recent study of a rat 2-Cys Prx demonstrated the opposite results with the binding efficiency for the electron donor (reduced thioredoxin) being greater for the dimeric form than for the decameric form (Matsumura et al., 2008). It is possible that oligomerization is one of the regulatory systems for the functions of 2-Cys Prx proteins. Since interconversion between the oxidized dimeric and decameric forms is influenced by factors such as redox state and protein concentration, this may be one of the regulatory mechanisms for the interactions of this protein with other proteins.

It has been reported that AT-rich genes such as those found in the *Plasmodium falciparum* genome are poorly expressed in yeast due to premature termination of transcription (Romanos et al. 1992). As an exception to this observation, the results of this study have shown that *P. pastoris* is capable of producing a *Pf*Prx-2 protein that has structural and biochemical characteristics comparable with those of native Prx proteins from other sources. The recombinant *Pf*Prx-2 protein was found to be

targeted to the host cell mitochondria indicating that *P. pastoris* recognizes the *P. falciparum* mitochondrial targeting signal sequence. Thus, there is potential for *P. pastoris* to be used to express large quantities of the *Pf*Prx-2 protein for structural studies and rational design of novel antimalarial drugs. The purification procedure using Ni-affinity chromatography resulted in relatively pure and active enzyme. The success of this study in developing an expression and purification system for *Pf*Prx-2 in *P. pastoris* should open the way for further investigations of this enzyme both in vivo and in vitro. This will facilitate the development of the *Pf*Prx-2 protein as a novel antimalarial drug target.

References

Alphey, M. S., Bond, C. S., Tetaud, E., Fairlamb, A. H. & Hunter, W. N. (2000) The structure of reduced tryparedoxin peroxidase reveals a decamer and insight into reactivity of 2-Cys peroxiredoxins. *Journal of Molecular Biology,* 300**,** 903-916.

Andricopulo, A. D., Akoachere, M. B., Krogh, R., Nickel, C., McLeish, M. J., Kenyon, G. L., Arscott, L. D., Williams, C. H., Davioud-Charvet, J., E. & Becker, a. K. (2006) Specific inhibitors of *Plasmodium falciparum* thioredoxin reductase as potential antimalarial agents. *Bioorganic and Medicinal Chemistry Letters,* 16**,** 2283-2292.

Atamna, H. & Ginsburg, H. (1993) Origin of reactive oxygen species in erythrocytes infected with *Plasmodium falciparum. Molecular and Biochemical Parasitology,* 61**,** 231-241.

Bathgate, B., Freebairn, E. M., Greenland, A. J. & Reid, G. A. (1992) Functional expression of the rat brown adipose tissue uncoupling protein in *Saccharomyces cerevisiae*. *Molecular Microbiology,* 6**,** 363-370.

Boucher, I. W., McMillan, P. J., Gabrielsen, M., Akerman, S. E., Brannigan, J. A., Schnick, C., Brzozowski, A. M., Wikinson, A. J. & Müller, S. (2006) Structural and biochemical characterization of a mitochondrial peroxiredoxin from *Plasmodium falciparum. Molecular Microbiology,* 61**,** 948-959.

Brocchieri , L. (2001) Low-omplexity regions in *Plasmodium* proteins: In search of a function *Genome Research,* 11**,** 195-197.

Chauhan, R. & Mande, S. C. (2001) Characterization of the *Mycobacterium tuberculosis* H37Rv alkyl hydroperoxidase AhpC points to the importance of ionic interactions in oligomerization and activity. *Biochemical Journal,* 354**,** 209-215.

Choi, J., Choi, S., Choi, J., Cha, M. K., Kim, I. H. & Shin, W. (2003) Crystal structure of *Escherichia coli* thiol peroxidase in the oxidized state: Insights into intramolecular disulfide formation and substrate binding in atypical 2-Cys peroxiredoxins *Journal of Biological Chemistry,* 278**,** 49478-49486.

González-Barroso, M. M., Ledesma, A., Lepper, S., Pérez-Magán, E., Zaragoza, P. & Rial, E. (2006) Isolation and bioenergetic characterization of mitochondria from *Pichia pastoris*. *Yeast,* 23**,** 307 - 313.

Harder, S., Bente, M., Isermann, K. & Bruchhaus, I. (2006) Expression of a mitochondrial peroxiredoxin prevents programmed cell death in *Leishmania donovani*. *Eukaryotic Cell,* 5**,** 861-870.

Kawazu, S., Komaki-Yasuda, K., Oku, H. & Kano, S. (2008) Peroxiredoxins in malaria parasites: Parasitologic aspects. *Parasitology International,* 57**,** 1-7.

Kitano, K., Kita, A., Hakoshima, T., Niimura, Y. & Miki, K. (2005) Crystal structure of decameric peroxiredoxin (AhpC) from *Amphibacillus xylanus*. *Proteins: Structure, Function, and Bioinformatics,* 59**,** 644-647.

Kitano, K., Niimura, Y., Nishiyama, Y. & Miki, K. (1999) Stimulation of peroxidase activity by decamerization related to ionic strength: AhpC protein from *Amphibacillus xylanus*. *Biochemistry,* 126**,** 313-319.

Komaki-Yasuda, K., Kawazu, S. & Kano, S. (2003) Disruption of the *Plasmodium falciparum* 2-Cys peroxiredoxin gene renders parasites hypersensitive to reative oxygen and nitrogen species. *FEBS Letters,* 547**,** 140-144.

König, J., Lotte, K., Plessow, G., Brockhinke, A., Baier, M. & Dietz, K.-J. (2003) Reaction mechanism of plant 2-Cys peroxiredoxin. Role of the C terminus and the quaternary structure. *Journal of Biological Chemistry,* 278**,** 24409-24420.

Kristensen, P., Rasmusssen, D. E. & Kristensen, B. (1999) Properties of thiol-specific antioxidant protein or calpromotin in solution. *Biochemical and Biophysical Research Communications,* 262**,** 127-131.

Matsumura, T., Okamoto, K., Iwahara, S., Horis, H., Takahashi, Y., Nishino, T. & Abe, Y. (2008) Dimer-oligomer interconversion of wild-type and mutant rat 2-Cys peroxiredoxin. *Journal of Biological Chemistry,* 283**,** 284-293.

McRee, D. E. (1993) *Practical Protein Cystallography,* San Diego, California 92101-4311, Academic Press, Inc.

Miranda-Vizuete, A., Damdimopoulos, A. E. & Spyrou, G. (2000) The mitochondrial thioredoxin system. *Antioxidants and Redox Signaling,* 2**,** 801–810.

Nagahara, N., Yoshii, T., Abe, Y. & Matsumura, T. (2007) Thioredoxin-dependent enzymatic activation of mercaptopyruvate sulfurtransferase: An intersubunit disulfide bond serves as a redox switch for activation. . *Journal of Biological Chemistry,* 282**,** 1561-1569.

Parsonage, D., Youngblood, D. S., Sarma, G. N., Wood, Z. A., Karplus, P. A. & Poole, L. B. (2005) Analysis of the link between enzymatic activity and oligomeric state in AhpC, a bacterial peroxiredoxin. *Biochemistry,* 44**,** 10583 - 10592.

Petsko, G. A. & Ringe, D. (2004) *Protein Structure and Function*, Sinauer Associates New Science Press Ltd.

Rahlfs, S. & Becker, K. (2001) Thioredoxin peroxidases of the malarial parasite *Plasmodium falciparum. European Journal of Biochemistry,* 268**,** 1404-1409.

Rhee, S. G., Chae, H. Z. & Kim, K. (2005) Peroxiredoxins: A historical overview and speculative of novel mechanisms and emerging concepts in cell signalling. *Free Radical Biology and Medicine,* 38**,** 1543-1552.

Romanos, M. A., Scorer, C. A. & Clare, J. J. (1992) Foreign gene expression in yeast: a review. *Yeast,* 8**,** 423-488.

Sarma, G. N., Savvides, S. N., Becker, K., Schirmer, M., Schirmer, R. H. & Karplus, P. A. (2003) Glutathione reductase of the malaria parasite *Plasmodium falciparum*: crystal structure and inhibitor development. *Journal of Molecular Biology,* 328**,** 893-907.

Schröder, E., Littlechild, J. A., Lebedev, A. A., Errington, N., Vagin, A. A. & Isupov, M. N. (2000) Crystal structure of decameric 2-Cys peorxiredoxin from human eruthrocytes at 1.7 Å resolution. *Structure,* 8**,** 605-615.

Schröder, E., Willis, A. C. & Ponting, C. P. (1998) Porcine natural-killer-enhancing factor-B: oligomerisation and identification as a calpain substrate in vitro. *Biochimica et Biophysica Acta,* 1383**,** 279-291.

Seo, M. S., Kang, S. W., Kim, K., Baines, I. C., Lee, T. H. & Rhee, S. G. (2000) Identification of a new type of mammalian peroxiredoxin that forms an intramolecular disulfide as a reaction intermediate. *Journal of Biological Chemistry,* 275**,** 20346-20354.

Smeets, A., Evrard, C., Landtmeters, M., Marchand, C., Knoops, B. & Declercq, J.-P. (2005) Crystal structures of oxidized and reduced forms of human mitochondrial thioredoxin 2. *Protein Science,* 14**,** 2610-2621.

Traoré, D. A. K., Ghazouani, A. E., Ilango, S., Dupuy, J., Jacquamet, L., Ferrer, J. L., Caux-Thang, C., Duarte, V. & Latour, J.-M. (2006) Crystal structure of the apo-PerR-Zn protein from *Bacillus subtilis*. *Molecular Microbiology,* 61**,** 1211 - 1219.

Wheeler, G. L. & Grant, C. M. (2004) Regulation of redox homeostasis in the yeast *Saccharomyces cerevisiae*. *Physiologia Plantarum,* 120**,** 12-20.

Wood, Z. A., Poole, L. B., Hantgan, R. R. & Karplus, P. A. (2002) Dimers to doughnuts: Redox-sensitive oligomerization of 2-cysteine peroxiredoxins. *Biochemistry,* 41**,** 5493– 5504.

Wood, Z. A., Schroder, E., Harris, J. R. & Poole, L. B. (2003) Structure, mechanism and regulation of peroxiredoxins. *Trends in Biochemical Sciences,* 28**,** 32-40.

Yano, K., Komaki-Yasuda, K., Kobayashi, T., Takemae, H., Kita, K., Kano, S. & and Kawazu, S. (2005) Expression of mRNAs and proteins for peroxiredoxins in *Plasmodium falciparum* erythrocytic stage. *Parasitology International,* 54**,** 35-41.

Chapter 5   Discussion

Effects of intercropping on P-nutrition and P-deficiency in wheat and lupin

Intercropping and crop rotation are traditional agricultural practices that have been shown to increase crop yields, improve resource utilization and reduce negative impacts on the environment (Zhang and Li, 2003). However, the mechanisms by which crop partners benefit from intercropping or crop rotation systems are not always well understood. Using a novel leaching system, this study provided a direct demonstration that improved growth and P uptake of wheat in mixed culture with white lupin is due to the ability of the lupins to extract P from a citric acid soluble soil P pool not normally available to wheat. Apart from providing a better understanding on the mechanism underlying the P-efficiency of white lupin and wheat, this study also demonstrated a simple, yet effective method for studying interactions between plants and soils.

In this study, the yield was assessed based on the dry biomass of plant shoots and roots. The next step would be to investigate the seed yields and mineral nutrition (in particularly P) of the seeds of wheat and lupin in monoculture versus intercropping. The results of such studies would provide useful information for farmers in order to establish an agronomic way of overcoming nutrition deficiency.

Biochemical and structural characterisation of 2-Cys Prx proteins from *P.*

falciparum

The results of Chapters 3 and 4 demonstrate the success in gene cloning and protein expression and purification of the *P. falciparum Pf*Prx-1 and *Pf*Prx-2. The cytosolic *Pf*Prx-1 was expressed in *E.coli* with reasonably high yield (12.5 mg per L culture) while that of the mitochondrial *Pf*Prx-2 expressed in *P. pastoris* was lower (0.5 mg per L culture). While producing recombinant protein with lower yield, the *P. pastoris* expression system had advantages in its capability to carry out post-translational processing of eukaryotic proteins (Romanos et al., 1992) and in this case, it successfully processed the recombinant *Pf*Prx-2 to produce active enzyme which was inactive when expressed in *E. coli*. The recombinant *Pf*Prx-2 produced here is likely to be more structurally similar to the native enzyme compared to *Pf*Prx-2 protein expressed in bacteria. This is the first published report on the expression of *Pf*Prx-2 in a eukaryotic expression host. The expression and purification system developed here can be easily up-scaled in order to produce large quantities of *Pf*Prx-2 protein for crystallization and X-ray crystallography analysis studies.

Both recombinant *Pf*Prx-1 and *Pf*Prx-2 were shown to possess typical Prx enzyme activity when assayed with H_2O_2. Both enzymes showed relatively low enzyme activity per mg protein and this is likely to be due to the use of *E. coli* Trx as the reducing substrate as compared with results from other studies (Rahlfs and Becker, 2001, Boucher et al., 2006). Future studies should be carried out with *P. falciparum*

cytosolic Trx and mitochondrial Trx together with *Pf*Prx-1 and *Pf*Prx-2 to confirm

this hypothesis. The removal of the His_6-tag seemed to decrease the Prx activity in

both recombinant enzymes in this study. In previous studies, this was found to be

due to the fact that the His_6-tag enhanced that stability of the decameric form of the

recombinant Prx protein (Cao et al., 2007). It would be interesting to carry out

structural studies in the presence and absence of the His_6-tag for the recombinant

*Pf*Prx-1 and *Pf*Prx-2 proteins in order to determine if they behave in the same way

as previously described by Cao et al. (2007).

With regards to structural analysis, both recombinant *Pf*Prx-1 and *Pf*Prx-2 proteins

existed predominantly as decamers which could dissociate to form dimers. These

oligomerization states were, however, dependent on many factors such as the

concentration of reducing agents, urea or pH. The results of this study are similar to

the findings on the oligomerisation characteristics of many other members of the Prx

family (Akerman and Müller, 2003, Boucher et al. 2006, Choi et al., 2003, Kitano et

al., 2005, Kristensen, P., 1999, Matsumura et al., 2008, Wood et al., 2003).

With regards to protein crystal structure, this study successfully produced crystals of

*Pf*Prx-1 recombinant protein and preliminary X-ray diffraction data were obtained

from these crystals. This is the first published data on *Pf*Prx-1 protein crystal

structure. The low resolution X-ray diffraction data, though not sufficient to solve

the *Pf*Prx-1 protein structure, nevertheless provide a glimpse into some of its

structural properties e.g. its group space, cell volume and diameters and, more

importantly, provide the basis for further experimentation. Future studies should

focus on the improvement of the size and quality of the protein crystals in order to solve the protein structure at higher resolution. Once the structure of *Pf*Prx-1 is solved, inhibitor screening and the characterization of enzyme-inhibitor complexes will demonstrate if the Prx proteins of malarial parasites are suitable candidates for targeted drug design.

Structure-based drug discovery is a useful tool for developing novel drugs because computational methods can be used to rapidly screen small molecule databases for compounds that bind to the active site of the target protein (Mehlin, 2005). This reduces the list of thousands of potential compounds that need to be tested in the laboratory to a more manageable number. This structure-driven screening method efficiently sorts out potential drug compounds from those that are unlikely to be effective. Structure-based computational methods have reported 'hit' rates of about 10% compared with 0.01% using conventional high-throughput screening techniques (Augen 2002).

The first and probably most important requirement for structure-based screening is the availability of high-quality structures of validated target proteins and this is a fundamental challenge as the total number of available X-ray crystal structures for *Plasmodium* proteins is very low (Buchholz et al., 2007). There have been 56 crystal structures of *P. falciparum* proteins deposited in the RSCB Protein Data Bank (http://www.rcsb.org/pdb/) to date. There are many reasons for this low number. First, *P. falciparum* is a challenging organism from which to clone and express proteins due to the genome's A-T richness, unique codon bias (Gardner et al., 2002)

and unusual glycosylation patterns (Mehlin 2005). Also, the presence of low-complexity regions in some *P. falciparum* proteins may prevent them from crystallizing (Aravind et al., 2003).

The results of this study, in general provide detailed information in the areas of biochemical and structural characteristics of the two typical 2-cys Prx proteins in *P. falciparum* recombinantly expressed in both bacterial and eukaryotic hosts. The results also provide the basis for future experiments in order to solve the crystal structures of those proteins and thus will aid in the structure-based screening process in order to develop novel drugs to combat malaria.

References

Akerman, S. E. & Müller, S. (2003) 2-Cys peroxiredoxin *Pf*Trx-Px1 is involved in the antioxidant defence of *Plasmodium falciparum. Molecular and Biochemical Parasitology,* 130**,** 75-81.

Augen, J. (2002) The evolving role of information technology in the drug discovery process. *Drug Discovery Today,* 7**,** 315-323.

Buchholz, K., Mailu, M., Schirmer, H. & Becker, K. (2007) Structure-based drug development against malaria. *Frontiers in Drug Design & Discovery: Structure-Based Drug Design in the 21st Century,,* 3**,** 225-255.

Boucher, I. W., McMillan, P. J., Gabrielsen, M., Akerman, S. E., Brannigan, J. A., Schnick, C., Brzozowski, A. M., Wikinson, A. J. & Müller, S. (2006) Structural and biochemical characterization of a mitochondrial peroxiredoxin from *Plasmodium falciparum. Molecular Microbiology,* 61**,** 948-959.

Cao, Z., Bhella, D. & Lindsay, J. G. (2007) Reconstitution of the mitochondrial PrxIII antioxidant defence pathway: General properties and factors affecting PrxIII activity and oligomeric state *Journal of Molecular Biology*, 372**,** 1022-1033.

Choi, J., Choi, S., Choi, J., Cha, M. K., Kim, I. H. & Shin, W. (2003) Crystal structure of *Escherichia coli* thiol peroxidase in the oxidized state: Insights into intramolecular disulfide formation and substrate binding in atypical 2-Cys peroxiredoxins *Journal of Biological Chemistry,* 278**,** 49478-49486.

Gardner, M. J., Hall, N., Fung, E., White, O., Beriman, M., Hyman, R. W., Carlton, J. M., Pain, A., Nelson, K. E. & al., e. (2002) The genome sequence of the human malaria parasite *Plasmodium falciparum. Nature,* 419**,** 498-511.

Kitano, K., Kita, A., Hakoshima, T., Niimura, Y. & Miki, K. (2005) Crystal

structure of decameric peroxiredoxin (AhpC) from *Amphibacillus xylanus*.

Proteins: Structure, Function, and Bioinformatics, 59**,** 644-647.

Kristensen, P., Rasmusssen, D. E. & Kristensen, B. (1999) Properties of thiol-

specific antioxidant protein or calpromotin in solution. *Biochemical and*

Biophysical Research Communications, 262**,** 127-131.

Matsumura, T., Okamoto, K., Iwahara, S., Horis, H., Takahashi, Y., Nishino, T. &

Abe, Y. (2008) Dimer-oligomer interconversion of wild-type and mutant rat 2-

Cys peroxiredoxin. *Journal of Biological Chemistry,* 283**,** 284-293.

Mehlin, C. (2005) Structure-based drug discovery for *Plasmodium falciparum*.

Combinatorial Chemistry and High Throughput Screening, 8**,** 5-14.

Rahlfs, S. & Becker, K. (2001) Thioredoxin peroxidases of the malarial parasite

Plasmodium falciparum. European Journal of Biochemistry, 268**,** 1404-1409.

Romanos, M. A., Scorer, C. A. & Clare, J. J. (1992) Foreign gene expression in

yeast: a review. *Yeast,* 8**,** 423-488.

Wood, Z. A., Schroder, E., Harris, J. R. & Poole, L. B. (2003) Structure, mechanism

and regulation of peroxiredoxins. *Trends in Biochemical Sciences,* 28**,** 32-40.

Zhang, F. & Li, L. (2003) Using competitive and facilitative interactions in

intercropping systems enhances crop productivity and nutrient-use efficiency.

Plant and Soil, 248**,** 305-312.

Appendix A. pET3d vector

The map of pET3d vector was obtained from pET System Manual (Novagen)
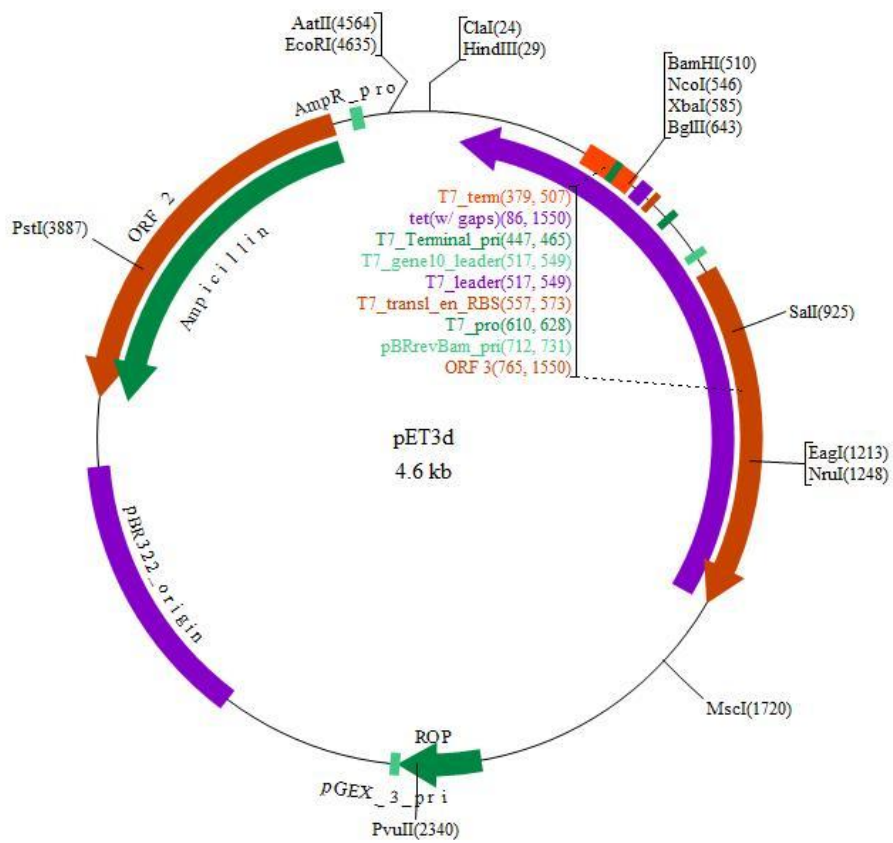
Appendix B: Sequencing result of the recombinant *Pf*Prx-1 protein coding sequence.

Letters in bold indicate restriction enzyme sites, in blue indicate His$_6$-tag, in red indicate Factor Xa recognition site and in italics indicating start and stop codons

A**CCATGG**AACATCATCACCATCATCATATTGAGGGACGC*ATG*GCATCA
TATGTAGGAAGAGAAGCTCCTTATTTTAAGGCTGAAGCAGTTTTTGCAGAT
AACACATTTGGAGAAGTAAATTTGCATGATTTTATTGGAAAGAAATATGT
ATTATTATATTTTTATCCATTAGATTTTACGTTTGTATGTCCATCTGAAATC
ATTGCATTAGATAAGGCTCTTGATGCATTTAAGGAAAGAAATGTTGAATT
AATAGGCTGTAGTGTGGATAGTAAATATACTCATTTGGCATGGAAAAAAA
CACCATTAACTAAAGGAGGTATAGGAAATATCCAACATACATTAATATCT
GATATTACTAAAGTATATCAAGAAGTTATAATGTGTTGTTTGGTGATAGT
GTATCATTAAGAGCATTTGTATTAATCGACAAGCAAGGTGTTGTTCAACAT
TTACTTGTTAATAATTTAGCTATTGGTAGATCAGTTGAGGAAGTCTTAAGA
ATTATTGATGCTGTACAACACCACGAACAACATGGAGATGTTTGCCCAGC
AAACTGGAAAAAGGGAAAGGTAGCCATGAAACCATCAGAAGAAGGTGTT
AGTGAATATTTATCAAAGTTG*TAA***GGATCC**

Appendix C: pPICZ B vector

The map of vector pPICZ A, B, C was obtained from "A Manual of Methods for

Expression of Recombinant Proteins Using pPICZ and pPICZα in *Pichia pastoris*"

Catalog no. K1740-01 (Invitrogen)
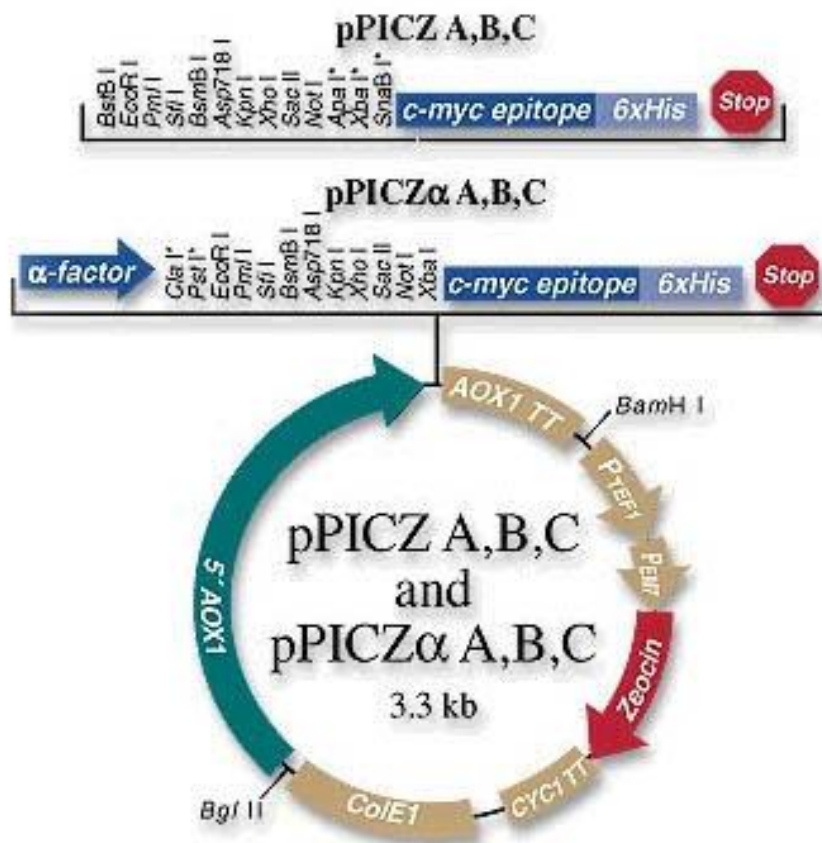
Appendix D: Sequencing result of the recombinant *Pf*Prx-2 protein coding sequence.

Letters in bold indicate restriction enzyme recognition site, in blue indicate His$_6$-tag, in red indicate Factor Xa recognition site, in green indicate myc-tag, in italics indicate start and stop codons

GGTAC**CTCGA**GACAATA*ATG*TCTTTTTTAAAAAAACTGTGCAGGAGCAA
TTTTTTCGGGAATTCAAGAAGATCCTTTTCGCTAGTGACAAAGAAGGCTT
ATAATTTCACAGCTCAAGGATTAAATAAAAATAATGAAATAATAAATGT
TGACCTTTCCTCTTTATAGGTCAGAAATACTGTTGTTTGTTATTTTATCC
ATTAAACTATACCTTCGTATGTCCAACAGAAATAATTGAATTTAATAAGC
ATATAAAGATTTTGAAAATAAAAATGTAGAGTTATTAGGTATATCCGT
AGATTCAGTATATAGTCATTTGGCATGGAAAAATATGCCTATTGAAAAA
GGAGGAATTGGAAATGTGGAATTTACTTTAGTATCAGATATAAATAAAG
ACATTTCTAAAAATTATAATGTACTTTATGATAATTCTTTTGCTTTAAGAG
GTTTATTTATTATTGATAAAAATGGATGTGTAAGACATCAAACCGTTAAT
GATTTACCAATAGGTAGAAATGTACAGGAAGTTTTAAGAACTATAGATT
CAATTATTCATGTAGATACAAGTGGAGAAGTTTGTCCAATCAACTGGAA
AAAGGGACAAAAGCATTCAAACCAACTACCGAATCGTTAATAGATTAT
ATGAATAATGCAAATAAAAA**ATTGAGGGACGC****GCGGCCGCC**AGCTTT
CTA**GAACAAAAACTCATCTCAGAAGAGGATCTGAATAGCGCCGTCGA**
C**CATCATCATCATCATCAT**TGA